Multiparametric Cardiovascular Magnetic Resonance for the Assessment of Cardiac Function and Metabolism in Hypertrophy and Heart Failure

MASLIZA MAHMOD

MBCHB MMED MRCP

WOLFSON COLLEGE

DIVISION OF CARDIOVASCULAR MEDICINE

RADCLIFFE DEPARTMENT OF MEDICINE

UNIVERSITY OF OXFORD

THESIS SUBMITTED FOR THE DEGREE OF
DOCTOR OF PHILOSOPHY
TRINITY TERM 2013

ACKNOWLEDGEMENTS

First of all, I would like to thank all my supervisors, Prof Stefan Neubauer, Dr Theodoros Karamitsos and Dr Houman Ashrafian. It was an honour to work with them and I will always be grateful for their guidance, advice, support and encouragement during critical stages of my studies and also preparation of this thesis. Dr Theodoros Karamitsos has been of tremendous help in the day-to-day help and guidance on running the projects.

To all fellow colleagues in OCMR, seniors (Sacha Bull, Alex Pitcher, Vanessa Ferreira, Erica Dall'Armellina, Ntobeko Ntusi, Malenka Bissell, Rajarshi Banerjee, Joseph Suttie, Sairia Dass) and less senior (Eylem Levelt, Margaret Loudon, Rina Ariga, Michael Pavlides, Victoria Stoll, Andrew Lewis). Thank you for always being there and making OCMR a stimulating office to work, and I appreciate your understanding especially negotiating scan slots. A special thank to Jane Francis for her support during scanning sessions. My gratitude to Hayley Harvey, who provided nursing support and looking after the heart failure patients, this was most helpful to me.

A special thank to my family who have always given continuous support in my work. My husband, Amerudin has always encouraged me to work hard, aim very high and has always reminded me to be humble. I will never forget his invaluable assistance especially with excel spreadsheets and thesis formatting! And not to forget, special thanks to my children (Melissa, Malek and Norman) for their endless patience and understanding especially during my long hours of work, cheering me along the way and keep my life lively and fun. Finally, a big thank you to my mother in-law Zabidah Mohamed who has given priceless support with the house work during my thesis writing stage, and for this I am truly thankful.

DECLARATION

I declare that the work presented in this thesis is my own. Dr Nikhil Pal assisted in recruitment of normal volunteers in this study. Dr Sacha Bull provided data on asymptomatic AS patients in Chapter 3. Dr Vanessa Ferreira and Dr Stefan Piechnick contributed some data on DCM patients in Chapter 6. Dr Sairia Dass provided ethics from her previous study for recruitment of participants in Chapters 3 and 4. Dr Cameron Holloway and Dr Banerjee Rajarshee contributed some normal volunteer data in Chapter 3. Dr Andrew Lewis helped with the processing of late gadolinium enhancement quantification data in Chapter 4. I recruited and imaged all the patients in this study with the invaluable assistance of the staff and fellows of the OCMR. I analysed all the CMR scans, interpreted the data, carried out the statistics and wrote the script.

During the course of my DPhil, I was funded by the National University of Malaysia and Ministry of Higher Education Malaysia Scholarship. The studies were also funded by the Oxford NIHR Biomedical Research Centre.

ABBREVIATIONS

AMARES	Advanced Method of Accurate, Robust and Efficient Spectroscopic fitting
AVA	Aortic Valve Area
AS	Aortic Stenosis
ATP	Adenosine Triphosphate
AVR	Aortic Valve Replacement
BNP	Brain Natriuretic Peptide
BOLD	Blood Oxygen Level Dependent
BP	Blood Pressure
CAD	Coronary Artery Disease
CCS	Canadian Cardiovascular Society
CMR	Cardiac Magnetic Resonance
DCM	Dilated Cardiomyopathy
ECG	Electrocardiogram
EDV	End Diastolic Volume
EF	Ejection Fraction
ESV	End Systolic Volume
FA	Fatty Acids
FWHM	Full-Width Half Maximum
HF	Heart Failure
HLA	Horizontal Long Axis
HOMA	Homeostasis Model of Assessment
jMRUI	Java Magnetic Resonance User Interface
LGE	Late Gadolinium Enhancement
LV	Left Ventricle/Ventricular
LVEF	Left Ventricular Ejection Fraction
LVMI	Left Ventricular Mass Index
MPRI	Myocardial Perfusion Reserve Index
MRI	Magnetic Resonance Imaging
MRS	Magnetic Resonance Spectroscopy
MTC	Myocardial Triglyceride Content
NEFA	Non-Esterified Fatty Acid
NYHA	New York Heart Association
PCr	Phosphocreatine
PET	Positron Emission Tomography

RF	Radio Frequency
ROI	Region Of Interest
RPP	Rate Pressure Product
SA	Short Axis
SD	Standard Deviation
SI	Signal Intensity
SNR	Signal To Noise Ratio
SPAMM	Spatial Modulation Of Magnetization
SSFP	Steady State Free Precession
STEAM	Stimulated Echo Acquisition Mode
SV	Stroke Volume
TE	Echo Time
TG	Triglyceride
TR	Repetition Time
TG	Triglyceride

TABLE OF CONTENTS

THESIS ABSTRACT

Both hypertrophied and failing hearts are characterised by pathological left ventricular (LV) remodelling, impaired myocardial energy status and alteration in substrate metabolism. Cardiac magnetic resonance imaging (CMR) and magnetic resonance spectroscopy (MRS) are powerful tools in the characterisation of these disease conditions. More recent techniques have allowed assessment of myocardial steatosis using ^{1}H-MRS and tissue oxygenation using blood oxygen level dependent (BOLD) CMR.

In hypertrophy and heart failure, studies on steatosis and the relationship with other parameters such as myocardial function and fibrosis, especially in humans are limited. I therefore investigated the presence of steatosis in severe aortic stenosis (AS) and dilated cardiomyopathy (DCM), and further assessed its relation to contractile function. This study found that myocardial triglyceride (TG) content is increased in both symptomatic and asymptomatic AS patients (lipid/water ratio 0.89±0.42% in symptomatic AS; 0.75±0.36% in asymptomatic AS vs. controls 0.45±0.17%, both $p<0.05$) and DCM patients (lipid/ratio 0.64±0.44% vs. controls 0.40±0.13%, $p=0.03$). Circumferential strain was lower in both AS (-16.4±2.5% in symptomatic AS; -18.9±2.9% in asymptomatic AS vs. controls 20.7±2.0%, both $p<0.05$) and DCM patients (-12.3±3.4% vs. controls -20.9±1.7%, $p<0.001$). In AS, myocardial contractility is related to the degree of steatosis, and were both reversible following aortic valve replacement (AVR), lipid/water ratio 0.92±0.41% vs. pre AVR 0.45±0.17%, $p=0.04$ and circumferential strain -17.2±2.0% vs. pre AVR -19.5±3.2%, $p=0.04$. A novel finding of this study was significant correlation of MRS-measured TG content with histological staining of

TG of the myocardium, taken from endomyocardial biopsy during AVR. In DCM, myocardial TG was independently associated with LV dilatation and correlated significantly with hepatic TG, which suggests that both cardiac and hepatic steatosis might be a common feature in the failing heart.

Additionally, although the hypertrophied heart is characterised by impaired perfusion, it is unknown if this is severe enough to translate into tissue deoxygenation and ischaemia. I assessed this by using adenosine vasodilator stress test and BOLD-CMR in patients with severe AS. It was found that AS patients had reduced perfusion (myocardial perfusion reserve index-MPRI 1.0±0.3 vs. controls 1.7±0.3, $p<0.001$), and blunted tissue oxygenation (blood-oxygen level dependent-BOLD signal intensity-SI change 4.8±9.6% vs. controls 18.2±11.6%, $p=0.001$) during stress. Importantly, there was a substantial improvement in perfusion and oxygenation towards normal after AVR, MPRI 1.5±0.4, $p=0.005$ vs. pre AVR and BOLD SI change 16.4±7.0%, $p=0.014$ vs. pre AVR.

Overall, the work in this thesis supports the powerful role of CMR in assessing LV function and elucidating metabolic mechanisms in the hypertrophied and failing heart.

CHAPTER 1: GENERAL INTRODUCTION

1.1. CARDIAC METABOLISM

Both hypertrophy and heart failure (Figure 1.1), though differing in their aetiologies, share features of abnormal metabolism characterised by impaired myocardial energetics and profound alterations in glucose and fatty acid (FA) metabolism. Deranged cardiac energy metabolism has been implicated in both hypertrophy[1, 2] and dilated cardiomyopathy (DCM).[3, 4, 5] Understanding these complex metabolic pathways is crucial to improving clinical risk stratification and developing targeted therapeutic interventions.

Figure 1.1. Left ventricular hypertrophy viewed in a longitudinal section (A). Transverse sections of the hearts are shown in B. Compared with a normal heart (*centre*), the pressure-overloaded heart (*left*) has an increased mass, a thick wall, and a smaller lumen. The dilated heart (*right*) has an increased mass, a larger lumen, and enlarged size in comparison to the normal heart (Figure from Kumar: Robins Basic Pathology, 9th ed).

In the normal heart, the majority (60-90%) of energy for cardiac function is derived from FA oxidation, with the remainder (10-40%) being derived from the glucose oxidation. The normal heart is capable of modulating rates of FA and glucose oxidation in response to substrate availability, which in turn allows the heart to keep constant energy level.[6] There are three components of cardiac energy metabolism **(Figure 1.2)**;

A. *Substrate utilisation* involves the uptake of fuel mainly fatty acids (FAs) and glucose. These are broken down by beta-oxidation and glycolysis producing Acetyl-CoA to be fed into the Krebs cycle in the mitochondria.

   In addition, adequate myocardial perfusion is essential to deliver both substrate and oxygen under resting and exercise condition.

B. *Oxidative phosphorylation* involves the production of high-energy phosphate compound adenosine triphosphate (ATP) from the mitochondrial respiratory chain.

C. *High-energy phosphate transfer* involves the transport of ATP to the consumption site, the myofibrils, which involves the creatine kinase energy shuttle.

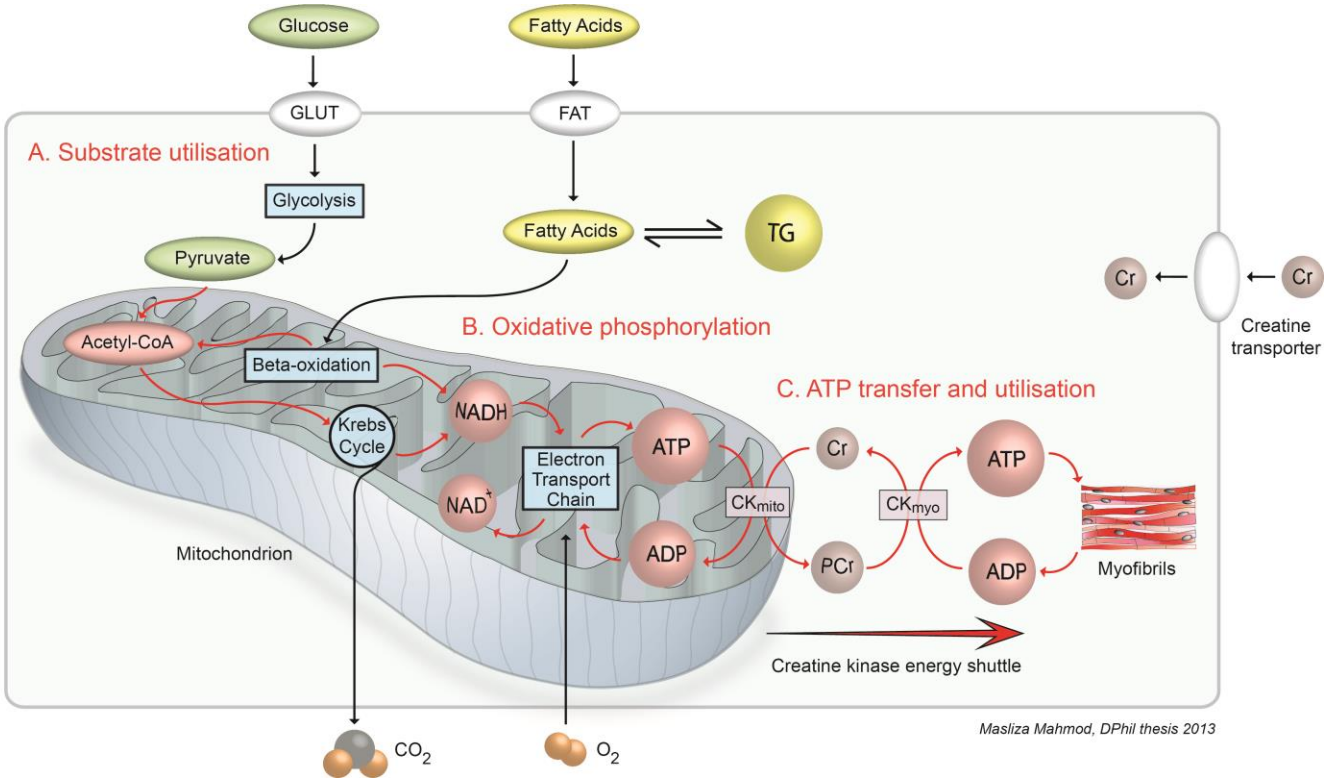

Figure 1.2. There are three components of cardiac energy metabolism. *A:* Substrate utilisation (FA and glucose uptake, and conversion to Acetyl-CoA to be fed into the Krebs cycle in the mitochondria). *B:* Oxidative phosphorylation (ATP production from the mitochondrial electron transport chain). *C:* High-energy phosphate transfer (ATP transport to the myofibrils, involving the creatine kinase energy shuttle).

Triglyceride and fatty acid metabolism

The sources of plasma triglyceride (TG) are from very low density lipoprotein (VLDL) produced by the liver and chylomicrons from the intestine upon dietary intake of fat. These TG particles are lipolysed by lipoprotein lipase (LPL) in the capillary wall to generate FA, which are subsequently taken up by the cells. Non-esterified fatty acids (NEFAs) are another form of FAs, bound to plasma albumin derived from lipolysis of triglycerides (TGs) stored in adipose tissue. These two forms of FAs are used for energy requirements, or alternatively to be stored as intracellular TGs **(Figure 1.3)**. In healthy conditions, almost all TGs present within the body are stored in adipose tissue, with only a small amount present in non-adipose tissues as the heart,[7] the liver[8] and skeletal muscle,[9] where levels are tightly regulated.

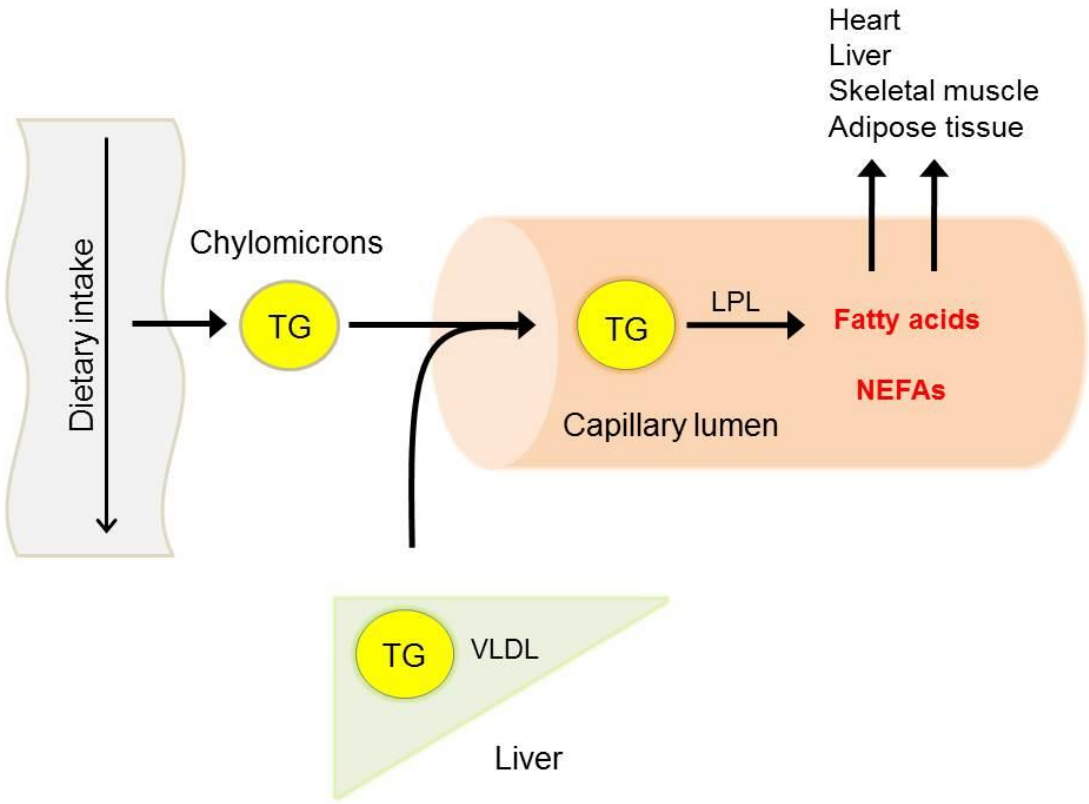

Figure 1.3. Triglyceride metabolism.

Mechanism of cardiac lipotoxicity

Myocardial steatosis is intracellular lipid accumulation arising from a mismatch between FA uptake and utilisation, and is implicated in the pathophysiology of the failing heart.[10-13] There are a number of experimental and clinical observations that suggest the association between steatosis and cardiac dysfunction.

1. FA overload as a result of *reduced FA oxidation*. Myocytes shift from FA to glucose utilisation in the hypertrophied and failing heart.[11, 13] This may be a beneficial compensatory mechanism in the short term as excess FA are stored as neutral TGs, but when the storage capacity is exceeded, these excess FA are transformed into toxic intermediates such as ceramide and diacylglycerols via non-oxidative pathways which is associated with apoptosis and myocardial dysfunction **(Figure 1.4)**.[14]

2. FA overload due to *increased FA uptake*. The increased sympathetic drive associated with HF is known to cause increased serum free FA.[15, 16] This will result in increased FA uptake and hyperactive β oxidation leading to production of reactive oxygen species and interference with calcium haemostasis impairing diastolic function. FA overload occurs when the oxidative capacity is exceeded leading to increased FA intermediates resulting in further lipotoxicity. Cardiac steatosis has been described in obesity and is associated with diastolic dysfunction in diabetes.[17, 18]

3. *Mechanical disruption* of contractile function. Infiltration of large lipid droplets can be accompanied by mechanical disassembly and loss of myofibrils leading to myocardial dysfunction in diabetic patients.[19]

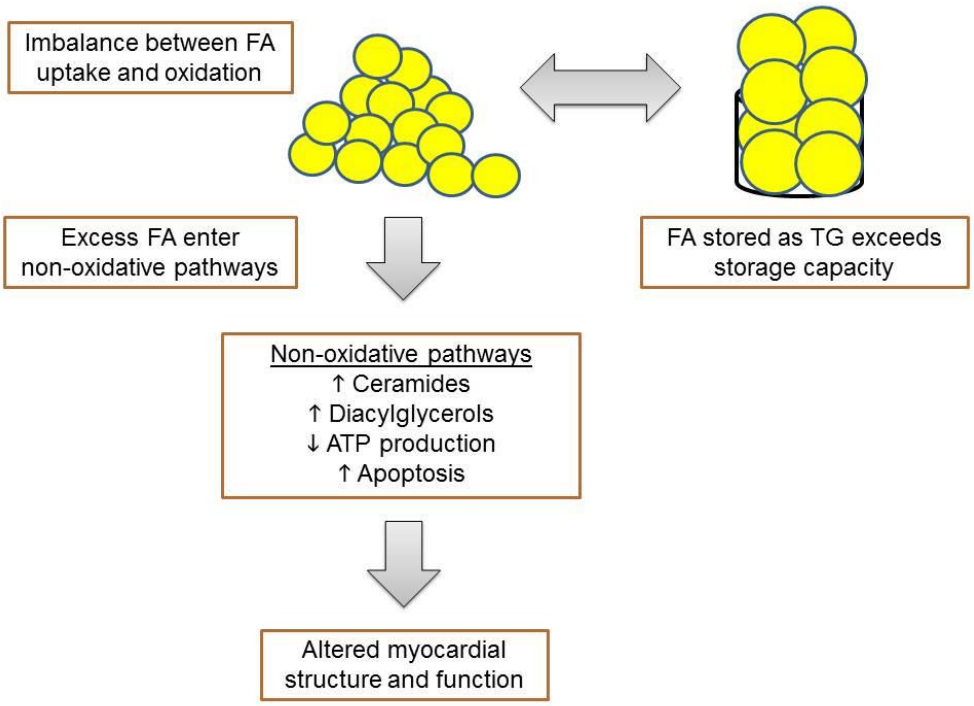

Figure 1.4. Proposed mechanisms of cardiac lipotoxicity.

Imbalance between FA uptake in relation to oxidative requirements results in FA overload which will lead to re-esterification of FA to TGs within the cells. When the storage capacity is exceeded, these excess FAs enter non-oxidative pathways. This has different effects, which ultimately alter myocardial structure and function. Although TGs per se are probably not harmful, however these TGs are reflection of increased potentially damaging intermediates.

However, all the 3 mechanisms can occur either in isolation or in combination, not exclusively to one another. Non-invasive assessment of the metabolic state of the myocardium can be done by two techniques; magnetic resonance spectroscopy (MRS) and positron emission tomography (PET), with the largest number of studies has been performed with MRS.[20] There are several types of MRS – ^{1}Hydrogen, ^{31}Phosphorus, ^{23}Sodium, ^{13}Carbon and more recently, hyperpolarization techniques, which can provide noninvasive assessment of myocardial metabolism.[21] The two most widely used techniques, ^{31}P-MRS gives information about energy status of the heart by measuring phosphocreatine (PCr) to ATP ratio and ^{1}H-MRS, which is a more recent technique used to measure myocardial lipids (triglycerides) as a measure of steatosis. If myocardial steatosis is present, it can provide a pathophysiological insight, and may become a potential prognostic indicator and/or therapeutic target. The main focus of this thesis is ^{1}H-MRS and therefore ^{31}P-MRS (energetics) will not be covered.

1.2. CARDIAC FUNCTION

Evaluation of left ventricular (LV) function by LV ejection fraction (LVEF) is well established in various cardiac conditions, and is used for clinical decision making. In aortic stenosis (AS), LVEF is used in deciding the appropriateness of valve surgery while in heart failure LVEF is used to guide therapy for example initiation or monitoring of pharmacotherapy, and implantation of cardiac resynchronisation therapy.[22, 23] However, LVEF is not a good surrogate marker of LV function as it varies with different loading conditions. Furthermore, subtle or regional myocardial dysfunction is usually undetectable until LV dysfunction becomes more advanced.[24] In AS, myocardial hypertrophy is a compensatory mechanism in attempt to neutralise the wall stress, therefore LVEF will be preserved until far advanced in the course of the disease.[25] In dilated cardiomyopathy (DCM), subclinical LV dysfunction has been shown in familial DCM with mutation carriers who had normal LVEF.[26] Thus, more accurate measure of LV contractile function is essential for the diagnosis and monitoring therapy in patient with non-ischaemic DCM.[27]

Assessment of myocardial deformation parameters can provide better quantification of global and regional systolic function, and might have increased sensitivity in detecting subtle myocardial dysfunction. Myocardial strain is defined as relative deformation of myocardium during contraction and relaxation.[28] Strain is a dimensionless quantity of myocardial deformation defined as the change of myocardial fibre length at end-systole compared to its original length at end-diastole, **Figure 1.5**. Strain rate (SR) is the change in strain per unit time.[29] With contraction, the myocardium is compressed or shortened (negative strain), while during relaxation, the myocardium lengthens (positive strain), **Figure 1.6**. Strain can

be measured in longitudinal, circumferential and radial directions and is thought to partially reflect sub-endocardial, mid-wall and sub-epicardial myocardial fibre function respectively, **Figure 1.7**. Diastolic strain rate (i.e. the rate of LV relaxation) is a measure of diastolic function.[30] LV twist (^{0}) is a wringing motion of the LV due to opposite rotation of the base with respect to the apex during systole. Looking from the base, basal segment is anticlockwise and apical is clockwise. This is due to shortening of the obliquely oriented fibres (subendocardium and subepicardium) and shear movement between longitudinal and circumferential fibres. LV torsion represents the twist normalised by the long-axis distance of the LV (^{0}/cm).[28] LV torsion is however beyond the scope of the thesis.

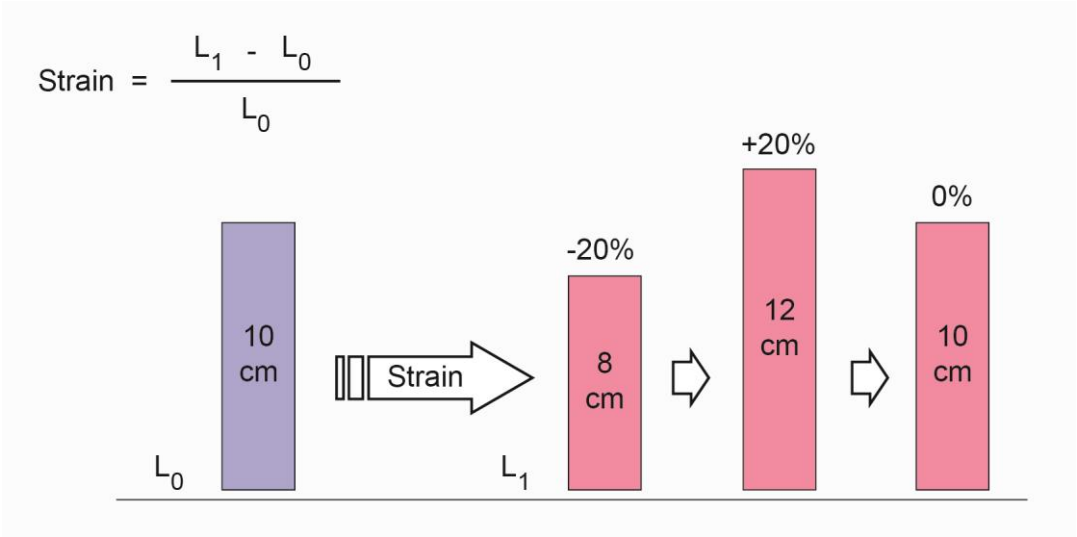

Figure 1.5. Strain is a dimensionless quantity of myocardial deformation defined as the change of myocardial fibre length at end-systole (L_1) compared to its original length at end-diastole (L_0) and is normally expressed as a percentage (Strain = L_1-L_0/ L_0)

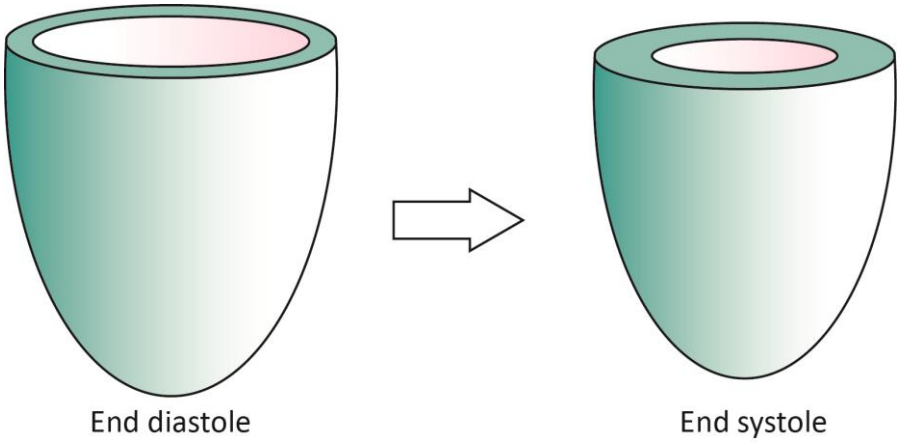

Figure 1.6. With contraction, the myocardium is compressed or shortened (negative strain), while during relaxation, the myocardium is enlarged or lengthened (positive strain).

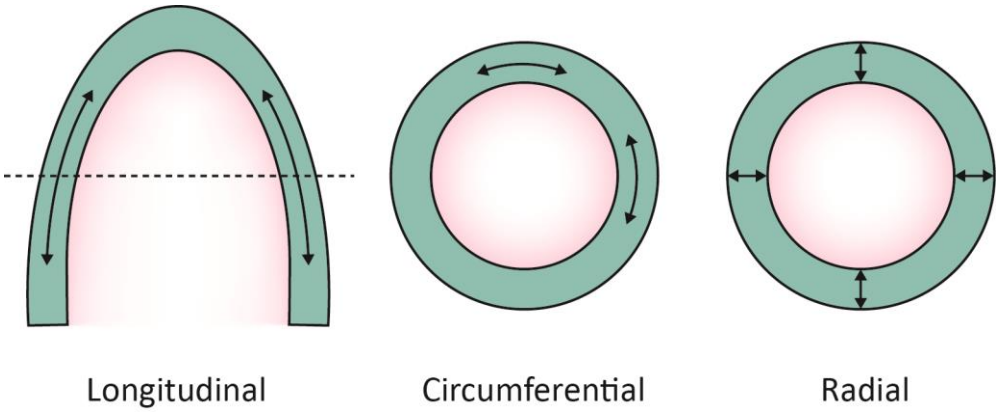

Figure 1.7. Schematic diagram demonstrating three dimensional; longitudinal (basal to apical shortening along the ventricular long axis), circumferential (circumferential shortening tangential to epicardial surface) and radial strain (myocardial thickening radially towards the centre of the ventricle).

Echocardiography with tissue Doppler imaging allows non-invasive measurement of myocardial strain but it is limited by angle dependency.[31] Tissue Doppler derived parameters are predominantly based on longitudinal and radial motion data,[32] but myocardial contraction is principally circumferential[33] and thus echo-based Doppler methods do not allow the most accurate evaluation of myocardial function. Speckle-tracking echocardiography has recently emerged as a quantitative ultrasound technique for assessment of myocardial deformation in longitudinal, circumferential and radial directions, based on tracking of speckle patterns created by interference of ultrasound beams in the myocardium, and is not angle dependent.[32, 34, 35] Myocardial strain quantification using speckle-tracking echocardiography has recently been validated against tagged MRI, and shows high feasibility and reproducibility.[36] However, limitations of this technique are dependence on good quality 2-dimensional echocardiographic images, which is essential to delineate endocardial border, and out-of-plane problem of short-axis imaging due to longitudinal motion.[35, 37] Three-dimensional speckle tracking is another approach for strain imaging but is currently limited by low temporal resolution and poor image quality when compared with 2D-STI.[27, 38]

Cardiac magnetic resonance (CMR) tissue tagging is a technique that can quantify myocardial deformation. It provides reproducible data on myocardial strain in longitudinal, circumferential and radial directions. Noninvasive markers that appear as dark lines (tags) in the acquired images follow myocardial motion during cardiac cycle, thus representing myocardial deformation. Persistent tags throughout cardiac cycle allow accurate assessment of both systolic and diastolic functions. However, due to T1 relaxation, the tag lines fade towards the end of diastole, but this can be overcome by implementing steady state free

precession (SSPP)[29] and scanning at higher field strength magnets to achieve longer tag persistence and better image quality.[29, 39] Current imaging sequences and acquisition techniques have improved temporal and spatial resolution, and shorten breath-hold durations.[28, 29] Although tagged MRI may be considered the gold standard for myocardial strain measurements, its routine use is limited by its high costs and poor availability.

In the thesis, I have focussed on only circumferential and longitudinal strain because these are the most important parameters of myocardial deformation when compared with radial strain. Myocardial contraction is predominantly circumferential, and provides ~60-70% of myocardial contraction, whereas longitudinal strain impairment is the earliest to occur. Radial strain impairment occurs relatively late, thus is less useful than circumferential or longitudinal strain.[28, 33]

1.3. OUTLINE OF THE THESIS

This is a multi-parametric CMR study to investigate cardiac metabolism and function in hypertrophied heart due to aortic stenosis (AS) and heart failure (HF) due to dilated cardiomyopathy (DCM).

1.3.1. HYPERTROPHIED HEART DUE TO AORTIC STENOSIS

AS is common, occurring in 2% of the population over 65 years of age, rising to 7% in men over 85 years.[40] AS is defined as severe when the aortic valve area (AVA) is less than 1.0 cm^2, mean gradient greater than 40 mmHg, or maximum jet velocity of greater than 4.0 m/s.[41, 42] The management of patients with severe AS is generally based on symptoms and left ventricular (LV) dysfunction. Aortic valve replacement (AVR) is the definitive treatment of symptomatic severe AS. In asymptomatic patients with severe AS, AVR is recommended if there is LV systolic dysfunction.[41, 42] The median survival without surgery in this group is 2-4 years depending on the symptoms.[43, 44]

For asymptomatic patients with preserved LV systolic function however, the management is controversial, and surgical intervention is not recommended according to current guidelines. Echocardiographic assessment of LV ejection fraction (LVEF) has a central role in clinical decision making. However LVEF is load-dependent and not considered to be a sensitive marker of systolic function, especially in the setting of LV hypertrophy (LVH).[45] Furthermore, reduced LVEF is a late development in the natural history of the disease and associated with a dismal prognosis (survival < 2 years)[46] and higher operative risk (mortality up to 50%) in those with no contractile reserve.[47] Early valve replacement exposes patients

to the risks of surgery and the ongoing risks of complications from prosthetic aortic valves. Waiting for symptoms to occur, however, risks the development of LV dysfunction and there is a small risk of sudden death.[48] Moreover, significant adverse LV remodeling is likely to occur and this may not be reversible after AVR.[49] Therefore, decision for earlier referral for AVR for asymptomatic severe AS may be beneficial. For example, a recent study identified a high risk group of "very severe asymptomatic AS" with exceptionally poor event free survival rate (3% at 6 years) as a subgroup of patients that would benefit from surgery before symptoms develop.[50] Another study showed that early surgery in patients with very severe AS (defined as AVA <0.75 and valve peak aortic velocity >4.5 m/s) is associated with improved long-term survival and decreased cardiac mortality compared to conventional management strategies in those with low operative risk.[51]

Myocardial factors currently identified as being associated with either an adverse prognosis in AS or poor recovery of the ventricle post AVR include a high degree of LVH,[52-54] a high percentage of fibrosis as measured by histology and CMR late gadolinium enhancement (LGE)[55] and reduced longitudinal strain.[56] However, metabolic changes and oxygenation in the myocardium of patients with AS have never been assessed before. The development of advanced cardiac imaging methods has enabled increasingly sophisticated assessments of myocardial metabolism, function and oxygenation to be carried out. Future challenges will be to determine whether these cardiac imaging parameters can identify changes in the myocardium of asymptomatic AS patients before irreversible myocardial damage occurs.

Thus, in addition to haemodynamic assessment of the aortic valve, a more sensitive marker of LV dysfunction (as discussed in 1.2) is needed. As elaborated in 1.1, assessment of myocardial metabolism and oxygenation can potentially be important markers to identify high risk asymptomatic AS patients to improve the timing of AVR. Importantly, myocardial metabolism and oxygenation can also be potential therapeutic targets for patients who are not suitable candidates for AVR or those who still have symptoms after AVR.

Figure 1.8 shows an example of a severe AS patient with associated LVH. Two main areas will be explored in AS:

(a) Myocardial steatosis: As discussed in section 1.1, deranged myocardial metabolism causes a switch of substrate utilisation from FA to glucose which is an adaptive response to increased hemodynamic workload. This study investigated the presence of steatosis in both asymptomatic and symptomatic severe AS, examined the relationship with cardiac function, and also whether there are changes following AVR. In a subgroup of patients, histological correlation was studied. This will be discussed in Chapter 3.

(b) Myocardial oxygenation: Cardiac myocyte hypertrophy is accompanied by reduced myocardial perfusion, even in the absence of epicardial coronary artery disease (CAD). Impaired coronary microvascular reserve is thought to be due to insufficient new blood vessels forming in pressure overload hypertrophy **(Figure 1.9)**. This study assessed whether this led to myocardial tissue deoxygenation, and changes following AVR were also examined. This will be discussed in Chapter 4.

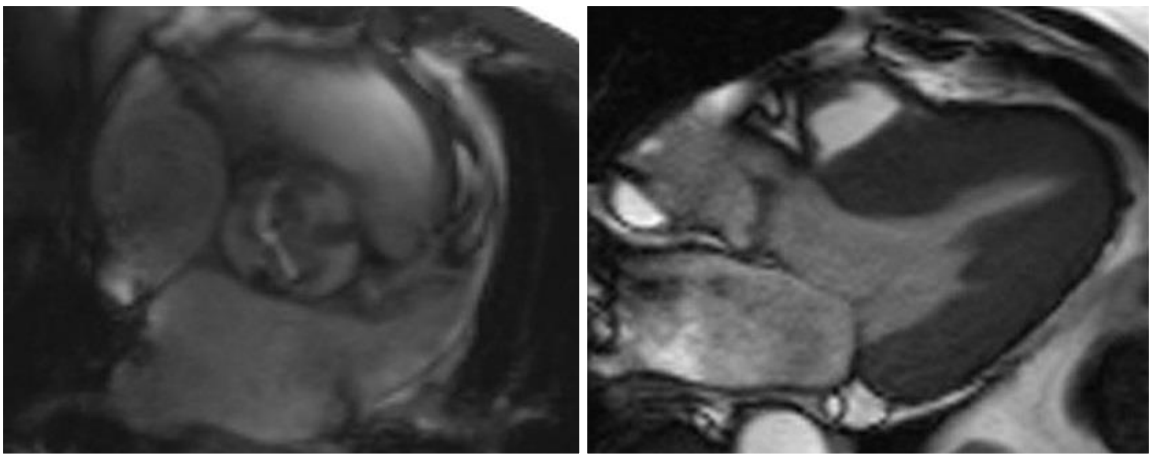

Figure 1.8: Cardiac magnetic resonance cine images showing an example of severe aortic valve stenosis (left) and associated left ventricular hypertrophy (right).

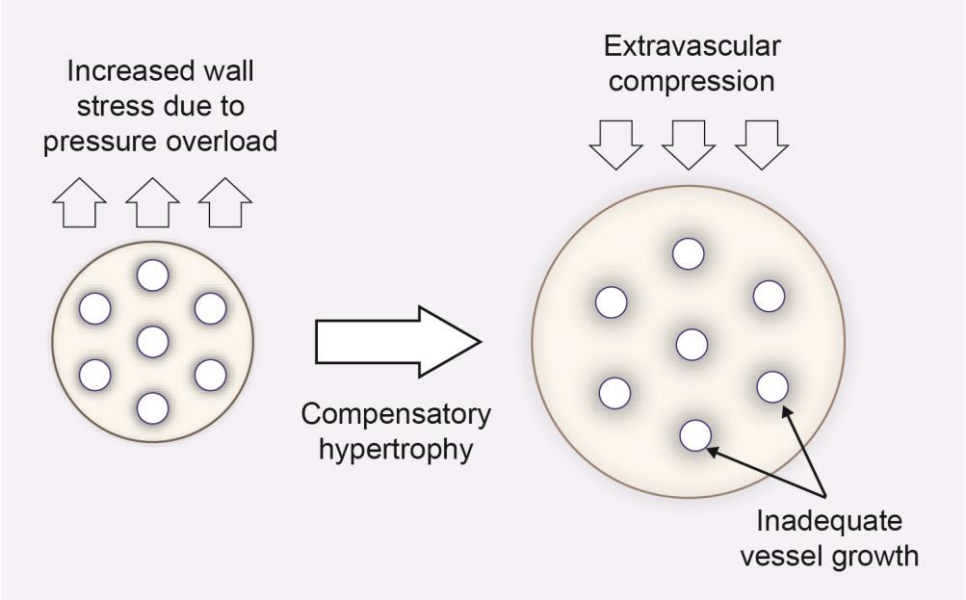

Figure 1.9 (new illustration)**.** Proposed mechanism of microvascular dysfunction in pressure overload hypertrophy. There is insufficient growth of vessels per unit myocardium leading to impaired coronary vascular reserve. Extravascular compression may also cause further impairment in perfusion.

1.3.2. HEART FAILURE DUE TO DILATED CARDIOMYOPATHY

1 to 2% of the population in developed countries has heart failure (HF).[57] Although pharmaceutical and device therapies have substantially ameliorated its prognosis, HF nevertheless reduces the quality and duration of life and exerts a substantial drain on healthcare resources.[57-59]

DCM is a primary myocardial disease characterized by LV dilatation and dysfunction in the absence of chronic increased afterload (e.g. aortic stenosis or hypertension), or volume overload (e.g. valvular incompetence).[60] DCM is the second most common cause of HF after CAD and the most common cardiomyopathy. The therapeutic aim is to treat the underlying cause but in the majority of patients, no causes is identified and (hence is called idiopathic DCM), and therefore the treatment is primarily reducing symptoms, prevention/delaying progression to HF and death.[61] Although there have been advances in the medical and surgical therapy of DCM in the last two decades, the condition still carries a very poor long-term prognosis.[62] Current medical therapy may not be tolerable by all patients due to underlying comorbidities (e.g. renal dysfunction) and side-effects (cough, hypotension and bradycardia);[59] not every patient is a suitable candidate of device therapy,[63] and heart transplantation is limited by the scarcity of the suitable organ.[64] Thus, the urgent need remains for novel, more effective HF therapies to optimise the management of patients with DCM.

Over the last 20 years, it has been proposed that HF is associated with a hyperadrenergic state that augments circulating plasma free fatty acids (FFA), which leads to impaired

glucose metabolism and insulin resistance.[65, 66] Insulin resistance inhibits uptake and metabolism of glucose which may prevent the heart from using its adaptive energy response to an insult.[67] This contributes to HF and the vicious cycle of neurohormonal activation, serving to potentiate the myocardial dysfunction and further increasing energy requirements **(Figure 1.10).** Therefore, despite a relatively higher dependence on glucose as a more efficient source of energy when compared with FA, both glucose uptake and oxidation are impaired due to persistence of myocardial insulin resistance. It has been proposed that excessive FA metabolism may also exacerbate HF by impairing myocardial calcium metabolism and increasing myocardial reactive oxygen species generation. It is therefore hypothesised that intramyocardial lipid accumulation (steatosis) may occur due to imbalance between free FA uptake and oxidation. If steatosis is indeed present, steatosis may be a potential prognostic marker and/or therapeutic target in DCM patients with HF.

Using magnetic resonance spectroscopy, it is possible to provide pathophysiological information of metabolic state of the myocardium that can be used as to guide optimal clinical management of patients with DCM. In particular, steatosis may become a potential therapeutic target using metabolic modulators. In this thesis, ^{1}H-MRS was used to assess myocardial TG content in patients with HF due to DCM.

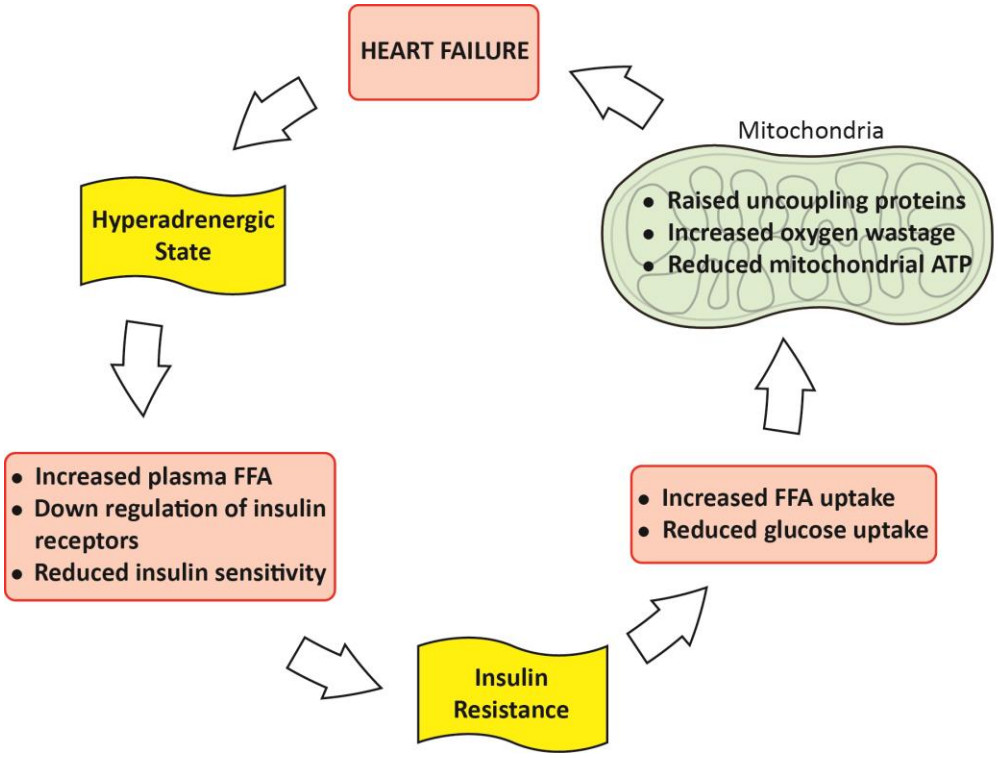

Figure 1.10 (new illustration)**.** Insulin resistance and fatty acid overload in heart failure

This thesis will therefore focus on.

(a) Myocardial steatosis in DCM: In view of impaired cardiac metabolism and insulin resistance as explained above, this study investigated if this led to cardiac steatosis, and further assessed its relation to cardiac function. Furthermore I also investigated if there was any relationship with hepatic TG content. This will be discussed in Chapter 5.

CHAPTER 2: GENERAL METHODS

2.1. OVERVIEW

This study was approved by the Mid and South Buckinghamshire Research Ethics Committee (ref: 07/H1607/66) for recruitment of AS (chapter 3 & 4) patients. For Chapter 5, subjects were participants of Syncria HF clinical trial (12 patients), GHF112670, approved by the Oxfordshire Research Ethics Committee A (10/H0707/54). Additional 8 DCM patients were derived from another project (Oxygen Supplement in HF). All subjects gave written informed consent for all study procedures.

2.2. ELIGIBILITY CRITERIA

Inclusion criteria

- Male or female, at least 18 years of age
- Willing to participate in a research study on a voluntary basis

Aortic stenosis

- Severe AS was defined as aortic valve area of <1.0 cm^2, mean gradient of >40 mmHg or maximum jet velocity of $\geq$4.0 m/s.[23, 41]
- No other significant valvular diseases
- Systolic BP <160 mmHg and diastolic BP <90 mmHg
- Normal LVEF (LVEF >50%)
- Non-obstructive CAD from invasive coronary angiography (symptomatic AS). No evidence of ischaemia from exercise test (asymptomatic AS).
  Exercise testing was chosen to exclude significant CAD in asymptomatic AS as it was not possible to obtain ethical approval for invasive coronary angiography in these patients. Alternatively, although dobutamine stress echo was a valid approach, the study was deemed too complicated to have both dobutamine and adenosine both to be performed in the same subjects. Thus, exercise testing was a safer approach in the current study, although it is possible that some potential subjects with normal coronary arteries were excluded on the grounds of false-positive exercise-induced ST depression.

Dilated cardiomyopathy

- LVEF <45%
- Non ischaemic etiology confirmed by either a coronary angiogram or a functional stress test. Patients must be on optimal anti failure therapy
- No history of liver disease or excessive alcohol intake

Healthy volunteers:

- Asymptomatic. No medical history. Not taking any medications
- Normal physical examination and ECG

Normal controls were not matched for comorbidities, therefore the data may be confounded by their comorbidities. However, to minimise this, patients were included only if their comorbidities (e.g. hypertension, dyslipidaemia) were well controlled, as shown in individual Chapters. Furthermore, where applicable, multivariate analyses will be performed to test this possibility.

Exclusion criteria

- History of significant CAD, valvular heart disease, hypertrophic cardiomyopathy, chemotherapy or pregnancy induced cardiomyopathy
- Diabetes mellitus based on history and abnormal fasting serum glucose or HbA1c.
- Previous coronary vascular intervention or cardiac surgery
- Any contraindications to MR scanning (metal implants, pacemakers, claustrophobia)
- History to suspect pregnancy *or* a positive pregnancy test
- Impaired renal function (eGFR <30 mL/min/m^2)

2.3. CLINICAL ASSESSMENT

On the day of scanning, history and physical examination were performed. History included assessment of inclusion and exclusion criteria as explained above and drug history including allergies. Physical examination included height and weight and blood pressure (BP) measurements. In addition, 12-lead electrocardiogram (ECG) was also performed.

2.4. CARDIAC MAGNETIC RESONANCE (CMR) SCAN PROTOCOLS

CMR scan protocols performed in this study included the following:

1. Cine imaging – to assess LV mass, volumes and EF.
2. Strain imaging (myocardial tagging) – to assess LV strain
3. Late gadolinium enhancement (LGE) – to assess myocardial fibrosis
4. Blood-oxygen level dependent (BOLD) and perfusion during adenosine vasodilator stress and rest - to assess myocardial oxygenation and perfusion
5. ^{1}H-magnetic resonance spectroscopy (MRS) – to assess TG content (for steatosis assessment)

2.4.1. LEFT VENTRICULAR FUNCTION

CMR is accurate, reproducible and well validated for measuring LV volumes and mass.[68] Cardiac volumes were acquired using Steady State Free Precession (SSFP) imaging as previously described.[69] Pilot, horizontal long axis, vertical long axis and short axis (SA) stack images were acquired with the patient in the supine position. Each slice was 7 mm thick with a 3mm gap and was retrospectively ECG-gated. The slices were obtained during a breath-hold at the end of normal expiration to minimise the effects of respiratory motion. LV SA epicardial (end-diastole) and endocardial (end-diastole and systole) borders were manually contoured **(Figure 2.1)** using Argus post-processing software package (Siemens Healthcare, Erlangen, Germany). LV end systolic (ESV) and end diastolic (EDV) volumes are used to calculate stroke volume (SV), ejection fraction (EF=SV/EDV). Myocardial mass is also calculated by subtracting the endocardial volume from the epicardial volume during

diastole. LV mass is calculated based on prior knowledge of myocardial specific gravity (1.05 g/cm3).[70] In addition, AVA measurement was obtained from direct planimetry of the aortic valve SSFP cine (see **Figure 1.8,** left panel, from chapter 1).

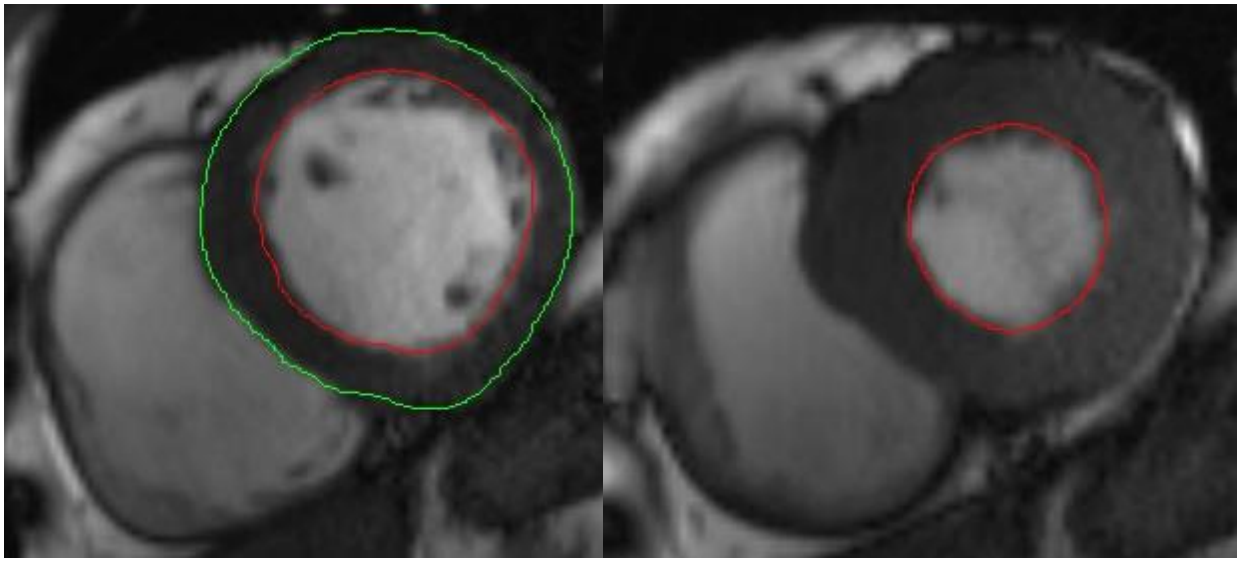

Figure 2.1: Epicardial and endocardial contours drawn in diastole (*left*) and endocardial contour in systole (*right*). Myocardial mass is calculated by subtracting the endocardial volume from the epicardial volume during diastole (*left*).

2.4.2. STRAIN IMAGING

CMR is a well validated tool for measurement of multidirectional strain using a sequence known as "tagging".[28] A gradient echo-based tagging pulse sequence was performed in the long axis and in the mid ventricular short-axis slice **(Figure 2.2)** with a segmented k-space, multi-shot sequence (repetition time 4.47ms, echo time 7.4ms, and flip angle 25^{o}).[71] Spatial modulation of magnetisation (SPAMM)[72] produced images with a grid-based pattern of horizontally and vertically modulated 'stripes' 7mm apart, acquired during a single breath hold, using a prospectively gated sequence . The temporal resolution (TR x no. of segments, 9) was 40.23 ms in all data sets, and 15–25 frames per cardiac cycle were recorded,

depending on heart rate. Tagged images were analysed using CimTag2D version 7 (Auckland Medical Research, Auckland, New Zealand). Outcome parameters measured in this study were; global mid ventricular peak systolic circumferential strain, with an example shown in **Figure 2.3**; global peak systolic longitudinal strain; circumferential diastolic strain rate and longitudinal diastolic strain rate.

A very recent study has shown that CMR tagging using the current technique has an excellent inter-study reproducibility, intraobserver and interobserver variability of strain measurements.[73] However, as the reproducibility tests were done in a different population (subjects without cardiovascular diseases), therefore repeatability in AS patients is unknown.

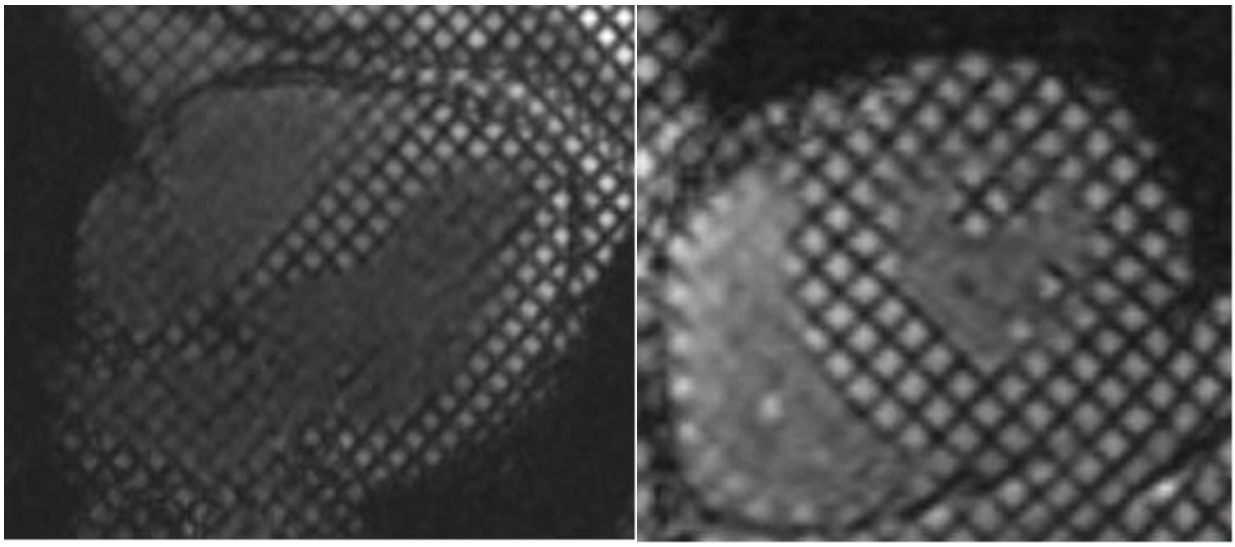

Figure 2.2. CMR tagging images of a long *(left)* and short axis *(right)* views in diastole.

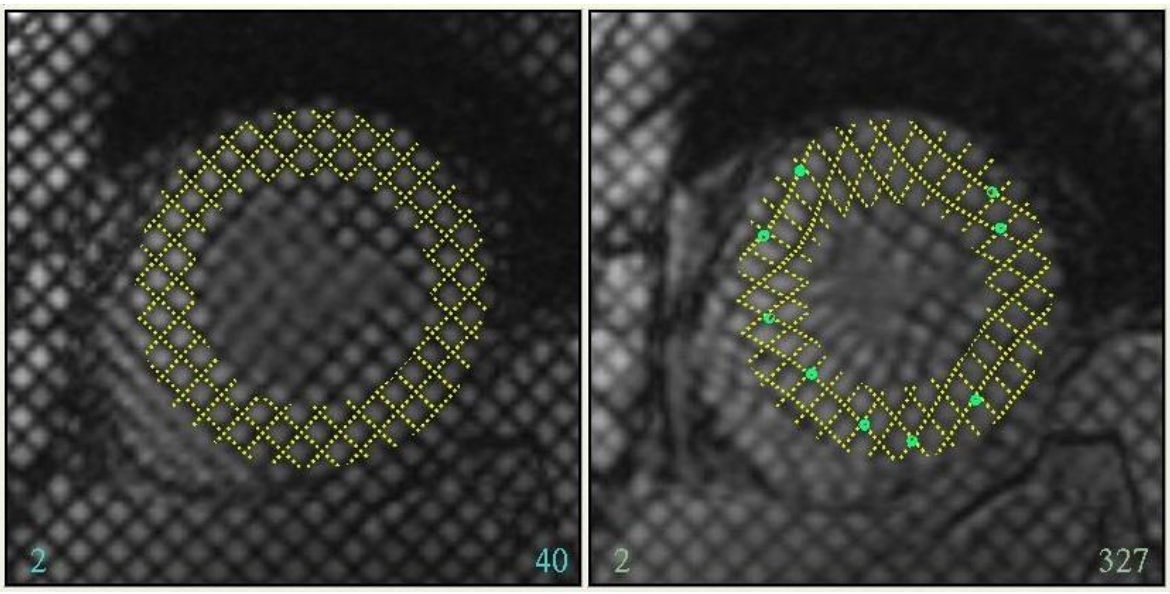

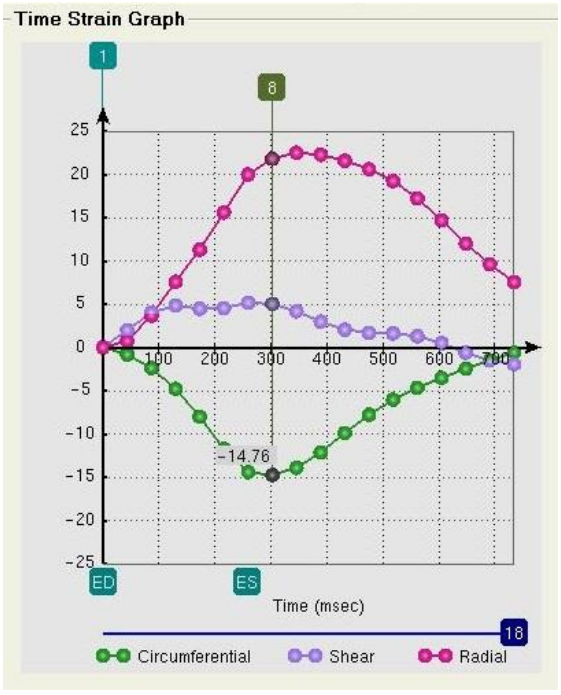

Figure 2.3. An example of CMR myocardial tagging in a short axis slice of the left ventricle. The deformation of the tags is tracked throughout the cardiac cycle (diastole, top-left and systole, top-right).

The resulting graph shows the result for average (mid-ventricular) peak circumferential strain (-14.76%), shown in green curve.

2.4.3. LATE GADOLINIUM ENHANCEMENT

LGE is the gold standard for the non-invasive measurement of regional myocardial fibrosis. Myocardial fibrosis, found in AS and DCM patients, is not only a powerful diagnostic tool, but also an independent predictor of cardiovascular events.[74, 75]

LGE imaging was acquired using a T1-weighted phase-sensitive inversion recovery sequence 5 minutes after an administration of 0.1 mmol/kg of body weight of a gadolinium-based contrast agent (Gadodiamide, Omniscan; GE Healthcare, Amersham, United Kingdom) or a top-up bolus (after rest perfusion imaging - for chapter 4) of the same dose, followed by a 15-ml saline flush were administered through an intravenous cannula inserted into the antecubital fossa. LGE was acquired earlier (at 5 minutes instead of 10 minutes) because a smaller dose of contrast was used. Some of the contrast was administered during stress perfusion and a top-up dose following rest perfusion was administered 20 minutes after the stress perfusion. The scan parameters used were: slice thickness 8 mm, flip angle 20°, Repetition time/Echo time = 3 ms/7.5 ms. Areas of LGE were visually scored as absent or present by consensus of 2 experienced operators. Absolute quantification was performed by using the full-width half maximum (FWHM) technique which uses half of the maximal signal within the fibrosis as the threshold. It was performed by manually tracing of endocardial and epicardial contours, avoiding papillary muscle and trabeculations **(Figure 2.4)**. The FWHM is the most reproducible method for quantification for quantification of fibrosis regardless of aetiology.[76] The region of interest (ROI) was drawn around hyperintensive myocardium to define maximal signal for the FWHM threshold. LGE was quantified as LGE = (LGE mass/LVM) x 100.

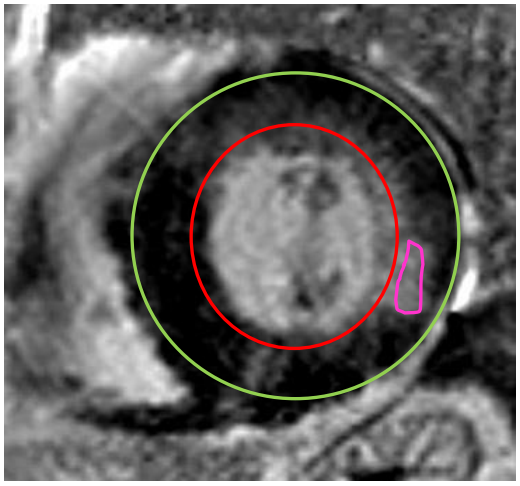

Figure 2.4.

Epicardial and endocardial borders are drawn, and a region of interest to define maximal intensity for the FWHM threshold.

2.4.4. BLOOD OXYGEND LEVEL DEPENDENT (BOLD) CMR AND PERFUSION

Study participants were instructed to avoid caffeine-containing food and drinks for at least 24 hours prior to CMR scan. For BOLD CMR, a single mid-ventricular slice was acquired using a T2-prepared ECG-gated SSFP sequence (repetition time 2.86 ms, echo time 1.43 ms, T2 preparation time 40 ms, matrix 168 x 192, field of view, 340 x 340 mm, slice thickness 8 mm, flip angle 44^0) was acquired at rest, prior to adenosine infusion and a single image of the same slice was repeated during peak adenosine stress (140µg/kg/min) typically 3 minutes after commencing adenosine. Shimming and centre frequency adjustments were performed if necessary to minimise off-resonance artefacts. Reproducibility test for BOLD imaging was not feasible in view of lack of ethical approval to repeat adenosine stress test in severe AS patients already undergoing a relatively long CMR scan protocol. Future work will involve obtaining ethical approval to perform CMR scan focussing on test-retest reliability of BOLD-CMR in these patients.

Stress first pass perfusion imaging was performed immediately after stress BOLD imaging, using a T1-weighted fast (spoiled) gradient echo sequence with saturation-recovery magnetisation preparation, as described previously.[77] A bolus of intravenous gadolinium-based contrast (gadodiamide [Omniscan; GEHealthcare, Amersham, United Kingdom]) at a dose of 0.03 mmol/kg (injection rate, 6 mL/s) followed by a saline flush of 15 mL at the same rate was given. Perfusion images were acquired in 3 SA slices at basal (between LV outflow tract and the papillary muscles), mid-ventricular (identical to the BOLD SA slice), and apical levels chosen according to recommended guidelines.[78] During adenosine infusion, study participants' heart rate and BP were recorded at 1-minute intervals. After discontinuing

adenosine, rest perfusion images were acquired at least 20 minutes after the stress study to allow sufficient contrast washout. After rest perfusion imaging, an additional bolus of 0.1 mmol/kg gadodiamide was administered (total dose: 0.16 mmol/kg). The LGE images were acquired after a 5-minute delay with the use of an inversion-recovery prepared, segmented gradient echo sequence, as previously described.[79] The inversion time was adjusted for optimal nulling of normal myocardium.

For BOLD analysis, QMass software (version 7.2, Medis, Netherlands) was used. Myocardial signal intensity was measured after manually tracing the endocardial and epicardial contours **(Figure 2.5)**. The mid-ventricular short-axis BOLD image was divided into 6 segments (inferior septum, anterior septum, anterior, anterolateral, inferolateral and inferior) according to the middle slice 6 segments of the 17-segment model. Mean signal intensities were calculated for resting and stress conditions by averaging signal measurements from images during rest and adenosine stress, respectively. BOLD signal intensity (SI) measurements were corrected for variations in heart rate between resting and stress as previously described.[80] By using Bland-Altman plot, I have performed inter-observer and intra-observer variability tests, with coefficient variations of 3% and 2% respectively, which is consistent with a previous study.[80]

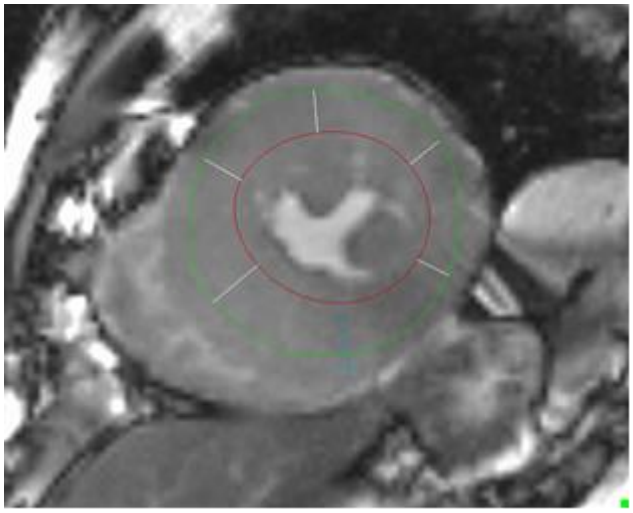

Figure 2.5

In this cardiac gated sequence, variations of heart-rate also affect the signal intensity due to its effect on T1 relaxation and the following equation was used for correction:

$$S = \frac{S_0}{1 - \beta e^{\frac{-T_R}{T_1}}}$$

S = Corrected signal intensity
β = saturation factor, e = exponential
T_1 = T1 relaxation time
S_0 = Measured signal intensity
T_R = Repetition time (replaced by R-R interval)

with T_1 =1220 ms[81] and β=0.59 (determined empirically for this sequence) where S_0 is the measured signal intensity, S is the corrected signal intensity and TR is the image dependent time between acquisitions of sections of k-space, governed by the heart rate. TR is replaced by the RR interval. The relative corrected signal intensity change was calculated as follows:

$$SI\ change\ (\%) = \frac{Mean\ SI_{stress} - Mean\ SI_{rest}}{Mean\ SI_{rest}} \times 100$$

An example of perfusion test performed during adenosine stress and rest is shown in **Figure 2.6.** Dark rim artefact is due to chemical shift artefact as a result of the difference in proton mechanics in different environment (e.g. blood and myocardium). This usually occurs both at rest and stress, and short lived. True subendocadial perfusion deficits only present during stress and persists longer, usually more than 5 heartbeats. The perfusion images were processed by tracing endocardial and epicardial contours using QMass software. A region of interest was drawn in the LV blood pool, avoiding any papillary muscles therein, to permit the derivation of an arterial input function. These 3 contours (epicardial, endocardial and LV blood pool) were drawn on a single image and propagated automatically throughout the perfusion series. The myocardium was divided into equiangular segments based on the

American Heart Association segmentation model.[78] Images were then checked for positioning and contours were manually adjusted for respiratory movement. Rest and stress myocardial perfusion upslopes were calculated using 5 point linear fit model of signal intensity vs. time and normalized to the LV blood pool upslope **(Figure 2.7)**.[82] Myocardial perfusion reserve index (MPRI) was derived for each of the 16 segments and per subject, defined as the ratio of stress to rest.

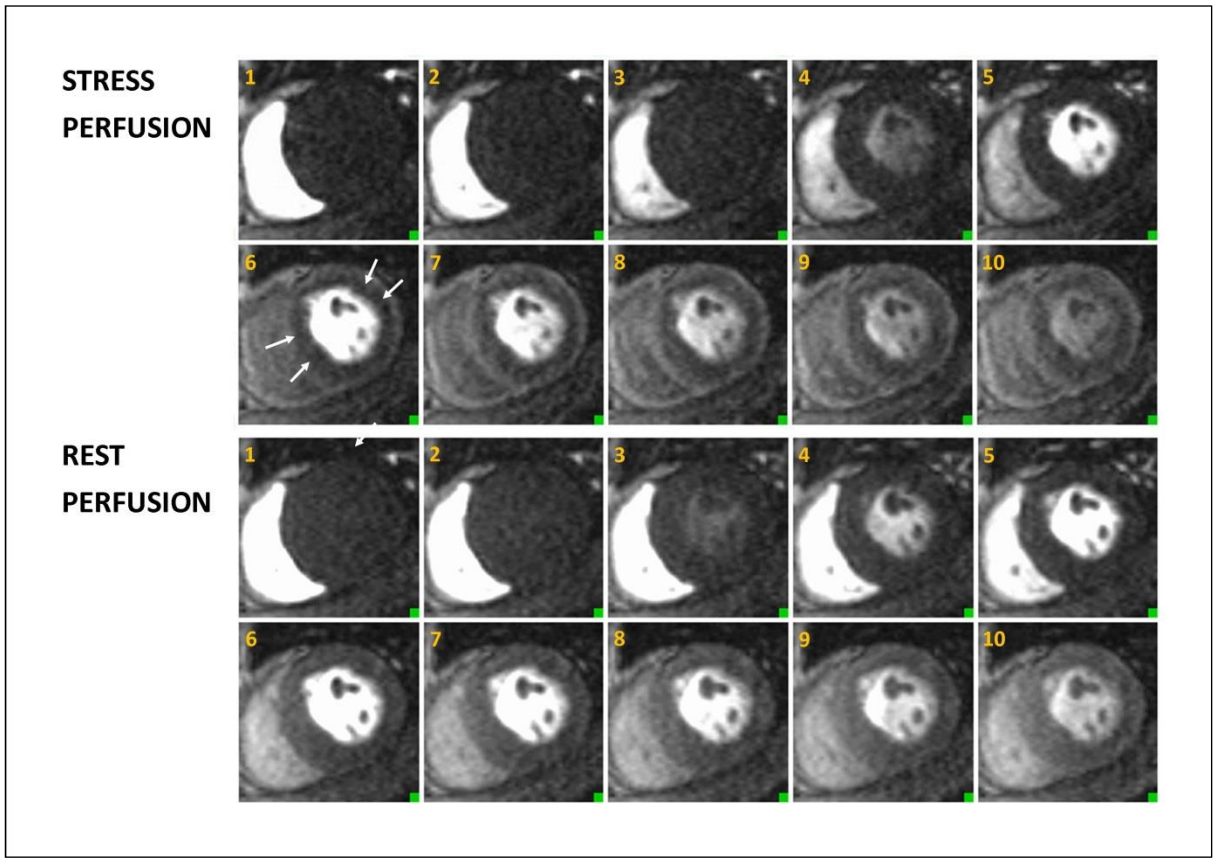

Figure 2.6. First pass myocardial CMR perfusion imaging. Series 1-10 show sequential perfusion images during adenosine stress in a patient with severe AS. Initially contrast enters the right ventricle (1-3), then left ventricle (4-5) and flushes through the myocardium (6-10). Note the circumferential perfusion defect in the stress perfusion images (dark rim shown by white arrows on image 6, upper panel, persisted until image no 10) which is not present in the rest images (lower panel).

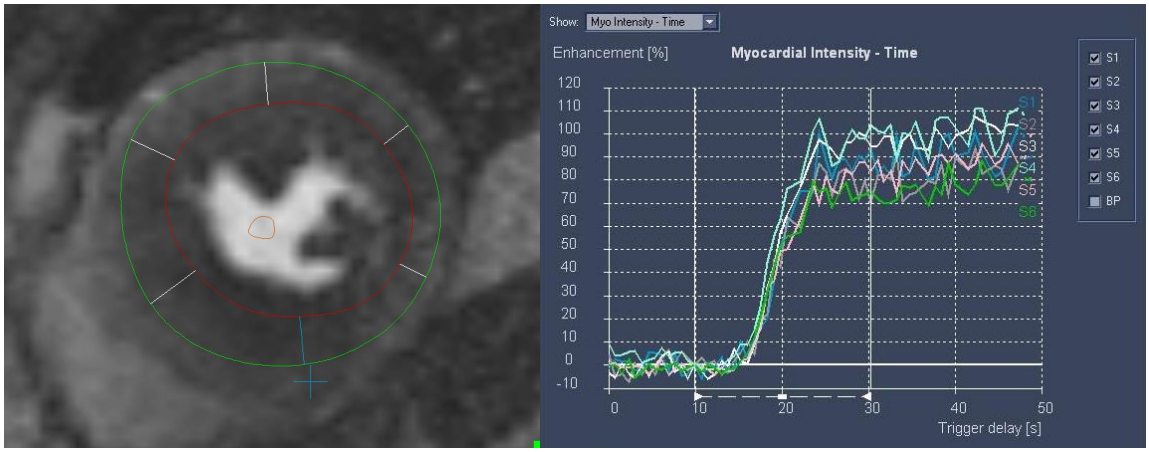

Figure 2.7. These relatively noisy SI curves are due to respiratory movement and missed triggering. To overcome this problem, manual correction of the contour, and where necessary phase deletion were performed.

2.4.5. 1H-MAGNETIC RESONANCE SPECTROSCOPY (MRS)

Recent developments in ^{1}H-MRS have demonstrated the feasibility of non-invasive myocardial lipid measurements in humans.[7, 10, 83] These methods have been validated in several body organs and animal models.[7, 84] They allow for the measurement of lipid (based on the specific resonance of methylene -CH_2) as a percentage of water signal in the same region of myocardium and also is able to distinguish between extracellular and intracellular lipids.[10] Technical challenges in the development of ^{1}H-MRS include low signal-noise ratio (SNR) due to low absolute metabolite concentrations, achieving adequate water suppression and long distances from the radio-frequency (RF) coils. Furthermore, increasingly at higher field strength, investigators must contend with shimming artefacts and field inhomogeneities. Some techniques have focused on respiratory navigation to minimise breathing artefacts, however our research group has recently validated an ECG gated breath-hold technique with excellent reproducibility.[85] The development of this rapid breath hold acquisition has rendered the measurement of myocellular lipid eminently feasible in a clinical research setting, however other metabolites (e.g. creatine) with lower concentrations remain require further validation.[85]

^{1}H-MRS was performed on a 3 T Siemens Tim Trio using the whole body coil and the 6-channel anterior and 24-channel posterior phased-array coils for signal receiving. Mid-ventricular long and SA cine were acquired to determine the trigger delay for mid-diastole. A calibration pulse sequence was implemented to evaluate the optimal water suppression pulse scaling factor. Cardiac gated spectra were acquired using different water correction scaling factors and the one yielding the most effective water-suppression was chosen. A

22x18x32 mm stimulated echo acquisition mode (STEAM) voxel was planned on the corresponding cine frame **(Figure 2.8).** A water spectrum (3 averages; repetition time [TR] of at least 4 s) was acquired in a single breath-hold to use as internal reference. Next, five to six water-suppressed scans (5 averages each; TR of at least 2 s) were acquired at mid-diastole in a series of single breath-holds. Reproducibility test was not feasible in the current work due to time constraint of the AS patients to have another MRI scan prior to their AVR. Although previous work has shown that the technique shows excellent reproducibility, it was done in healthy volunteers, and without repositioning the voxel.[85] Future work will involve performing a repeatability ^{1}H-MRS test in AS patients, and by rescanning them after they have come out completely from the scanner.

Individual coil signals were combined within Matlab using specially written modules. The water-suppressed scans were constructively averaged, including frequency correction. Spectra were quantified using the Advanced Method of Accurate, Robust and Efficient Spectroscopic (AMARES) fitting algorithm. Metabolite peaks (including lipids/TGs) were analyzed and prior knowledge was used for all peak locations by using soft constraints. All peaks were fitted using Lorentzian lineshapes.[85] As ^{1}H-MRS analysis has no subjective element to it and is not operator dependent, inter-observer and intra-observer variability tests were not performed.

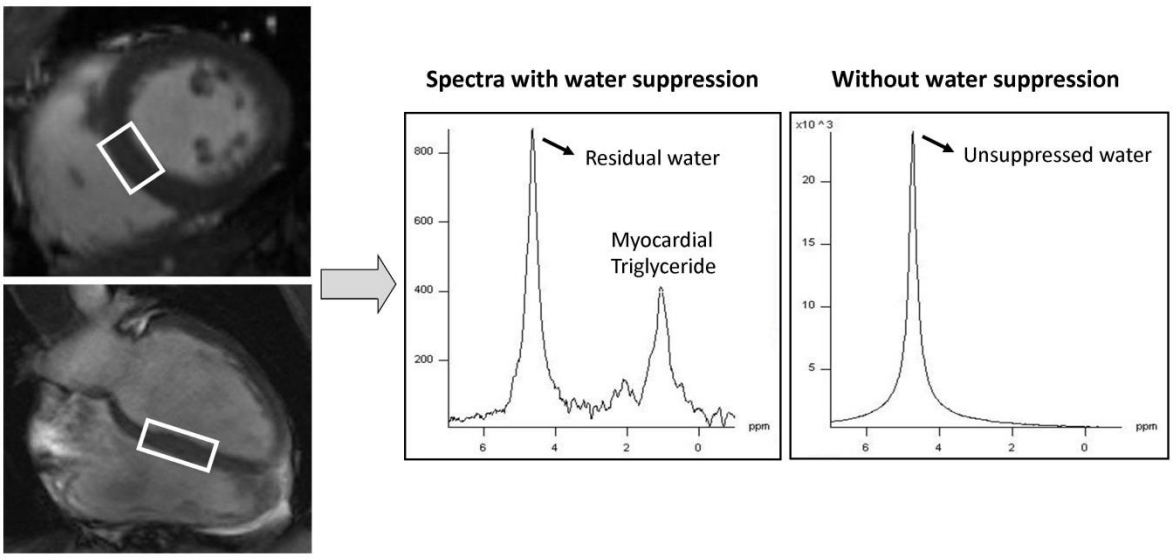

Figure 2.8. Spectra were acquired from the interventricular septum to avoid contamination from the epicardial fat. Spectra with water suppression were obtained and spectra without water suppression were used as internal reference. Myocardial lipid was calculated as a percentage of the lipid peak to the water peak.

Please note that biopsies were taken through the LVOT, therefore the LV septum should be easily accessible. However, there may also be sampling errors where samples are taken from the anterior septum resulting in inconsistencies between spectroscopic measurement and histological findings. This can happen as there were multiple surgeons involved.

To obtain hepatic ^{1}H-MRS, an 8-ml voxel (2x2x2cm) was positioned in the liver, avoiding gross vascular structures and adipose tissue depots. Both spectra with and without water suppression were obtained to calculate hepatic TG content as a percentage relative to water (triglyceride/water x 100), see **Figure 2.9.**[86]

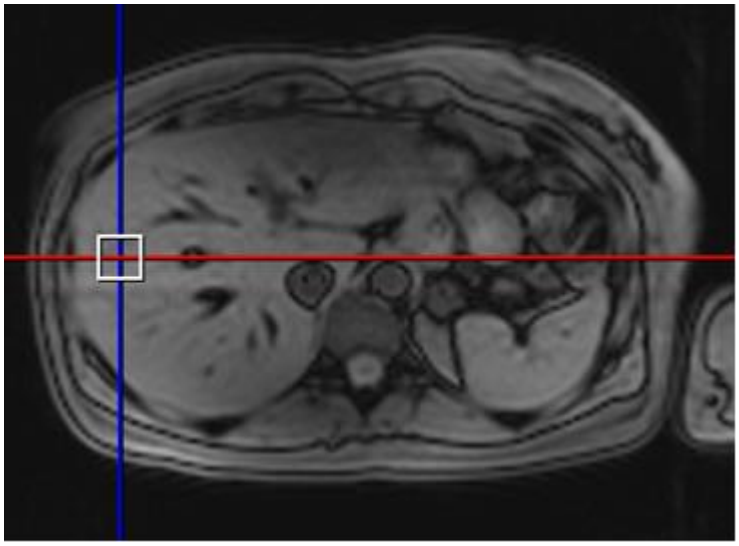

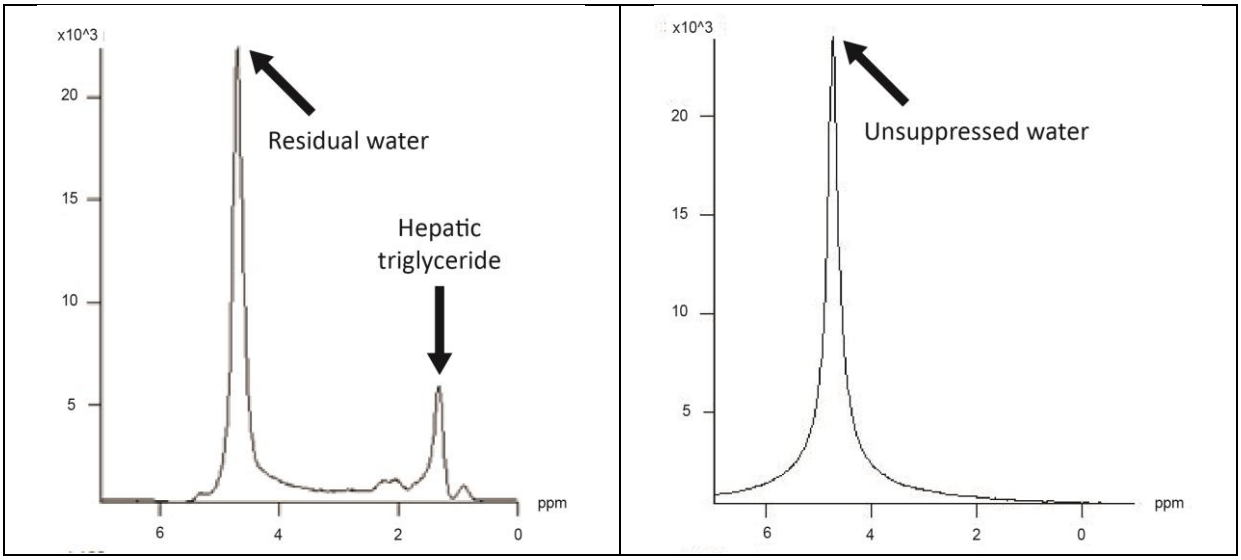
x10^3
20
15
10
5
Residual water
Hepatic
triglyceride
ppm
6
4
2
0
x10^3
20
15
10
5
Unsuppressed water
ppm
6
4
2
0

Figure 2.9.

CHAPTER 3: MYOCARDIAL STEATOSIS AND LEFT VENTRICULAR CONTRACTILE DYSFUNCTION IN PATIENTS WITH SEVERE AORTIC STENOSIS

3.1. ABSTRACT

Background: AS leads to LVH and LV dysfunction. Previous studies have shown that the hypertrophied heart, such as in AS, undergoes a shift in substrate utilisation, with a preference to glucose metabolism and down regulation of FA oxidation. We hypothesised that cardiac steatosis is involved in the pathophysiology, and also assessed whether it is reversible post AVR.

Methods and results: Thirty-nine severe AS patients (symptomatic=25, asymptomatic=14) with normal LVEF and no significant CAD and 20 age- and gender-matched healthy controls underwent cardiac ^{1}H-MRS and imaging for the determination of steatosis (myocardial triglyceride content - MTC) and cardiac function including circumferential strain (measured by MR tagging). Strain was reduced in both symptomatic and asymptomatic AS (-16.4±2.5% and -18.1±2.9% respectively vs. controls -20.7±2.0%, both $p<0.05$). Myocardial steatosis was found in both symptomatic and asymptomatic AS patients (0.89±0.42% and 0.75±0.36%, respectively vs. controls 0.45±0.17, both $p<0.05$). Importantly, multivariable analysis indicated that steatosis was an independent predictor of impaired LV strain. Spectroscopic measurements of MTC correlated significantly with histological analysis of lipids from biopsies obtained during AVR. At 8.0±2.1 months after AVR, steatosis and strain had recovered towards normal.

Conclusions: Pronounced myocardial steatosis is present in severe AS, regardless of symptoms, and is independently associated with the degree of LV strain impairment. MTC measured by MRS correlates with histological quantification of lipids. Steatosis and strain impairment are reversible after AVR. Our findings suggest a novel pathophysiologic

mechanism in AS, myocardial steatosis, which may be amenable to treatment, thus potentially delaying onset of LV dysfunction.

3.2. INTRODUCTION

AS is characterised by pressure overload of the LV, resulting in compensatory LVH. Under normal conditions, excess FAs are sequestered as TGs and stored in adipocytes as lipid droplets, with a small amount also stored in non-adipose tissues such as the myocardium, where levels are tightly controlled.[87] However, there is increasing evidence implicating altered myocardial substrate utilisation and consequent excessive TG accumulation (steatosis) in myocardial disease.[11, 87] Previous studies have assessed the presence of myocardial steatosis using MRS, and examined its functional associations in obesity, impaired glucose tolerance, type 2 diabetes mellitus and in normal individuals when subjected to prolonged exercise and diet restrictions.[18, 88-90] These studies have shown that myocardial triglyceride content (MTC) can be an independent predictor of both systolic and diastolic function, implying a causal relationship between steatosis and such functional changes. Measuring MTC is difficult however, and while myocardial biopsy is the gold standard, it is invasive and unsuitable as a routine diagnostic test. ^{1}H MRS is a noninvasive technique that can be used to quantify MTC *in vivo,*[10, 83] and may be more suitable for routine diagnosis.

To date, no MRS studies have assessed the presence of steatosis and its relationship to indices of myocardial function in patients with AS. Although LVEF is the most commonly used method to assess myocardial function, it is not a sensitive measure of systolic dysfunction in AS.[29] In contrast, myocardial strain is a measure of myocardial deformation which represents an index of contractility,[25, 91] and has been shown to be impaired in AS despite normal LVEF.[25] Myocardial strain can be measured using noninvasive CMR tagging.

Therefore, the purpose of the present study was threefold: First, to assess whether myocardial steatosis is present in patients with severe (both symptomatic and asymptomatic) AS, by measuring MTC using ^{1}H-MRS, validated against histological analysis. Secondly, to study the association between steatosis with myocardial strain as assessed by MR tagging, to test if steatosis independently predicts myocardial dysfunction. Thirdly, to evaluate changes in cardiac steatosis and strain after AVR, to test for reversibility of steatosis and strain changes.

3.3. METHODS

Study population

Thirty-nine patients with isolated severe AS (25 symptomatic, 14 asymptomatic) were prospectively recruited. Symptomatic patients were being worked-up for AVR and had unobstructed coronary arteries on coronary angiography. The 14 asymptomatic patients (as judged by their treating physician) also had an exercise stress test to confirm the absence of symptoms. Twenty healthy volunteers of similar age and gender served as controls. Eligibility criteria for all participants are detailed in Chapter 2.

Study protocol

All study subjects underwent CMR scanning at 3T as follows;

1. Cine imaging to measure LV function, mass and volume
2. Tagging CMR to assess LV strain
3. Late gadolinium enhancement to assess fibrosis
4. ^{1}H-MRS to quantify myocardial lipidosis

Details of CMR and MRS protocols and analysis are described in Chapter 2. In addition, all subjects had transthoracic echocardiography which was performed using a Philips iE33 echocardiographic system (Philips Medical Systems, The Netherlands). Measurements of peak aortic valve gradient and LV diastolic function were performed according to the guidelines of the American Society of Echocardiography.[92] The following diastolic indices

were obtained; transmitral early (E) and late (A) diastolic velocities, deceleration time (DT), mitral annular (septum) early (E') diastolic velocity, with calculation of E/E' ratio.

In addition, venous blood was drawn for non-esterified fatty acids (NEFA), which is a measure of free FA, and for other routine laboratory parameters. Within the subsequent 2-8 weeks, AVR was performed on the 25 patients with symptomatic AS. For patients who consented for tissue biopsies and where it was technically feasible, endomyocardial biopsies were taken intraoperatively from the LV outflow tract. To minimise sampling inaccuracies, biopsies were taken from the LV septum where spectroscopic measurements were acquired. The samples were sent to the histopathology laboratory for lipid analysis. Patients who had AVR had a repeat MRI scan 6-12 months (mean 8.0±2.1 months) after AVR.

Histological analysis of endomyocardial biopsy

Fresh biopsies were immediately placed in normal saline and sent to the pathology laboratory for lipid analysis. One section of the heart tissue was frozen and subsequently stained with oil red O (ORO) for lipid staining[93] and another section was placed in formalin and stained with haematoxylin and eosin (H&E). Semiquantitive analysis of lipids was performed by a pathologist who was blinded to the results of lipid content obtained from MRS measurements. Lipid deposition was graded as: (0) no positive staining, (+1) scanty ORO-positive droplets and (+2) extensive ORO-positive droplets according to previously published criteria.[93] Interobserver and intraoberver variability results are not known as these were not performed in the current study. However, in a recent study using this

technique in the myocardial tissue of obese mice shows excellent interobserver variability, r=0.94, p<0.001.[94]

3.4. STATISTICAL ANALYSIS

All data are expressed as mean ± standard deviation and were checked for normality using Kolmogorov–Smirnov test. Categorical data are presented as numbers and percentages. Comparisons between the 3 groups were performed by one-way analysis of variance (ANOVA) with post hoc Bonferroni corrections. The chi-square test or Fisher's exact test was used to compare discrete data as appropriate. Bivariate correlations were performed using Pearson's or Spearman's method as appropriate. Multivariable linear regression analysis was used to identify independent predictors of systolic strain and diastolic strain rates. To generate the multivariable models, only those variables with significant correlations on bivariate analyses were entered as covariates. Categorical variables were directly entered as independent variables in the multivariate model, and there were no adjustments needed as all the categorical variables in the study are dichotomous.[95] Comparisons between pre- and post-AVR measurements in AS patients were performed with paired two-tailed Student *t*-test. Comparisons between AS patients and controls at baseline and post-AVR were performed using Student *t*-test or Mann-Whitney U test as appropriate. A *P*-value <0.05 was considered significant. All statistical analyses were performed with IBM SPSS Statistics, version 19.

3.5. RESULTS

Baseline Study Characteristics

Demographic, clinical, echocardiographic and biochemical data are shown in **Table 1.** Recruitment for severe asymptomatic AS data are shown in **Figure 3.1**. There were no significant differences in age, gender, body mass index, BP and heart rate among study groups. Blood glucose and biochemical lipid parameters were similar across all groups. Liver function results were normal in all study subjects.

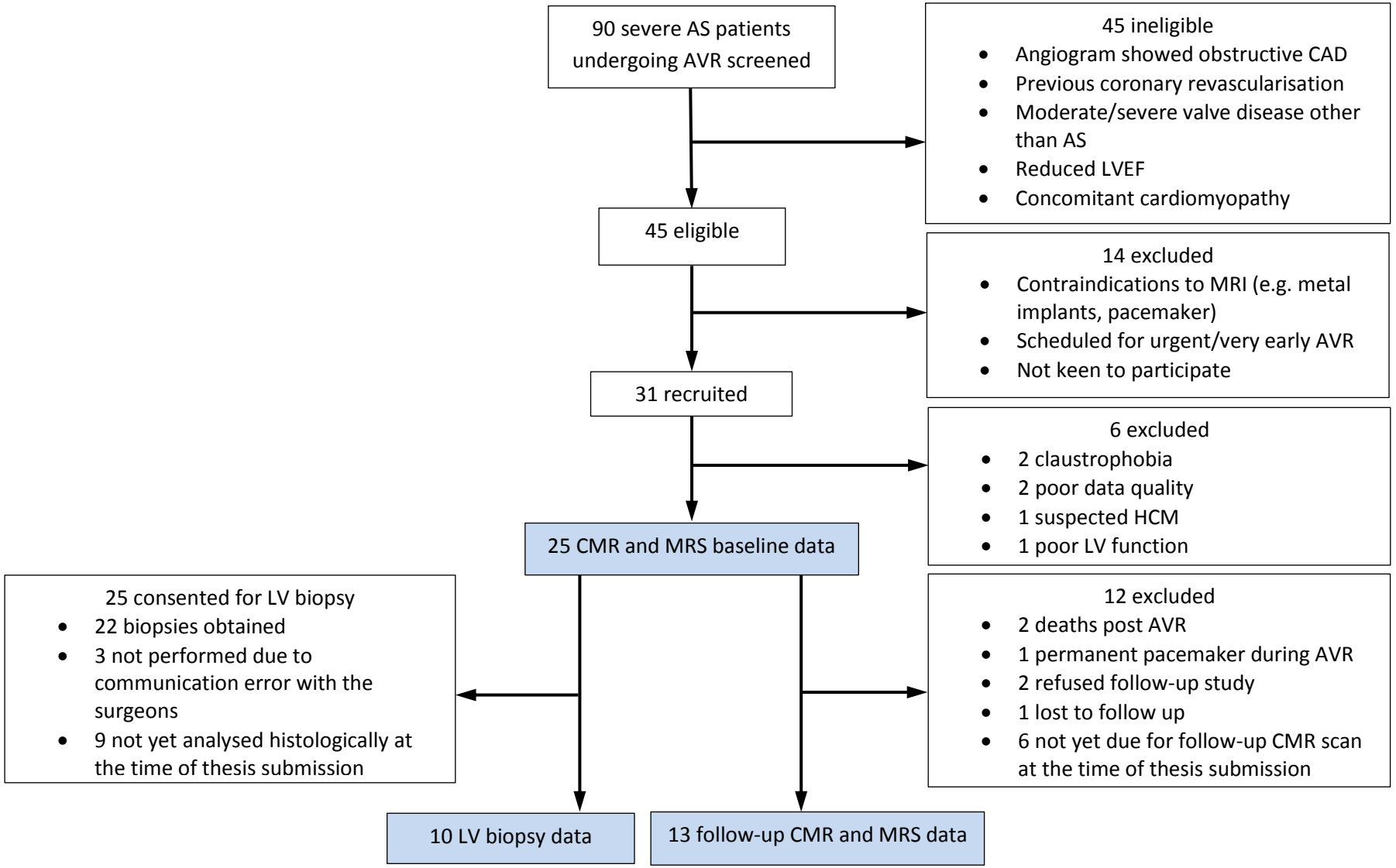

Figure 3.1. Recruitment data for severe symptomatic aortic stenosis

Table 1: Clinical and echocardiographic characteristics

	Severe Aortic Stenosis		Normal Controls (n = 20)	P value[¶]
	Symptomatic (n = 25)	Asymptomatic (n = 14)		
Age (years)	68±10	63±16	63±4	0.09
Male, n (%)	16 (64)	11 (78)	12 (60)	0.15
Symptoms, n (%)				
Dyspnoea	19 (80)	–	–	
Angina	7 (28)	–	–	
Syncope	1 (4)	–	–	
Past medical history, n (%)				
Hypertension	9 (36)	3 (21)	–	
Diabetes	6 (24)	–	–	
Dyslipidaemia*	6 (24)	2 (14)	–	
Medications, n (%)				
Beta blockers	4 (16)	–	–	
ACE-I/ARB-II	9 (36)	5 (36)	–	
Statin	11 (46)	3 (21)	–	
Body mass index (kg/m^2)	28±4	27±4	26±4	0.14
Systolic BP (mmHg)	134±17	134±18	130±12	0.66
Diastolic BP (mmHg)	75±9	76±8	76±8	0.70
Heart rate (bpm)	67±10	65±13	62±9	0.43
Echocardiograpy				
Peak AV gradient (mmHg)	81±14	74±14	–	0.14[‡]
E-wave deceleration (ms)	273±109	255±108	210±43	0.15
E/A ratio	0.8±0.4	0.9±0.3	0.9±0.3	0.22
E/E' ratio	15.1±5.1*	12.6±5.4†	9.2±2.7	0.001
Biochemical, mmol/L				
Blood glucose, mmol	5.6±1.7	5.3±0.5	5.1±0.9	0.36
NEFA	0.6±0.3	0.6±0.1	0.5±0.3	0.20
Triglycerides	1.3±0.8	1.2±0.5	1.0±0.3	0.58
Low-density lipoprotein	2.8±1.2	3.1±0.2	3.3±0.9	0.10
High-density lipoprotein	1.4±0.4	1.5±0.3	1.5±0.4	0.83

Values are mean ± SD or percentages.
[¶]P-values are for one-way analysis of variance (ANOVA) for all groups unless specified.
*P (with post hoc Bonferroni correction) <0.05 vs. normal and >0.05 vs. asymptomatic severe AS.
†P (with post hoc Bonferroni correction) >0.05 vs. normal.
[‡]P-value is student *t* test for symptomatic vs. asymptomatic aortic stenosis.
ACE indicates angiotensin-converting enzyme-inhibitors; ARB, angiotensin-receptor antagonist-II; AV, aortic valve; A, atrial contraction; BP, blood pressure; E, early diastolic filling phase; E', mitral annular velocity; NEFA, non-esterified fatty acids. *Dyslipidaemia was defined as abnormal fasting serum lipid levels, or diagnosis made by their treating physicians.

Assessment of left ventricular mass and function

CMR results for LV volumes and function results are summarised in **Table 2**. As anticipated, AS patients had significantly higher LV mass index (LVMI) and increased LV wall thickness, and high normal LVEF when compared to the normal controls. Systolic circumferential strain and longitudinal strain were impaired in asymptomatic AS patients and further deteriorated in symptomatic AS.

Table 2: Cardiovascular MRI and spectroscopy

	Severe Aortic Stenosis		Normal Control (n = 20)	P value[¶]
	Symptomatic (n = 25)	Asymptomatic (n = 14)		
Lipid/water ratio (%)	0.89±0.42*	0.75±0.36[†]	0.45±0.17	<0.001
Circumferential strain (%)	-16.4± 2.5*	-18.1±2.9[†]	-20.7±2.0	<0.001
Longitudinal strain (%)	-12.6±2.0*	-13.2±2.9[†]	-16.6±1.6	<0.001
Circumferential diastolic SR (s^{-1})	56±13*	59±12[†]	76±12	<0.001
Longitudinal diastolic SR (s^{-1})	43±12*	40±14[†]	54±12	0.006
LV ejection fraction (%)	75±5*	73±8[†]	69±4	0.003
LV end-diastolic volume (ml)	137±47	143±27	143±28	0.69
LV end-systolic volume (ml)	35±19	39±16	45±11	0.15
LV mass index (g/m^2)	94±33*	94±29[†]	54±13	<0.001
LV wall thickness (mm)	16±2*	15±3[†]	9±1	<0.001
LGE present, n (%)	20 (80)[‡]	9 (64)	2 (10)	<0.001
Aortic valve area (cm^2)	0.83±0.12	0.86±0.14	-	0.47[χ]

Values are mean ± SD or percentages.
[¶]P values are for one-way analysis of variance (ANOVA) for all groups unless specified.
*P (with post hoc Bonferroni correction) <0.05 vs. normal and >0.05 vs. asymptomatic severe AS,
†P (with post hoc Bonferroni correction) <0.05 vs. normal.
[‡]P (with post hoc Bonferroni correction) <0.05 vs. asymptomatic severe AS and normal.
[χ] P-value is student *t* test for symptomatic vs. asymptomatic aortic stenosis.
LV indicates left ventricular; LGE, late gadolinium enhancement; SR, strain rate.

Assessment of left ventricular diastolic function

Tagging MR results showed that circumferential and longitudinal diastolic strain rates were also impaired in AS when compared to normal volunteers. Echocardiographic parameters showed that there was a stepwise increase in E/E' ratio with the greatest increase seen in the symptomatic AS group, whereas E/A ratios were similar in all the study groups **(Table 1).**

Assessment of myocardial fibrosis using late gadolinium imaging

LGE was analysed qualitatively in this chapter. Areas of LGE were identified in the majority of patients with severe AS, with the greatest prevalence in symptomatic AS (80%) versus 64% in the asymptomatic group. The predominant pattern of LGE was patchy, involving mainly the basal inferior and infero-lateral walls. For comparison, only 10% of control subjects had LGE, which was only seen in the left/right-ventricular insertion points. None of the subjects had any evidence of previous myocardial infarction.

Measurement of steatosis using ^{1}H-MRS

Patients with severe AS had significantly higher MTC than controls, with the highest level in the symptomatic AS patients (nearly two-fold) and a lesser, but also significant, 67% increase in the asymptomatic group. As diabetes was only present in the symptomatic AS patients, we further explored the relationship between MTC and diabetic status, and serum glucose. There were no significant correlations were found between MTC and these variables (results not shown), suggesting that diabetes was not a confounding variable of steatosis in the AS cohort.

When comparing AS patients with and without LGE, those with LGE had higher MTC compared to those without: 0.82±0.44% vs. 0.56±0.28 respectively, p=0.016. Patients with LGE had significantly higher LVMI, and impaired systolic strain and diastolic strain rates in both circumferential and longitudinal directions (all p<0.05), despite similar aortic valve area and peak aortic valve gradient (p>0.05; results not shown).

^{1}H-MRS vs. histological analysis

Biopsy samples from 10 patients* with severe AS were available for analysis. There was a significant correlation between MTC and the number of positive staining ORO myocytes (r_S=0.66, p=0.036). There was also an inverse correlation between the number of ORO staining myocytes and circumferential systolic strain (r_S=-0.79, p=0.01), **Figure 3.2.**

*****Although there are 22 samples available, only 10 samples were analysed as the pathologist who was in charge had only analysed 10 samples before leaving. The replacement pathologist was not available to analyse the rest of the samples at the time the thesis was written.

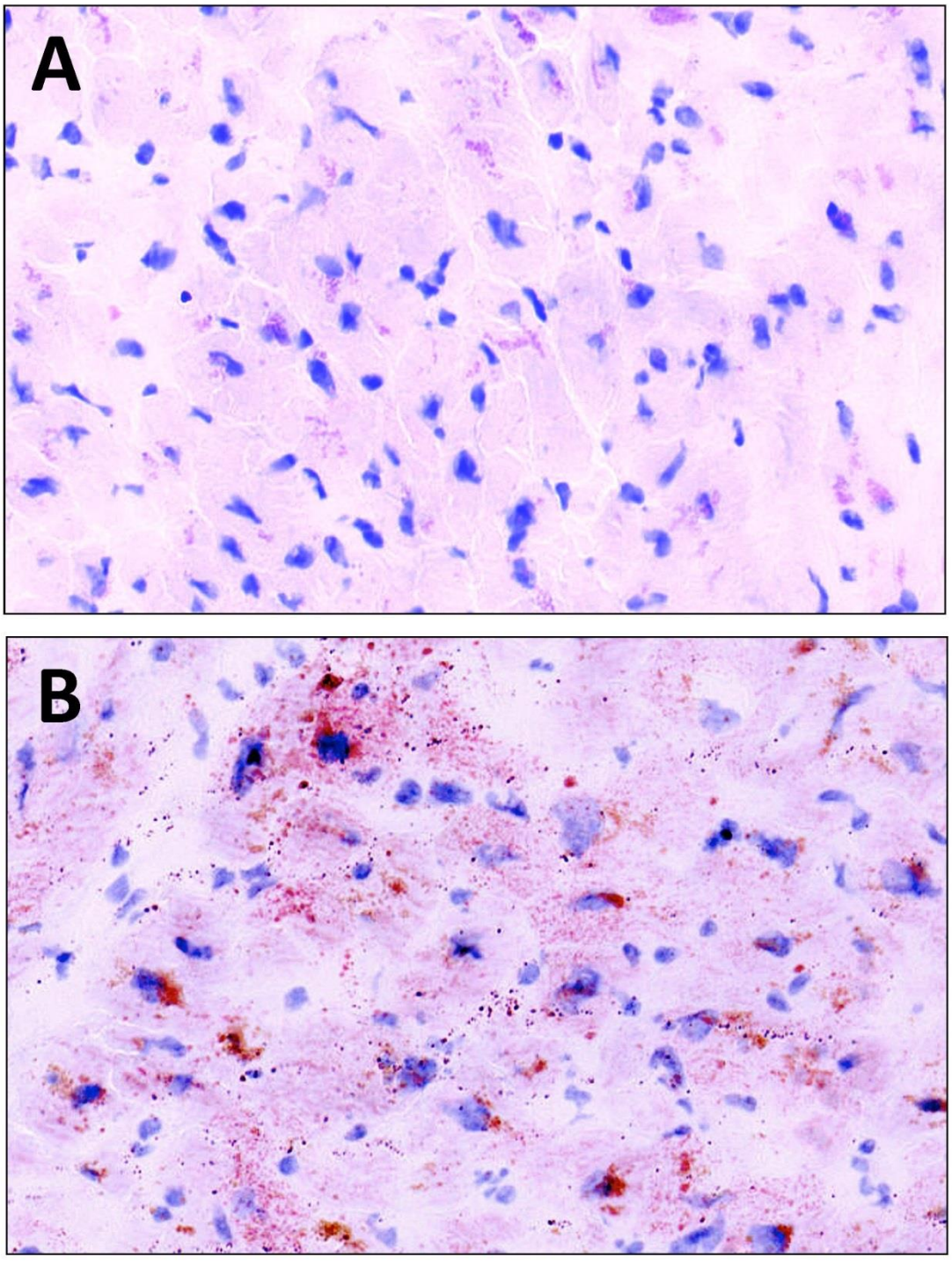

Figure 3.2. Representative photomicrographs showing Oil Red O (ORO) staining in low **(A)**, and high **(B)** myocardial lipid deposition (appears as red spots) from left ventricular septal biopsies of two patients with severe aortic stenosis. Lipid/water ratios for these patients were 0.30 and 1.10, respectively.

Association between parameters of systolic function and other study variables

Peak circumferential and longitudinal strains represented CMR parameters of LV systolic function. **Table 3**, **Figure 3.3 (a) and (b)** show bivariate Pearson correlations**,** and multiple regression analysis of circumferential and longitudinal strain with several parameters in all study subjects. Steatosis (MTC) and LGE were independent predictors of circumferential strain, whilst steatosis and LVMI were independent predictors of longitudinal strain.

Table 3: Associations of multiple study parameters with circumferential and longitudinal systolic strain

	Circumferential strain				Longitudinal strain			
	Bivariate		Multivariate		Bivariate		Multivariate	
	R	P-Value	β	P-Value	R	P-Value	β	P-Value
Age	0.11	0.41	–	–	-0.10	0.45	–	–
Diabetes	0.29	0.03	0.16	0.15	0.23	0.09	–	–
Hypertension	0.19	0.15	–	–	0.22	0.10	–	–
Dyslipidaemia	0.12	0.35	–	–	0.23	0.09	–	–
Body mass index	0.16	0.21	–	–	0.20	0.14	–	–
Aortic valve area	-0.07	0.64	–	–	0.30	0.57	–	–
Peak aortic valve gradient	-0.05	0.73	–	–	-0.13	0.49	–	–
Left ventricular ejection fraction	0.11	0.43	–	–	0.14	0.33	–	–
Left ventricular mass index	0.45	0.001	0.07	0.96	0.53	<0.001	0.33	0.023
Late gadolinium enhancement	0.54	<0.001	0.35	0.01	0.41	0.002	0.05	0.74
Lipid/water ratio	0.55	<0.001	0.41	0.003	0.51	<0.001	0.35	0.015

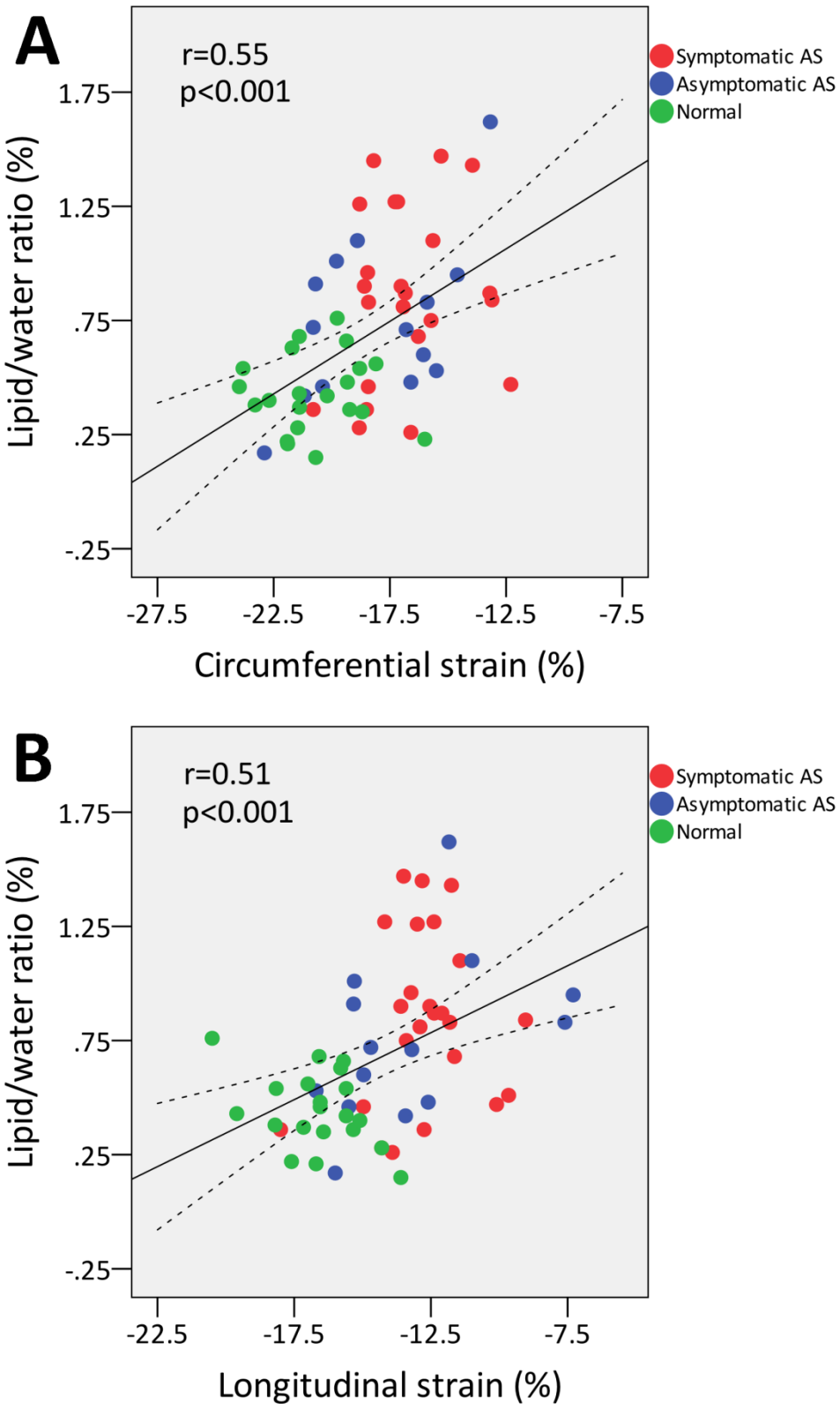

Figure 3.3 (a). Correlations between lipid/water ratio and **(A)** peak circumferential strain, **(B)** peak longitudinal strain.

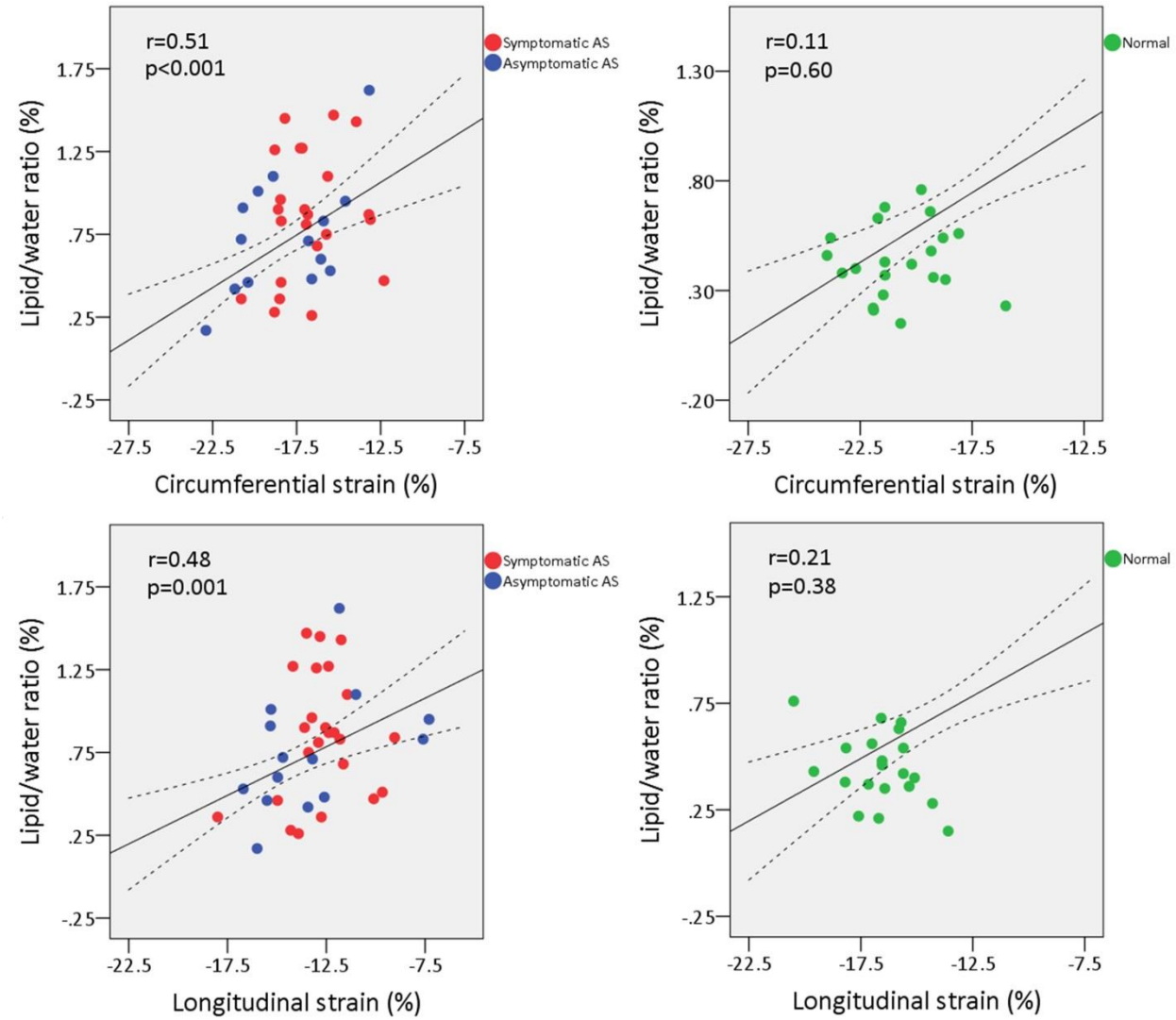

Figure 3.3 (b). Correlations between lipid/water ratio and strain in both AS patients (left hand panel) and controls (right hand panel).

Association between parameters of diastolic function and other study variables

Circumferential and longitudinal diastolic strain rates represented CMR parameters of LV diastolic function. For echocardiographic LV diastolic parameter, we studied the most suitable parameter for diastolic function, E/E'. **Table 4** shows similar analyses for diastolic strain rates and E/E'. LVMI and the presence of LGE were independent predictors of circumferential diastolic strain rate, whilst only LVMI was an independent predictor of longitudinal strain rate. Only the presence of LGE showed a significant independent association with E/E'.

Thus, in AS, steatosis was a strong independent predictor of systolic dysfunction, but not of diastolic dysfunction.

Table 4: Associations of multiple study parameters with circumferential and longitudinal diastolic strain rate, and E/E'

	Circumferential diastolic SR*				Longitudinal diastolic SR*				E/E'†			
	Bivariate		Multivariate		Bivariate		Multivariate		Bivariate		Multivariate	
	R	P	β	P	R	P	β	P	R	P	β	P
Age	-0.19	0.14	–	–	-0.10	0.56	–	–	0.21	0.13		
Diabetes	-0.01	0.97	–	–	-0.01	0.97	–	–	0.28	0.03	0.17	0.23
Hypertension	-0.03	0.85	–	–	-0.03	0.86	–	–	0.23	0.09		
Dyslipidaemia	0.03	0.84	–	–	0.03	0.86	–	–	0.25	0.07		
Body mass index	-0.07	0.58	–	–	0.23	0.09	–	–	0.30	0.03	0.19	0.18
Aortic valve area	0.19	0.24	–	–	0.10	0.54	–	–	-0.10	0.57		
Peak AVA gradient	-0.10	0.55	–	–	0.11	0.51	–	–	-0.06	0.74		
LVEF	-0.03	0.83	–	–	0.07	0.63	–	–	0.07	0.63		
LV Mass index	-0.53	<0.001	-0.35	0.02	-0.58	<0.001	-0.50	0.003	0.31	0.02	0.13	0.41
LGE	-0.52	<0.001	-0.41	0.003	-0.35	0.01	-0.10	0.65	-0.38	0.006	-0.37	0.01
Lipid/water ratio	-0.31	0.02	-0.03	0.85	-0.30	0.03	-0.05	0.75	0.31	0.02	0.16	0.29

*Derived from cardiovascular magnetic resonance measurements.
†Derived from echocardiographic measurement.
AVA indicates aortic valve area; E, transmitral early diastolic velocity; E', mitral annular early diastolic velocity; LGE, late gadolinium enhancement; LV, left ventricular; LVEF, left ventricular ejection fraction; SR, strain rate.

Changes post aortic valve replacement

Thirteen patients had follow up CMR scans 8.0±2.1 months after AVR. There was near complete reversal of myocardial steatosis to control group levels (from 0.92±0.41% pre surgery to 0.47±0.25% post surgery, p=0.04), with no significant differences between the post-AVR levels and normal controls (p=0.73), as shown in **Table 5**. Three examples (normal control, AS patient before and after AVR) are shown in **Figure 3.4**. There was substantial regression of LV hypertrophy (LVMI from 96±35 g/m^2 to 69±18 g/m^2, p=0.001) although LVMI in patients 8 months post AVR was still significantly higher compared to normal controls (p=0.015). There was no change in LVEF (from 74±5% to 74±5%, p=1.0) post AVR. Of the 13 patients who underwent AVR and follow-up CMR, 2 patients had new left bundle branch block resulting in disco-ordinate septal movement which affected strain measurements, and these were excluded from the pre and post AVR strain comparisons. Systolic and diastolic strain indices improved significantly post AVR and were similar to measurements in controls: circumferential strain increased from -17.0±2.0% to -19.5±3.2%, p=0.04; circumferential diastolic strain rate from 60±11s^{-1} to 75±12s^{-1}, p=0.012; longitudinal diastolic strain rate from 42±6$s^{-1}$to 55±11s^{-1}, p=0.002. The only exception was longitudinal strain, which showed no significant change: -13.0±2.0% to -13.6±2.1% (p=0.26). These findings are presented on **Figure 3.5 (a) and (b).**

Table 5. Cardiac MRI and spectroscopy before and after AVR in symptomatic AS

Cardiac MRI and Spectroscopy	All symptomatic AS patients (n = 25)	Follow-up patients (n = 13)		Controls
		Pre AVR	Post AVR	
Cardiac lipid/water	0.89±0.42	0.92±0.41	0.47±0.25*	0.45±0.17
Circumferential strain	-16.4±2.5	-17.0±2.0	-19.5±3.2*	-20.7±2.0
Circumferential diastolic strain rate	56±13	60±11	75±12*	76±12
Longitudinal strain	-12.6±2.0	-13.0±1.7	-13.6±2.1†	-16.6±1.6
Longitudinal diastolic strain rate	43±12	42±6	55±11*	53±12
Left ventricular mass index	94±33	96±35	69±18‡	54±13
Left ventricular ejection fraction	75±5	74±5	74±5†	69±4

*p<0.05 versus pre AVR and >0.05 versus controls; †p>0.05 versus pre AVR and <0.05 versus controls; ‡p<0.05 versus pre AVR and controls.
Note: For strain, n=11 were used for follow-up analysis as two patients were excluded due to new left bundle branch block post AVR.

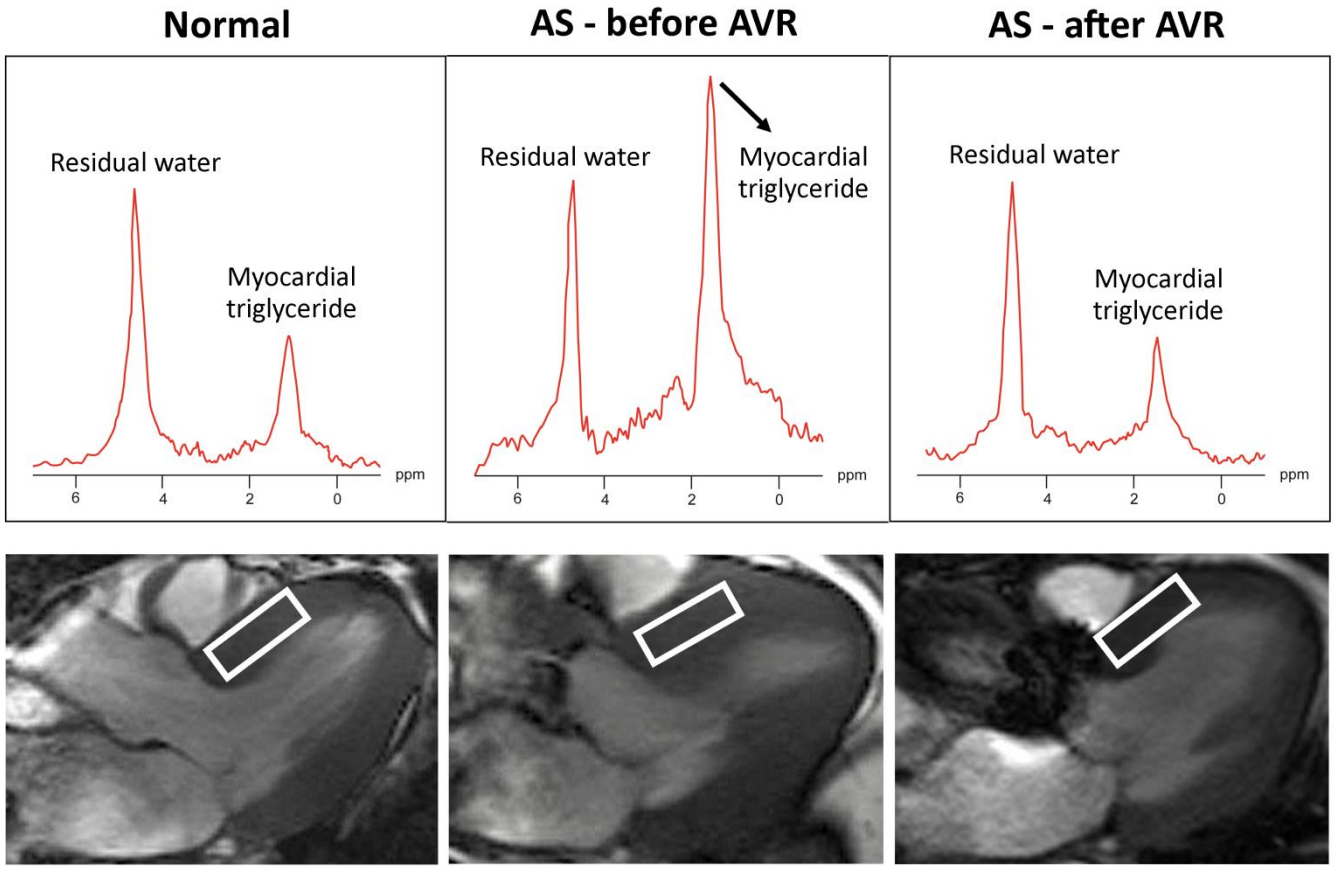

Figure 3.4. Myocardial spectra (with water suppression) from a normal volunteer showing a smaller triglyceride peak relative to that of residual water. Myocardial spectra (with water suppression) from a patient with severe aortic stenosis before and after aortic valve replacement (AVR) showing a greater triglyceride peak relative to that of water, which has normalised after AVR. Corresponding left ventricular outflow tract cine images show correct placement of the magnetic resonance spectroscopy voxel at the interventricular septum, to avoid contamination from epicardial fat.

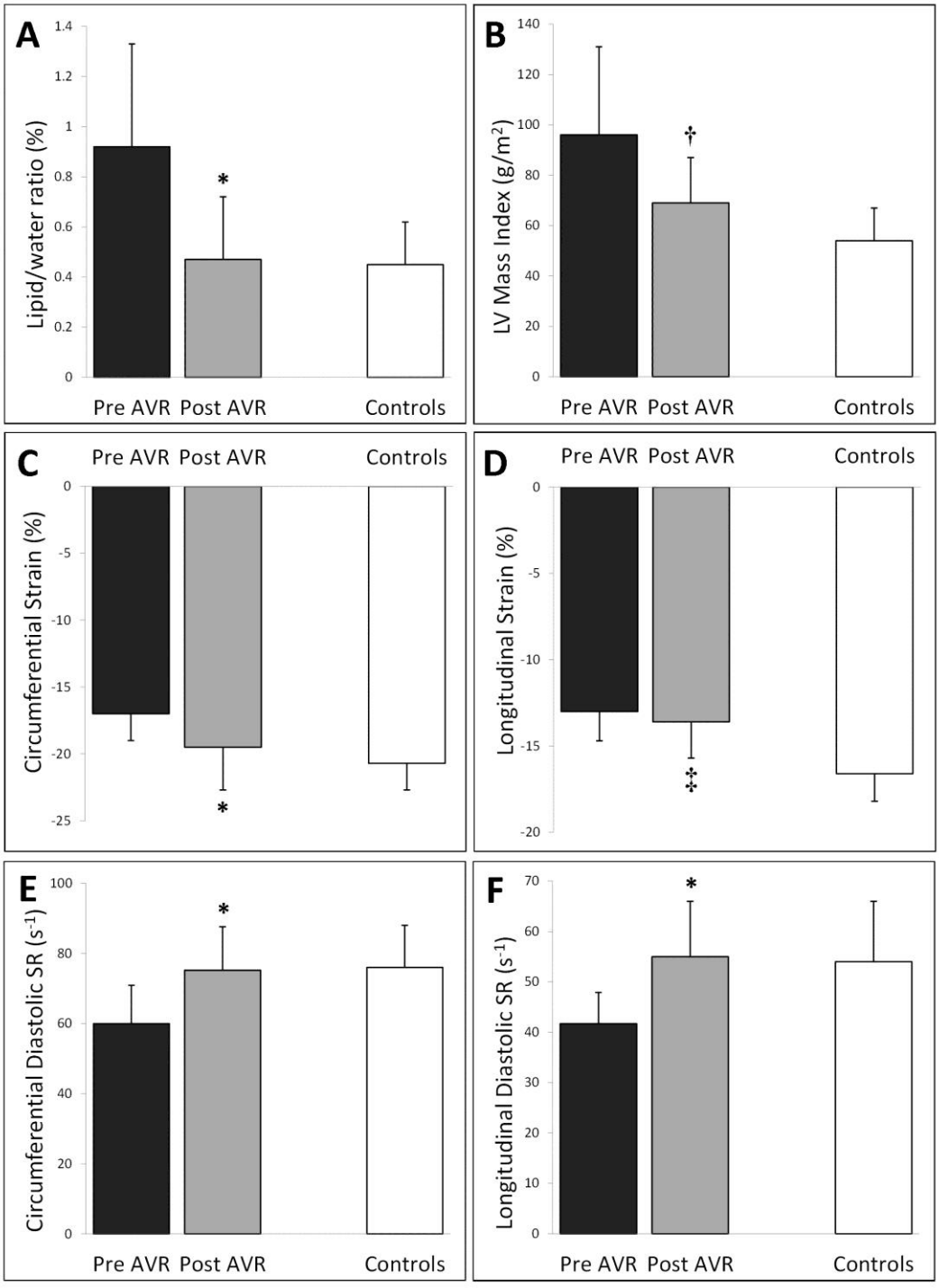

Figure 3.5 (a). Changes in **(A)** lipid/water ratio, **(B)** left ventricular mass index, **(C)** circumferential strain, **(D)** longitudinal strain, **(E)** circumferential diastolic strain rate and **(F)** longitudinal strain rate after aortic valve replacement.

*p<0.05 versus pre AVR and >0.05 versus controls; †p<0.05 versus pre AVR and controls; ‡p>0.05 versus pre AVR and <0.05 versus controls.

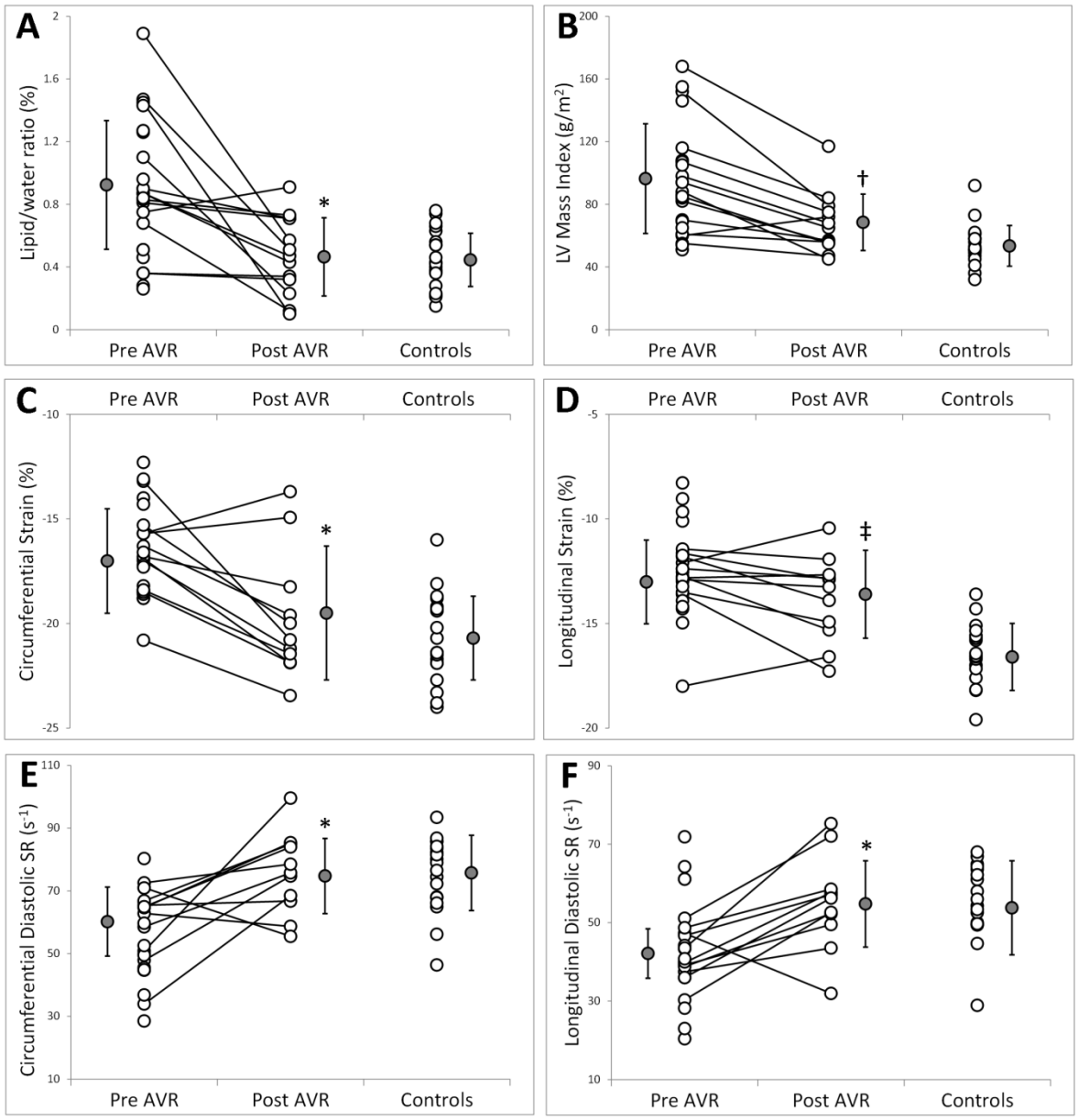

Figure 3.5 (b). Spaghetti plots showing individual responses post aortic valve replacement.

As these results might be confounded by the presence of diabetes (6 pre AVR and 4 post AVR), we repeated the analysis in the subgroup of patients without diabetes before (n=19) and after AVR (n=9). The results were similar to the entire cohort (results are available in Appendix 2).

3.6. DISCUSSION

The present study demonstrated three important findings: firstly, that myocardial steatosis is pronounced in both symptomatic and asymptomatic severe AS and is independently associated with impaired systolic but not diastolic strain. Secondly, that myocardial steatosis and strain changes are reversible post AVR. Finally, steatosis as measured by ^{1}H-MRS could be validated against histological analysis.

Myocardial steatosis in AS

This is the first study to show the presence of myocardial steatosis in severe AS *in vivo,* using ^{1}H-MRS. MTC determined by ^{1}H-MRS has previously been shown to correlate with biochemical determination of myocardial triglyceride in Zucker rats[10] and skeletal muscle from dogs.[7] We extend these findings by confirming that MTC as measured by MRS correlates closely with histological analysis of human myocardial biopsies obtained intraoperatively (r_s=0.66) in patients with severe AS. Steatosis existed in our AS cohort despite no significant difference in age, gender, BMI, serum glucose and lipid profile compared to normal controls, all of which have been shown to contribute to myocardial steatosis.[89, 96] Importantly, our data showed that myocardial TG is increased in both symptomatic and asymptomatic severe AS patients despite similar degree of aortic valve stenosis and LV remodelling. Since this is the first study to show lipid abnormalities in AS patients, we hypothesise that there may be worsening of the degree of metabolic abnormalities with clinical worsening of AS, which cannot be detected by the conventional tests, e.g. stenosis severity, pressure gradient and LV mass, suggesting that lipid assessment may potentially be useful as a more accurate/objective assessment in the future to

characterise asymptomatic AS which may guide the timing of AVR. Although the mechanisms underlying cardiac steatosis are incompletely understood, it is likely that impaired myocardial FA oxidation characteristic of cardiac hypertrophy contributes to triglyceride accumulation.[62]

The important question is whether steatosis is involved in the pathophysiology of contractile dysfunction in AS, or is just an epiphenomenon. The present data demonstrate that in severe AS, steatosis is independently associated with strain, similar to that described in previous animal and human studies.[18, 93] Moreover, when compared to other independent variables (LGE and LVMI), MTC (and ORO staining of lipid deposition from myocardial biopsies) was associated with systolic strain abnormalities with the highest statistical significance, suggesting that steatosis is at the very least a sensitive marker of myocardial contractile dysfunction. This concurs with a previous study demonstrating a significant association between high myocardial lipid staining and reduced LVEF in AS patients who had metabolic syndrome.[97] One explanation for this observation is that the association is causative and mediated by the generation of toxic intermediates such as ceramides from non-oxidative fatty acid metabolism.[98, 99] In addition, lipid vacuole infiltration has been shown to mechanically dissemble the myocardial contractile apparatus leading to contractile dysfunction in diabetic patients.[19] Thus, while our data do not prove a direct causal link, they are clearly suggestive of a pathophysiological role of steatosis in the development of systolic dysfunction in AS.

Our data did not show any association between steatosis and LV diastolic function. LVMI and the presence of LGE were, however, independent determinants of abnormal diastolic

parameters in our study. These findings are not surprising, as LVH and myocardial fibrosis[100, 101] are well-established causes of diastolic dysfunction. In contrast, Rijzewijk[102] and Ng *et al*[18] demonstrated that steatosis in their diabetic cohort is independently associated with LV diastolic dysfunction using MRI-derived E/A ratio and deceleration time, and longitudinal strain rate measured by echocardiographic speckle tracking, respectively. The discrepancies between these reports are likely attributable to the different patient populations investigated, but warrant further study. It may be possible that in diabetes where plasma FA is elevated, increased FA influx and rate of β-oxidation is associated with increased production of reactive oxygen species (ROS) which is known to interfere with calcium haemostasis leading to diastolic dysfunction.[103] Thus in pressure overload hypertrophy we speculate that diastolic dysfunction is not the main feature of lipotoxicity because of intact calcium homeostasis as a result of suppressed FA oxidation hence no excess ROS production.

Reversibility of steatosis and strain changes following aortic valve replacement

We showed that there is a significant reduction in steatosis after AVR. Significant improvements in most parameters of myocardial function were also observed, despite incomplete LVH regression.

Improvement in myocardial metabolism and function post AVR is likely to reflect a mitigation of the pressure overload leading to reduced LV wall stress.[104, 105] Rajappan *et al*, using positron emission tomography, demonstrated that coronary vascular and myocardial blood flow improvements after AVR were related to reduced afterload rather than the

regression of LVH.[106] We hypothesise that the relief of LV wall stress post AVR causes a switch in myocardial substrate metabolism from glucose back to FA, thus reducing FA overload, toxicity and steatosis with subsequent improvement in cardiac function.[104, 105, 91, 107] Reversal of metabolic dysregulation and improved ventricular function have been reported in another model of improved LV loading, after bariatric surgery for weight reduction in obese patients.[108] Postoperative longitudinal systolic function did not improve significantly post AVR in our AS cohort, but this is primarily determined by LVH regression[109], which was only partial in our study. Furthermore, it was evident from our data that LV mass index was an important determinant of longitudinal systolic strain.

3.7. CLINICAL IMPLICATIONS

The present study provides novel insights into metabolic alterations and their consequences in aortic stenosis. We demonstrated that steatosis and subclinical myocardial dysfunction occur regardless of symptoms in severe AS. Furthermore, the presence of myocardial steatosis and its significant association with myocardial strain is likely to be relevant clinically. Depressed LVEF is a late phenomenon and recognition of subtle changes in LV systolic function, while LVEF is still preserved, may permit more timely surgical intervention. It is conceivable that, in future, steatosis may also emerge as a parameter for guidance of AVR timing. Most importantly, we showed that steatosis improved after AVR; thus, if steatosis is indeed a pathophysiological factor in AS, then a reduction in steatosis might be a potential new therapeutic target to delay the development of LV dysfunction. We are currently setting up a clinical trial that tests this intriguing possibility. Such a trial, if positive, would also provide confirmatory evidence of a causal relationship between steatosis and systolic dysfunction in AS.

3.8. STUDY LIMITATIONS

This study is limited by a relatively small sample size, in line with its proof-of-principle nature. Furthermore, the AS population was heterogenous, including patients with hypertension, dyslipidaemia and diabetes which are known to be associated with metabolic abnormalities. However, we only included patients with well-controlled BP and diabetes. We were careful to assess whether the observed association between steatosis and strain might be confounded by the presence of diabetes. However, diabetes was not predictive of strain changes when MTC, LVMI and LGE were included in the multivariate model.

Furthermore, and most importantly, steatosis was reversible post AVR, and this group included 4/13 (31%) diabetics. All analyses were repeated excluding the diabetic patients, and this did not affect any of the statistical significances in our study (Appendix 1).

3.9. CONCLUSION

Severe aortic stenosis is characterized by pronounced myocardial steatosis and subclinical LV contractile dysfunction. Eight months post AVR, steatosis regresses along with normalisation of myocardial circumferential strain despite only partial regression of LVH. Myocardial lipid assessment may serve as a useful adjunct to standard clinical information for risk stratification of patients with severe AS, but future studies are needed to investigate this further.

CHAPTER 4: IMPAIRED MYOCARDIAL OXYGENATION RESPONSE DURING VASODILATOR STRESS IN PATIENTS WITH SEVERE AORTIC STENOSIS: INSIGHTS FROM OXYGENATION-SENSITIVE CARDIOVASCULAR MAGNETIC RESONANCE

4.1. ABSTRACT

Background: LVH in AS is characterised by reduced myocardial perfusion reserve due to coronary microvascular dysfunction. However, whether this hypoperfusion is associated with myocardial tissue deoxygenation is uncertain. The aim of this study was to assess myocardial oxygenation and perfusion in patients with severe AS but no obstructive CAD before and after AVR.

Methods and Results: Twenty patients with isolated severe AS underwent CMR at 3 Tesla. Myocardial function, perfusion (myocardial perfusion reserve index-MPRI) and oxygenation (blood-oxygen level dependent-BOLD signal intensity-SI change) during adenosine stress and rest, and fibrosis (late gadolinium enhancement-LGE) were assessed. Fifteen aged- and gender-matched healthy volunteers served as healthy controls. When compared with normals, AS patients had blunted oxygenation response during stress (BOLD SI 4.6±9.8% vs. controls 18.2±11.6%, p=0.002) and reduced MPRI (1.0±0.3 vs. controls 1.7±0.3, p<0.001). Myocardial perfusion but not oxygenation significantly correlated with myocardial fibrosis. At 8.0±2.1 months post AVR, BOLD SI change and MPRI improved significantly.

Conclusions: Myocardial perfusion is impaired in severe AS and this is translated into a blunted oxygenation response during vasodilator stress. Following AVR, perfusion and oxygenation improve significantly.

4.2. INTRODUCTION

As discussed in Chapter 1, AS is characterized by pressure overload LVH and impaired myocardial perfusion reserve.[110] This has been shown by a variety of imaging modalities such as positron emission tomography (PET)[111] and CMR[112] which demonstrate reduced myocardial perfusion, suggesting there is limited oxygen availability in the myocardial tissue. In the absence of coronary stenoses, this finding is indicative of microvascular dysfunction, but it remains unclear whether the hypoperfusion seen in severe AS during stress leads to myocardial tissue deoxygenation and ischemia. Such knowledge is important as myocardial tissue hypoxia may play a significant pathophysiological role in the natural history of AS patients as development of symptoms is followed by rapid clinical deterioration which indicates poor prognosis.[113] Furthermore, some studies have shown that myocardial perfusion reserve is restored following AVR[106] but it is unknown whether the same applies to myocardial oxygenation.

CMR provides the unprecedented capability to assess myocardial perfusion *and* oxygenation in the same setting during vasodilator stress. Assessment of myocardial perfusion reserve during vasodilator stress is an established CMR technique during the first pass of a gadolinium based contrast agent.[114, 115] Oxygenation-sensitive CMR can non-invasively assess myocardial tissue oxygenation by measuring blood-oxygen level-dependent (BOLD) signal intensity (SI) differences which reflect deoxygenated haemoglobin concentration during adenosine stress and rest.[80, 116-120] Oxygenation measurements using BOLD CMR have been shown to be proportional to changes in coronary sinus oxygen saturation.[117] As recently shown in patients with CAD, oxygenation-sensitive CMR can not only identify de-

oxygenated myocardial segments subtended by stenosed vessels, but also segments with microvascular dysfunction and intermediate SI changes to adenosine stress when compared to normal volunteers.[80, 116, 119] Importantly, myocardial perfusion can be dissociated from oxygenation, i.e. hypoperfusion is not necessarily commensurate with tissue hypoxia. The oxygen demand of the heart muscle may vary in different states, e.g. it may be reduced in hibernating myocardium in line with the downregulated contractility[121] or may be increased in hypertrophic cardiomyopathy due to the increased energy cost of contraction.[122, 123] Thus, compared to perfusion, regional myocardial oxygenation may be a superior parameter reflecting more directly the imbalance between oxygen demand and supply that characterizes ischemia.

Therefore, the purpose of the present study was, to comprehensively assess coronary microvascular status in patients with severe AS and no obstructive CAD by assessing myocardial perfusion *and* oxygenation during adenosine stress. We hypothesised that tissue oxygenation and perfusion during stress are impaired in severe AS but relatively quickly restored after AVR. If our hypothesis is proven true, it would suggest a central role of myocardial ischemia in patients with severe AS despite the absence of epicardial coronary stenoses.

4.3. METHODS

Study population and protocol

Twenty symptomatic AS patients, with no CAD, undergoing AVR and fifteen healthy volunteers underwent CMR scanning protocol at 3T as follow;

1. Cine imaging to measure LV function and mass
2. Late gadolinium enhancement to assess fibrosis
3. Rest and adenosine stress BOLD imaging to assess oxygenation
4. Rest and adenosine stress perfusion to measure myocardial perfusion reserve index.

The methods and analysis are described in Chapter 2. Additionally, valvulo-arterial impedance-VAI (the sum of the systolic BP and the transaortic valvular pressure gradient divided by indexed stroke volume) was calculated as an estimate of global LV afterload.[124] For LGE analysis, it was only deemed to be present when the area of signal enhancement could be seen in both phase-swapped images and in a cross-cut long-axis image.[75] LGE quantification was performed using cmr42 software (version 4.0, Circle Cardiovascular Imaging). The full-width-half-maximum (FWHM) technique was used to quantify fibrosis as previously described.[76] Fibrosis volume was expressed as a percentage of total myocardial mass.

4.4. STATISTICAL ANALYSIS

All data are expressed as mean ± standard deviation and checked for normality using Kolmogorov–Smirnov test. Categorical data are presented as numbers and percentages. Comparisons between the 2 groups were performed by Student *t*-test. The chi-square test or Fisher's exact test was used to compare discrete data as appropriate. Bivariate correlations were performed using Pearson's or Spearman's method as appropriate. Multivariable linear regression analysis was used to identify independent correlates of MPRI and BOLD SI change. Comparisons between pre- and post-AVR measurements in AS patients were performed with paired two-tailed Student *t*-test. Comparisons between AS patients and controls at baseline and post-AVR were performed using independent Student *t*-test or Mann-Whitney U test as appropriate. A *P*-value <0.05 was considered significant. All statistical analyses were performed with IBM SPSS Statistics, version 19.

4.5. RESULTS

Baseline Study Characteristics

Demographic, clinical, echocardiographic and biochemical data are shown in **Table 1.** There were no significant differences in age, gender, body mass index, BP and pulse rate between AS patients and normal controls. Blood glucose and biochemical lipid parameters were also similar in both groups.

Table 1: Baseline characteristics

	Severe AS (n = 20)	Normal controls (n = 15)	P value
Age (years)	67±9	63±4	0.09
Male, n (%)	14 (70)	8 (53)	0.16
Symptoms, n (%)			
Dyspnoea	13 (65)	–	
Angina	7 (35)	–	
Syncope	1 (5)	–	
Past medical history			
Hypertension	6 (30%)	–	
Dyslipidaemia	5 (25%)	–	
Medications, n (%)			
ACE-I/ARB-II	4 (20)	–	
Beta-blockers	4 (20)	–	
Statin	11 (37)	–	
Body mass index (kg/m^2)	27±4	26±3	0.44
Systolic blood pressure (mmHg)	132±17	130±9	0.92
Diastolic blood pressure (mmHg)	75±10	76±8	0.75
Heart rate (bpm)	64±9	62±9	0.57
Peak AV gradient (mmHg)	81±13	-	
Biochemical (mmol/L)			
Blood glucose	5.2±1.0	5.0±0.7	0.71
Total cholesterol	4.6±1.0	5.5±0.6	0.013
Triglycerides	1.1±0.4	1.2±0.3	0.15
High-density lipoprotein	1.4±0.4	1.5±0.4	0.43

Values are mean ± SD or percentages. ACE indicates angiotensin-converting enzyme-inhibitors; ARB, angiotensin-receptor antagonist-II.

Cardiovascular MR imaging

CMR results are summarised in **Table 2**. There was striking reduction in BOLD SI change (~ 4-fold drop in SI) in AS patients when compared to the normal controls. There was also significant reduction in MPRI. As expected, AS patients had significantly higher LVMI and increased LV wall thickness, and high normal LVEF when compared to the normal controls.

LGE imaging demonstrated that myocardial fibrosis was most prevalent in AS (84%) versus 13% in the normal controls. The predominant pattern of LGE was patchy involving mainly basal inferior and infero-lateral wall. Control subjects (n=2) had LGE involving the inferior left/right-ventricular insertion point, which can be seen in normal subjects.[125] None of the subjects had any evidence of previous myocardial infarction. Using FWHM method for LGE quantification, as expected the burden of LV fibrosis was significantly higher in the AS group.

Table 2: CMR results in AS patients vs. normal controls

	Aortic Stenosis (n = 20)	Normal (n = 15)	P value
BOLD signal intensity change (%)	4.6±9.8	18.2±11.6	0.002
MPRI	1.0±0.3	1.7±0.3	<0.001
Baseline RPP (x 10^3) [(beats/min).mmHg]	8.5±1.5	8.0±1.5	0.36
Stress RPP (x 10^3) [(beats/min).mmHg]	11.3±2.5	11.7±2.6	0.63
Adenosine duration (min)	6.3±1.7	6.3±1.1	0.92
LV ejection fraction (%)	74±6	69±4	0.005
LV end-diastolic volume (ml)	146±47	142±32	0.73
LV end-systolic volume (ml)	40±20	44±12	0.45
LV mass index (g/m^2)	100±35	56±13	<0.001
LV wall thickness (mm)	17±3	10±1	<0.001
Aortic valve area (cm^2)	0.83±0.10	–	
Valvulo-arterial impedance (mmHgml/m^2)	4.0±0.9	2.6±0.6	<0.001
LGE present, n (%)	16 (84)	2 (13)	<0.001
LGE volume (%)	17.6±13.8	0.79±0.55	<0.001

Values are mean ± SD or percentages. BOLD, blood oxygen level dependent; LV, left ventricular; LGE, late gadolinium enhancement; MPRI, myocardial perfusion reserve index; RPP, rate pressure product.

Relationship among oxygenation, perfusion and other study variables

Table 3 shows bivariate Pearson correlations of MPRI and BOLD SI change with several parameters in study subjects. MPRI had a negative correlation with NYHA functional class, AVA, VAI, LV wall thickness, LVMI and LGE. BOLD SI change had negative correlation with CCS and NYHA functional class, LV wall thickness, LVMI, VAI, and positive correlation with MPRI. Further analyses showed an expected positive correlation between LGE volume and LV wall thickness ($r=0.72$, $p<0.001$) and VAI ($r=0.60$, $p<0.001$).

Table 3. Associations of multiple study parameters with MPRI and BOLD SI change

	MPRI		BOLD	
	R	**P-Value**	**R**	**P-Value**
NYHA Class	-0.47	0.005	-0.39	0.02
CCS Class	-0.23	0.18	-0.42	0.01
Aortic valve area	0.57	0.007	-0.14	0.54
Valvulo-arterial impedance	-0.37	0.03	-0.47	0.005
Peak aortic valve gradient	-0.41	0.066	-0.35	0.12
LV wall thickness	-0.72	<0.001	-0.46	0.006
LV mass index	-0.74	<0.001	-0.39	0.02
Presence of LGE	-0.53	0.001	-0.27	0.12
Volume of LGE	-0.42	0.015	-0.14	0.53
MPRI	–	–	0.48	0.006
BOLD signal intensity change	0.48	0.006	–	–

BOLD indicates blood oxygen level dependent; CCS, Canadian Cardiovascular Society; LV, left ventricular; LGE, late gadolinium enhancement; MPRI, myocardial perfusion reserve index; NYHA, New York Heart Association.

Cardiac MRI post aortic valve replacement

Results are summarised in **Table 4** with examples shown in **Figure 4.1** and **4.2**. Ten patients had follow up CMR scans 8.0±2.1 months after AVR. There was significant improvement in change in BOLD SI (from 4.9±8.4% to 16.4±7.0%, p=0.013 and p=0.69 vs. normal) and MPRI (from 1.1±0.4 to 1.5±0.4, p=0.01 and p=0.37 vs. normal). There was significant regression of LVH (LVMI from 100±36 g/m^2 to 71±19 g/m^2, p=0.02; LV wall thickness from 16±2 mm to 14±2 mm, p=0.003) although LVMI and LV wall thickness in patients 8 months post AVR was still significantly higher compared to normal controls (p=0.03 for LVMI and p=0.001 for LV wall thickness). There was no significant reduction in LGE volume, from 17.2±14.1% pre AVR to 14.7±12.7% post AVR, (p=0.48).

Table 4. Cardiac MRI before and after AVR in AS patients

	All patients pre AVR (n = 20)	Follow-up patients (n = 10)		Controls
		Pre AVR	Post AVR	
BOLD signal intensity change	4.6±9.8	4.9±8.4	16.4±7.0*	18.2±11.6
MPRI	1.0±0.3	1.1±0.4	1.5±0.4*	1.7±0.3
Baseline RPP (x 10^3) [(beats/min).mmHg]	8.5±1.5	8.5±1.3	8.1±1.4†	8.0±1.5
Stress RPP (x 10^3) [(beats/min).mmHg]	11.3±2.5	12.0±3.5	11.4±1.8†	11.7±2.6
Adenosine duration (min)	6.3±1.7	6.4±0.8	6.0±1.2†	6.3±1.1
Left ventricular mass index (g/m2)	100±37	100±36	71±19‡	56±13
Left ventricular wall thickness (mm)	17±3	16±2	14±2‡	10±1
LV ejection fraction (%)	74±6	75±6	74±5¶	69±4
LGE volume (%)	17.6±13.8	17.2±14.1	14.7±12.7†	0.79±0.55

Values are mean ± SD or percentages. BOLD indicates blood oxygen level-dependent; LV, left ventricular; LGE, late gadolinium enhancement; MPRI, myocardial perfusion reserve index; RPP, rate pressure product.

*p<0.05 vs pre AVR and >0.05 vs controls; †p>0.05 vs pre AVR and controls; ‡p<0.05 vs pre AVR and controls; ¶p>0.05 vs pre AVR and <0.05 vs controls.

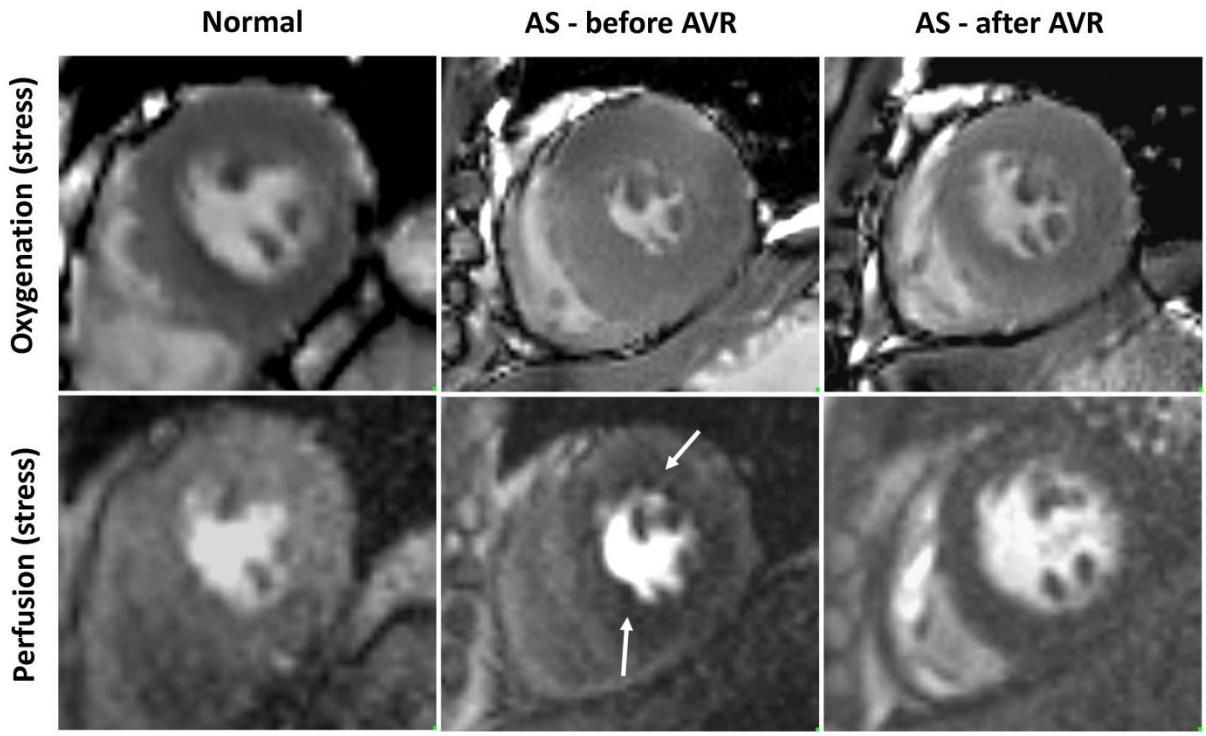

Figure 4.1: Myocardial oxygenation and perfusion examples for a normal volunteer, a patient with severe aortic stenosis (AS) before and after aortic valve replacement (AVR). Note the perfusion defect in the pre AVR patient, which has reduced after AVR.

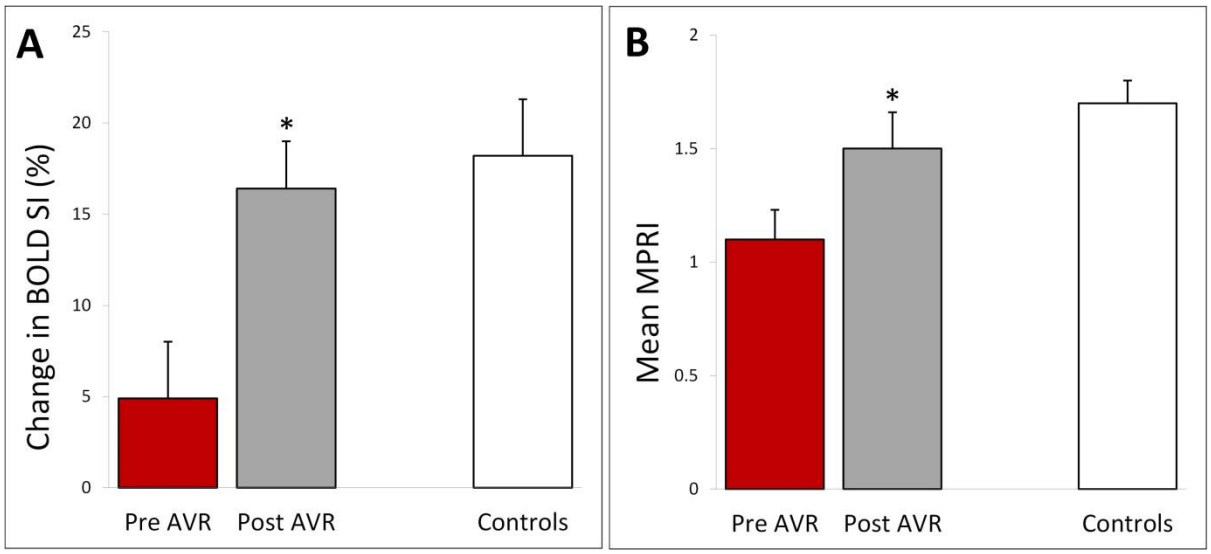

Figure 4.2. Changes in **(A)** BOLD SI change and **(B)** mean MPRI after aortic valve replacement.

*p<0.05 vs pre AVR and >0.05 vs controls.

4.6. DISCUSSION

The major finding of the present study is that, there is significant impairment in myocardial perfusion and oxygenation response to vasodilator stress in patients with severe AS and normal epicardial coronaries when compared to normal volunteers. Eight months after AVR, myocardial tissue perfusion and oxygenation improve significantly.

Our data confirmed a previous finding of reduced perfusion reserve during vasodilator stress using CMR in severe AS patients.[112] Microvascular dysfunction is a well-established phenomenon in pressure overload hypertrophied heart.[126, 127] This can be due to decreased capillary density per unit myocardium due to inadequate growth of new vessels and extravascular compression as a result of LV wall stress.[126, 127] Not surprisingly, our data showed that the degree of impairment in perfusion reserve correlated with the extent of hypertrophy, aortic valve stenosis, LV afterload and myocardial fibrosis. Steadman *et al* similarly reported that myocardial perfusion is related to LVMI, LWT and LGE. On the contrary, that study did not find AVA was related to myocardial perfusion.[112] The discrepancies are likely due to their more heterogenous AS cohort with a greater number of hypertensives (59% vs. 30%) and diabetics (22% vs. none), and lower mean LVEF (56.5% vs. 74%). On the other hand, Rajappan *et al* showed that AVA and LV afterload are important correlates of myocardial perfusion in their AS cohort.[111] Rajappan however did not find significant associated between perfusion reserve and LVMI. The reason for the difference is unclear but it may be that half of the patients in that study were asymptomatic (50% vs. none in the current study). In the current study, MPRI derived from the signal intensity curves instead of MPR (measured from absolute myocardial blood flow quantification) was

measured. This was because the absolute blood flow quantification technique was not available. Although MPR is more accurate, MPRI derived from the signal intensity curves can provide useful information on coronary circulation and may be proportional to the coronary flow reserve.[128, 129]

In the absence of obstructive CAD, the hypertrophied ventricle is vulnerable to ischemia especially under stress.[130] This is thought to be the explanation why patients with AS have symptoms of effort angina despite normal epicardial coronary arteries.[131] Whether de-oxygenation occurs as a consequence of impaired perfusion reserve during stress in AS, has never been demonstrated. Myocardial hypoperfusion does not always reflect hypoxia as oxygen demand may vary in different pathophysiologic states. For example, in hypertension, myocardial oxygen utilization per unit LV weight is reduced in the presence of LVH.[132] Cardiac hypertrophy is an adaptive mechanism in response to pressure overload, to normalize increased wall stress according to the Law of Laplace.[133] Our group recently demonstrated that dissociation can exist between myocardial perfusion and oxygenation.[80, 119, 134] Impaired stress perfusion can be compatible with normal oxygenation when myocardial oxygen demand is down-regulated such as in hibernation,[80, 119] and stress oxygenation can be reduced in spite of normal perfusion, when the oxygen demand is increased such as in hypertrophic cardiomyopathy carriers.[134] Our current study now shows that, in the context of AS, perfusion and oxygenation during stress are closely associated, and both are impaired. This is in line with observations in patients with LVH due to long-standing hypertension.[135] We also showed that both perfusion and oxygenation impairments in AS showed significant associations with the degree of LVH. Conversely, there

was no significant relationship between oxygenation and fibrosis, which is expected because scar tissue has negligible oxygen requirements.

Another important finding from this study is the significant relationship between tissue oxygenation and global LV afterload. Increased global LV afterload as shown by increased in valvulo arterial-impedance (hence increase in myocardial wall stress and oxygen demand) is an important prognostic marker in patients with asymptomatic moderate to severe AS.[136] Degenerative AS by itself is a manifestation of atherosclerotic process in the ageing population, thus reduced systemic arterial compliance including the aorta is not an uncommon finding in patients with AS. Therefore, the left ventricle faces both vascular and valvular stenotic load leading to greater myocardial wall tension (and thus oxygen demand).[124] To compensate for the increase in LV wall stress, myocardial hypertrophy occurs as a necessary adaptation to normalise LV wall tension aims at restoring myocardial oxygen consumption towards normal.[137]

Changes following aortic valve replacement

Importantly, we showed that impaired perfusion and oxygenation both returned to normal 8 months after AVR, clearly demonstrating that such abnormalities are reversible following the relief of valve obstruction. It is likely that improvement in microcirculatory dysfunction after AVR is the result of a combination of both, relief of mechanical obstruction with reduced LV wall stress, and LVH regression.[104, 105, 138] There was no significant fibrosis regression post AVR, in keeping with a previous study which showed that myocardial fibrosis was essentially unchanged 9 months after AVR.[139]

4.7. CLINICAL IMPLICATIONS

The current findings suggest that substantial microvascular insufficiency likely leading to myocardial tissue ischaemia is present in severe AS patients, at least during vasodilatory stress. A reduced capacity to augment myocardial oxygenation may potentially lead to poor clinical outcome as prognosis is worse after development of symptoms such as angina. Ischaemia itself can lead to LV dysfunction,[135] suggesting that BOLD-CMR is an important test for myocardial oxygenation. It is conceivable that in the future oxygenation-sensitive CMR may become a valuable test in addition to conventional clinical information for evaluation of patients with severe AS. Future studies in larger AS cohorts will be necessary to assess the incremental diagnostic and/or prognostic value of oxygenation-sensitive CMR in these patients. Importantly, myocardial tissue hypoxia may be a potential avenue for therapy targeted at ameliorating ischaemia such as perhexiline[140] either as an add-on therapy to those who are still symptomatic after AVR or to delay disease progression especially in patients who are not fit to undergo surgical AVR.

4.8. STUDY LIMITATIONS

We included a small number of AS patients with hypertension and dyslipidaemia which may contribute to myocardial perfusion abnormalities. However, only patients with well-controlled BP were included and patients who had dyslipidaemia were well treated by statin (as shown by blood lipid measurements). It would be extremely challenging to recruit patients with severe AS without these conditions which are very common in the elderly population. The strength of our study is that, both CAD and diabetes were excluded from our study cohort resulting in a relatively homogenous patient population. Diastolic perfusion

time (DPT) was not measured in the current study, therefore we are unable to comment of its effect on myocardial perfusion and oxygenation. Nevertheless, previous studies have shown inconsistent results between DPT and myocardial perfusion reserve.[111, 112] As our study population is relatively small, particularly the group of patients being rescanned after AVR, confirmation of our findings in larger scale studies is warranted. Due to the cross-sectional study design, we are unable to prove direct causality of disease mechanisms described above, therefore longitudinal and interventional trials would be essential to confirm these.

4.9. CONCLUSIONS

In severe AS without epicardial CAD, the presence of reduced myocardial perfusion is associated with a striking blunted oxygenation response to adenosine stress suggestive of severe microvascular impairment. Oxygenation-sensitive CMR is a promising tool to become an adjunct for the clinical evaluation of patients with aortic stenosis.

CHAPTER 5: MYOCARDIAL STEATOSIS AND LEFT VENTRICULAR CONTRACTILE DYSFUNCTION IN DILATED CARDIOMYOPATHY

5.1. ABSTRACT

Background: HF is characterised by impaired myocardial substrate metabolism and insulin resistance. We hypothesised that myocardial steatosis is involved in the pathophysiology of HF due to DCM and assessed whether it was related to cardiac structure and function. We also investigated if there was any relationship with hepatic TG.

Methods and Results: Twenty DCM patients were studied using cine imaging and ^{1}H-MRS for the determination of LV volumes and ejection fraction and myocardial TG content, respectively. A subgroup of patients (n=12) underwent ^{1}H-MRS of the liver for the determination of hepatic TG content. Twenty aged- and gender-matched subjects served as healthy controls. When compared with normals, DCM patients had significantly increased myocardial TG content (0.64±0.44% vs. 0.40±0.13%, p=0.03), increased LV volumes and reduced LVEF and circumferential strain. Multivariable analysis indicated that steatosis was an independent associate of increased LV volume. Furthermore, there was high correlation between myocardial and hepatic TG content, r=0.78, p=0.003.

Conclusions: Myocardial steatosis may be involved in the pathophysiology of adverse LV remodelling in DCM. Its correlation with hepatic TG content suggests that both myocardial and hepatic steatosis may be a common feature of HF due to DCM.

5.2. INTRODUCTION

Myocardial metabolism in HF is complex and studies on myocardial substrate utilisation have produced conflicting results. Most studies have shown that FA oxidation is unaffected or slightly increased in early HF, but decreased in the late stage of the disease with energy supply mainly from glucose oxidation.[62, 141-143] This metabolic substrate shift towards a preference for glucose may in part be a consequence of glucose being energetically more efficient (lower oxygen usage) than fat.

However, despite a relatively higher dependence on glucose, there is evidence that both glucose uptake and oxidation are impaired, and that myocardial insulin resistance persists in these patients.[15, 66] Myocardial TG content is increased in conditions with increased insulin resistance (thus elevated circulating FA) such as diabetes and obesity,[90, 103] where hepatic steatosis is also present.[8] We hypothesised that cardiac steatosis might be a common disease pathway in other forms of insulin resistance state such as DCM. Therefore we used CMR and MRS to investigate the relationship between myocardial TG content and cardiac function, and if there was any relation with hepatic TG content.

5.3. METHODS

Study Population

Twenty patients with DCM and twenty healthy volunteers were recruited. Eligibility criteria for both study cohorts were detailed in Chapter 2.

Study Protocol

All subjects underwent cardiac MR and ^{1}H-MRS (details described in Chapter 2). A subgroup of DCM patients (n=12) underwent CMR tagging (for strain imaging) and ^{1}H-MRS of the liver (for hepatic TG measurements). Fasting venous blood was drawn for blood glucose, lipid profile, non-esterified FA (NEFA), homeostasis model of assessment (HOMA) index and insulin.

5.4. STATISTICAL ANALYSIS

All data are expressed as mean ± standard deviation and checked for normality using Kolmogorov–Smirnov test. Categorical data are presented as numbers and percentages. Comparisons between the 2 groups were performed by Student *t*-test. The chi-square test or Fisher's exact test was used to compare discrete data as appropriate. Bivariate correlations were performed using Pearson's or Spearman's method as appropriate. Multivariable linear regression analysis was used to identify independent correlates of circumferential strain. A *P*-value <0.05 was considered significant. All statistical analyses were performed with IBM SPSS Statistics, version 19.

5.5. RESULTS

Baseline Study Characteristics

Demographic, clinical, echocardiographic and biochemical data are shown in **Table 1.** There were no significant differences in age, gender, body mass index, BP and pulse rates between DCM patients and normal controls. Fasting blood glucose and lipid profiles were similar in both groups. DCM patients had features suggestive of insulin resistance; HOMA index of 4.5±2.6 and insulin level of 14.2±9.2 mU/L.

Table 1: Clinical and echocardiographic characteristics

	DCM (n = 20)	Normals (n = 20)	P value
Age (years)	61±9	60±6	0.81
Male, n (%)	14 (70)	13 (65)	0.75
NYHA functional class, n (%)			
I	2 (15)	–	
II	17 (85)	–	
III	1 (5)	–	
Medical history, n (%)			
Atrial fibrillation	8 (40)	–	
Hypertension	8 (40)	–	
Diabetes	-	–	
Significant coronary artery disease	-	–	
Dyslipidaemia	4 (20)	–	
Medications, n (%)			
ACE-I /ARB-II blocker	18 (90)	–	
Beta-blocker	17 (85)	–	
Spironolactone	10 (50)	–	
Diuretics	11 (55)	–	
Digoxin	3 (15)	–	
Anticoagulation	9 (45)	–	
Statin	7 (35)	–	
Body mass index (kg/m^2)	28±5	26±4	0.08
Systolic blood pressure (mmHg)	126±10	128±10	0.48
Diastolic blood pressure (mmHg)	77±14	75±6	0.65
Heart rate (bpm)	64±12	60±9	0.24
Biochemical (mmol/L)			
Blood glucose	5.3±0.7	5.1±0.9	0.59
Total cholesterol	5.1±1.0	5.4±0.3	0.33
Triglycerides	1.4±0.7	1.1 0.3	0.14
Low-density lipoprotein	3.0±0.9	3.1±1.0	0.68
High-density lipoprotein	1.3±0.5	1.3±0.3	0.99
Non esterified free FA	0.5±0.1	0.5±0.3	0.58
HOMA index*	4.5±2.6	–	
Insulin (mU/L)*	14.2±9.2	–	

Values are mean ± SD or percentages. ACE indicates angiotensin-converting enzyme-inhibitors; ARB, angiotensin-receptor antagonist-II; HOMA, homeostasis model of assessment. *Not available in normals.

Cardiovascular MR imaging and spectroscopy

CMR results are summarised in **Table 2**. As expected, DCM patients had significantly higher LV volumes and mass, reduced function (LVEF and strain) when compared to the normal controls. LGE imaging demonstrated that myocardial fibrosis was most prevalent in DCM (75%) versus 10% in the normal controls. The predominant pattern of LGE was mid-wall involving mainly in the septum and inferior wall. An example of a DCM patient with mid-wall fibrosis is shown in **Figure 5.1**. Control subjects had LGE involving the inferior left/right-ventricular insertion point (n=2).

Table 2: Cardiovascular MRI and spectroscopy

	DCM (n = 20)	Normal (n = 20)	P value
Cardiac lipid/water ratio (%)	0.64±0.44	0.40 ± 0.13	0.03
Hepatic lipid/water ratio (%)*	3.1 (5.2)†	–	
LV ejection fraction (%)	39±9	70±3	<0.001
LV end-diastolic volume (ml)	229±78	146±29	<0.001
LV end-systolic volume (ml)	146±71	44±11	<0.001
LV mass index (g/m^2)	78±26	54±12	0.001
Peak global circumferential strain (%)ᵞ	-12.3±3.4	-20.9±1.7	<0.001
LGE present, n (%)	15 (75)	2 (10)	<0.001

Values are mean ± SD or percentages. †value is median and IQR.
*N=12 for DCM; hepatic lipid/water ratio was not measured in normal. ᵞN=12 for DCM.
LV indicates left ventricular; LGE, late gadolinium enhancement.

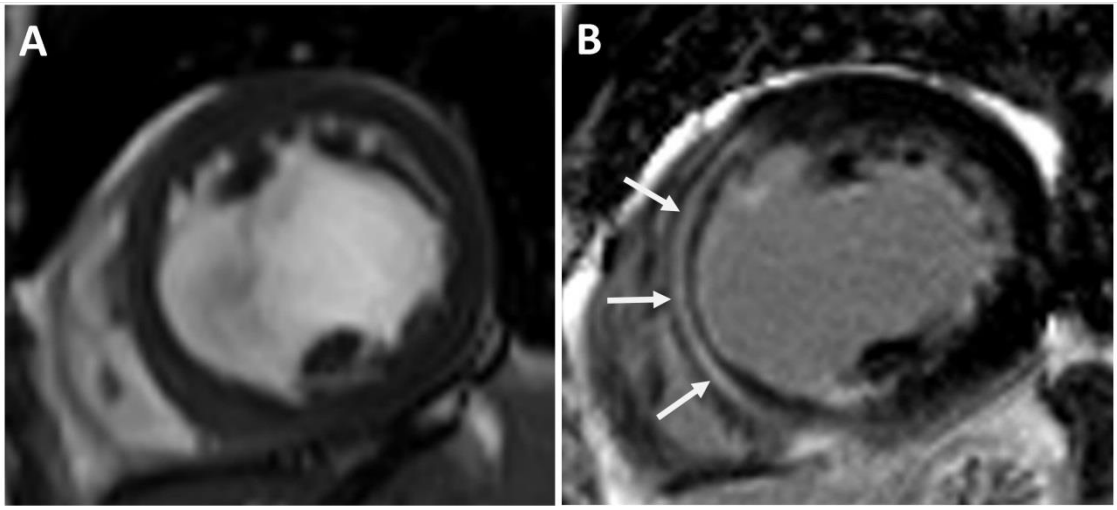

Figure 5.1. An example of a DCM patient dilated heart (A) and mid-wall fibrosis (B - white arrows).

DCM patients had significantly increased myocardial TG content when compared to the normal controls. The median level of liver TG content in the DCM cohort was 3.1% (IQR 5.2) with 4/12 (33%) had levels of >5%.

Relationship between MTC and other study variables

Myocardial TG content significantly correlated with BMI (r=0.40, p=0.01), LVEDV (r=0.54, p<0.001), LVESV (r=0.47, p=0.003), circumferential strain (r=0.42, p=0.02), but not with NYHA (r=0.21, p=0.20), age (r=-0.18, p=0.25), LVEF (r=-0.31, p=0.056) or LGE (r=0.28, p=0.08).

Table 3 shows bivariate correlations, and multiple regression analyses to determine independent associates of LVEDV and LVEF. LVEDV increased with increasing NYHA class, BMI, LVMI and strain whilst LVEF declined with increasing NYHA class, BMI, LV volumes and mass (LVEDV, LVESV, LVMI), strain and presence of LGE, but not with myocardial TG. Multivariable analyses showed that steatosis (myocardial TG) was an independent correlate of LVEDV, whilst both LVEDV and presence of LGE were independent predictors of LVEF. In view of the small sample size, we were careful in selecting the most appropriate variables in order to limit the number of independent variables. To determine independent associates of LVEDV, LVESV and LVMI were not included in the multivariate analysis as these are related to LVEDV. To determine independent associates of LVEF, LVESV and LVMI were not included due to highly related (multicollinearity i.e. tolerance value of <0.1), and strain was excluded as it is related to LVEF. NYHA class was excluded from both multivariate analyses on the grounds that it is not independent of LVEDV or LVEF.

Table 3: Associations of multiple study parameters with left ventricular end diastolic volume and left ventricular ejection fraction

	Left ventricular end diastolic volume				Left ventricular ejection fraction			
	Bivariate		Multivariate		Bivariate		Multivariate	
	R	P-Value	β	P-Value	R	P-Value	β	P-Value
Age	-0.23	0.16	–	–	-0.05	0.77	–	–
NYHA functional class	0.69	<0.001	–	–	-0.83	<0.001	–	–
Body mass index	0.52	0.001	0.17	0.34	-0.33	0.041	0.10	0.26
Left ventricular end diastolic volume	–	–	–	–	-0.71	<0.001	-0.46	<0.001
Left ventricular end systolic volume	0.95	<0.001	–	–	-0.86	<0.001	–	–
Left ventricular ejection fraction	–	–	–	–	–	–	–	–
Left ventricular mass index	0.45	0.001	–	–	-0.69	<0.001	–	–
Circumferential strain	0.59	<0.001	0.20	0.32	-0.92	<0.001	–	–
Presence of LGE	0.67	<0.001	0.29	0.17	-0.77	<0.001	-0.60	<0.001
Myocardial triglyceride content	0.54	<0.001	0.39	0.03	-0.31	0.056	–	–

NYHA indicates New York Heart Association; LGE, late gadolinium enhancement

There was highly significant correlation between myocardial TG and hepatic TG content, r=0.78, p=0.03. An example of myocardial and liver TG spectra is shown in **Figure 5.2.** There was no significant correlation between liver TG content and BMI.

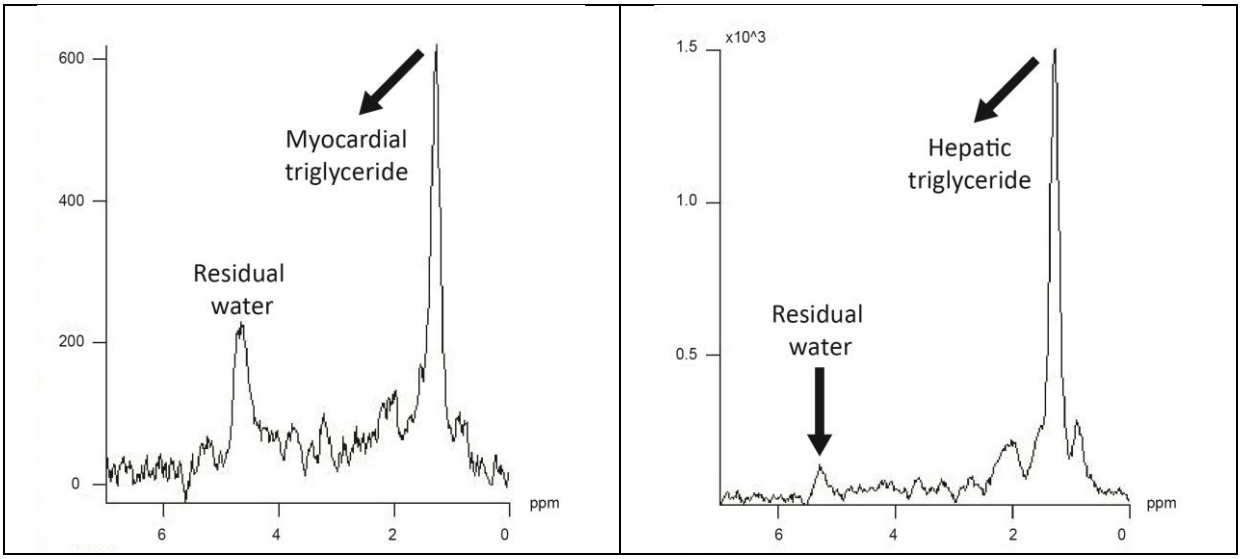

Figure 5.2: Examples of water suppressed spectra showing myocardial triglyceride peak (*left*) and hepatic triglyceride peak (*right*).

5.6. DISCUSSION

The present study showed that, by using in vivo MRS technique, cardiac steatosis is present and is independently associated with LV size in patients with non-ischaemic DCM. Furthermore, myocardial TG highly correlates with hepatic TG content.

There is some evidence demonstrating that heart failure causes insulin resistance albeit in the absence of diabetes or obesity.[65, 144] This is consistent with increased levels of HOMA index and insulin in our DCM cohorts, despite no evidence of diabetes or obesity. A previous study investigating idiopathic DCM showed that these biochemical abnormalities were two-fold increase when compared to normal controls.[145] Although it is believed that circulating FA is elevated in DCM patients, NEFA level was similar in our DCM and normal cohorts, and this could be explained by the high proportion of DCM patients who were taking anti failure therapy (e.g. beta-blockers) which might have affected plasma FA levels.[146, 147]

Because abnormal substrate metabolism and insulin resistance are seen in the failing heart, it is hypothesised that both factors could potentially contribute to intramyocardial lipid overload. Cardiac steatosis has been demonstrated in HF from animal studies,[11, 148] but data from humans are scarce and limited to individual case reports and findings from explanted hearts.[93, 149] Data on ^{1}H-MRS measured myocardial lipid levels in patients with DCM is limited. Only one published report by Nakae *et al* in the recent years, did not find significant difference in myocardial TG content in patients with idiopathic DCM and the normal controls.[150] The reason for the difference in these 2 reports is unclear, but potentially because of the smaller number of patients in the previous study (n=12 vs. n=20). The

current findings however are consistent with the level of myocardial TG in another cohort of DCM patients (n=15) assessed by our group previously, with lipid/water ratio of 0.7±0.3%.[151]

The present data demonstrated that in DCM, steatosis is independently associated with LV dilatation, in line with the lipotoxicity hypothesis as discussed in Chapter 1. Excessive accumulation of TG in the myocardium can induce pathologic remodelling of the heart characterised by apoptosis, progressive chamber dilatation and contractile dysfunction.[93, 152] We selected LVEDV as a dependent variable in the multivariate analysis as it is a good reflection of LV remodelling, whereas LVESV may be less reproducible than LVEDV as asymmetric LV contraction may result in less accurate measurements of LVESV.[153] We found that myocardial steatosis correlated with the degree of LV strain impairment but not LVEF (although there is a trend towards worsening of LVEF with increasing myocardial TG, p=0.56), suggesting that strain may be more accurate (less load dependent compared with LVEF) measure of LV contractile function. Nevertheless, we selected LVEF as it is an established technique for assessment of LV function, in particular when there is relatively advanced LV functional impairment, and is the most widely used clinical marker for systolic heart failure.[154] On the other hand, strain (myocardial deformation assessment) is useful for detection of subclinical LV dysfunction in a variety of conditions known to have myocardial dysfunction despite preserved LVEF.[155] Furthermore, only a small number of patients underwent strain imaging (n=12 for strain vs. n=20 for LVEF), hence LVEF was more appropriate dependent variable for LV function in the multivariate model. It is not surprising that that myocardial fibrosis, which was predominantly mid-wall pattern, as previously shown[75, 156] had significant independent association with LVEF.[75, 157] Interestingly, given the established association between fibrosis and ventricular remodelling, regression analysis

suggests that steatosis is a stronger/more important associate with LV remodelling when compared with fibrosis. Given the modest correlation found in our study (R=0.39), the significance of this finding is uncertain. Future longitudinal, larger scale studies are needed to assess this.

It is well known that diabetes and obesity have been associated with lipid accumulation in various organs such as skeletal muscle and the liver.[158-161] Although it seems obvious that hepatic TG will be increased in parallel to cardiac TG in HF patients, the data supporting this are lacking in humans. In a rat model of congestive HF, it has been shown that abnormal hepatic metabolism leads to increased level of TG in the liver.[162] Our data showed that about a third (33%) of our DCM patients had hepatic TG content of above the upper limit of normal (> 5%)[86] despite no identifiable risk factors for fatty liver disease such as diabetes, excessive alcohol intake or abnormal liver function tests. This is the first study using in vivo MR technique demonstrating the presence of cardiac steatosis which corresponds to hepatic TG content in patients with idiopathic DCM. This is in accordance with a recent study showing significant correlation between cardiac and hepatic TG contents in non-diabetic obese subjects.[163] This supports the notion that lipid accumulation also occurs in the heart of insulin resistance state other than the liver, suggesting that myocardial *and* hepatic triglyceride accumulation might be a common feature in DCM.[164] In healthy subjects given high fat and energy diet, however this does not seem to be the case. Only hepatic TG but not myocardial TG was affected suggesting that the same mechanism may not be a feature in normal condition.[165] Further studies would be essential to further investigate this.

5.7. STUDY LIMITATIONS

The main limitation of this study is the small study population, particularly patients having CMR tagging and liver spectroscopy. Therefore confirmation of the findings in a larger scale studies is warranted. The cross-sectional nature of the current data does not allow one to draw conclusions as to whether steatosis occurs before or after fibrosis. Longitudinal studies in patients with less severe DCM with assessment of steatosis and LGE may be able to answer this question.

5.8. CONCLUSIONS

In conclusions, DCM is characterised by insulin resistance and myocardial steatosis which is independently associated with LV remodelling. Interestingly, myocardial steatosis correlates highly with hepatic TG content. Our study gives insights into the pathophysiology of LV dysfunction in patients with HF due to non-ischaemic DCM. Therefore cardiac steatosis may become a potential biomarker in this condition, and that therapies aimed at lipotoxity and insulin resistance might be beneficial to improve cardiac function in patients with DCM.

CHAPTER 6: GENERAL CONCLUSIONS

This work was carried out to assess myocardial metabolism and function in two different disease entities, hypertrophy and heart failure. I have shown that multiparametric MR assessment (LV function including myocardial strain, perfusion, oxygenation, LGE, and spectroscopy) in a single centre setting was largely well tolerated, even by the more elderly AS patients and those with a higher degree of aortic valve stenosis. In DCM patients, LV function, strain, LGE, and proton spectroscopy of the heart and liver were also feasible.

In Chapters 3 and 5, I have shown that increased myocardial TG content was evident in both hypertrophied and dilated hearts, supporting the theory that both these conditions share a common feature of metabolic derangements, and that cardiac steatosis may not be restricted to only obesity and diabetes. Importantly, I demonstrated that patients with high myocardial TG levels have significantly greater impairment of LV strain in AS, and LV dilatation in DCM. The present research studies provide a proof of concept of ^{1}H-MRS as a valid and feasible, non-invasive assessment of the metabolic derangements of the myocardium. Together with strain imaging, the method offers a strategy for early diagnosis of myocardial complications that may occur due to lipotoxic disorders. Remarkable improvement in steatosis post AVR suggests that myocardial steatosis is indeed a modifiable condition. These initial data may serve as a starting point for future prospective studies to determine if metabolic modulation (e.g. peroxisome proliferator-activated receptor - PPAR agonist) that reduce myocardial TG,[166, 167] leads to improvement in LV function.

In Chapter 4, I have shown that patients with severe AS have blunted oxygenation in addition to impaired perfusion during vasodilator stress. BOLD CMR is an exciting new technique for measuring tissue oxygenation in the myocardium and has excellent potential to be used as a surrogate endpoint of clinical research. Compared to perfusion, BOLD-CMR is a more direct measure of myocardial microvascular status without the need to use a contrast agent. The current study yields important insights into the potential mechanism of myocardial ischaemia in AS patients and provides a new avenue for potential drug trial aimed at ischaemic cascade (e.g. perhexiline),[140] which may be useful for patients who are not fit to undergo surgical AVR or who still have symptoms post AVR.

The current studies are limited by small sample sizes in line with their proof of principle nature. Furthermore, these studies are cross-sectional and therefore, it is not possible to determine whether the observed associations between myocardial TG and LV contractive function are causal. However, our findings are entirely consistent with experimental and animal studies that establish a causal link between steatosis, the production of lipotoxic metabolites and resulting cardiac dysfunction. Although CMR is safe and does not entail exposure to ionizing radiation, it precludes its use in patients who are contraindicated to have MRI (e.g. pacemaker, metal implants, claustrophobia) and not tolerating a vasodilator stress test. The additional time taken to acquire spectroscopy, BOLD, strain and the length of post-processing time, the variability of measures and lack of multicentre trial evidence in these areas with outcome data to support the routine use. Finally, due to the relatively long and complex scan protocol in high risk AS patients, it was not feasible to perform repeatability tests in the current study, thus reproducibility of BOLD-CMR, ^{1}H-MRS and strain parameters in AS patients is unknown.

In summary, CMR offers the opportunity for sophisticated analysis of cardiac metabolism and function in the hypertrophied and failing heart. Many of the CMR and MRS measurements in my studies (e.g. lipidosis assessment with ^{1}H-MRS and myocardial oxygenation assessment with BOLD-CMR) have the potential to become important imaging biomarker tools for diagnostic and prognostic assessment as well as for monitoring therapy in the near future.

REFERENCES

1. Shivu GN, Abozguia K, Phan TT, Ahmed I, Henning A, Frenneaux M. (31)p magnetic resonance spectroscopy to measure in vivo cardiac energetics in normal myocardium and hypertrophic cardiomyopathy: Experiences at 3t. *Eur J Radiol*. 2008
2. Neubauer S, Horn M, Pabst T, Harre K, Stromer H, Bertsch G, Sandstede J, Ertl G, Hahn D, Kochsiek K. Cardiac high-energy phosphate metabolism in patients with aortic valve disease assessed by 31p-magnetic resonance spectroscopy. *J Investig Med*. 1997;45:453-462
3. Neubauer S, Krahe T, Schindler R, Horn M, Hillenbrand H, Entzeroth C, Mader H, Kromer EP, Riegger GA, Lackner K, et al. 31p magnetic resonance spectroscopy in dilated cardiomyopathy and coronary artery disease. Altered cardiac high-energy phosphate metabolism in heart failure. *Circulation*. 1992;86:1810-1818
4. Neubauer S, Horn M, Pabst T, Godde M, Lubke D, Jilling B, Hahn D, Ertl G. Contributions of 31p-magnetic resonance spectroscopy to the understanding of dilated heart muscle disease. *Eur Heart J*. 1995;16 Suppl O:115-118
5. Neubauer S, Horn M, Cramer M, Harre K, Newell JB, Peters W, Pabst T, Ertl G, Hahn D, Ingwall JS, Kochsiek K. Myocardial phosphocreatine-to-atp ratio is a predictor of mortality in patients with dilated cardiomyopathy. *Circulation*. 1997;96:2190-2196
6. Stanley WC, Recchia FA, Lopaschuk GD. Myocardial substrate metabolism in the normal and failing heart. *Physiol Rev*. 2005;85:1093-1129
7. Szczepaniak LS, Babcock EE, Schick F, Dobbins RL, Garg A, Burns DK, McGarry JD, Stein DT. Measurement of intracellular triglyceride stores by h spectroscopy: Validation in vivo. *Am J Physiol*. 1999;276:E977-989
8. Ishii M, Yoshioka Y, Ishida W, Kaneko Y, Fujiwara F, Taneichi H, Miura M, Toshihiro M, Takebe N, Iwai M, Suzuki K, Satoh J. Liver fat content measured by magnetic resonance spectroscopy at 3.0 tesla independently correlates with plasminogen activator inhibitor-1 and body mass index in type 2 diabetic subjects. *Tohoku J Exp Med*. 2005;206:23-30
9. Sinha R, Dufour S, Petersen KF, LeBon V, Enoksson S, Ma YZ, Savoye M, Rothman DL, Shulman GI, Caprio S. Assessment of skeletal muscle triglyceride content by (1)h nuclear magnetic resonance spectroscopy in lean and obese adolescents: Relationships to insulin sensitivity, total body fat, and central adiposity. *Diabetes*. 2002;51:1022-1027
10. Szczepaniak LS, Dobbins RL, Metzger GJ, Sartoni-D'Ambrosia G, Arbique D, Vongpatanasin W, Unger R, Victor RG. Myocardial triglycerides and systolic function in humans: In vivo evaluation by localized proton spectroscopy and cardiac imaging. *Magn Reson Med*. 2003;49:417-423
11. Chiu HC, Kovacs A, Ford DA, Hsu FF, Garcia R, Herrero P, Saffitz JE, Schaffer JE. A novel mouse model of lipotoxic cardiomyopathy. *J Clin Invest*. 2001;107:813-822
12. Wittels B, Spann JF, Jr. Defective lipid metabolism in the failing heart. *J Clin Invest*. 1968;47:1787-1794
13. Bishop SP, Altschuld RA. Increased glycolytic metabolism in cardiac hypertrophy and congestive failure. *Am J Physiol*. 1970;218:153-159
14. Brindley DN, Kok BP, Kienesberger PC, Lehner R, Dyck JR. Shedding light on the enigma of myocardial lipotoxicity: The involvement of known and putative regulators of fatty acid storage and mobilization. *Am J Physiol Endocrinol Metab*. 2010;298:E897-908
15. Opie LH. The metabolic vicious cycle in heart failure. *Lancet*. 2004;364:1733-1734
16. Tuunanen H, Knuuti J. Metabolic remodelling in human heart failure. *Cardiovasc Res*. 2011;90:251-257

17. Kankaanpaa M, Lehto HR, Parkka JP, Komu M, Viljanen A, Ferrannini E, Knuuti J, Nuutila P, Parkkola R, Iozzo P. Myocardial triglyceride content and epicardial fat mass in human obesity: Relationship to left ventricular function and serum free fatty acid levels. *J Clin Endocrinol Metab*. 2006;91:4689-4695
18. Ng AC, Delgado V, Bertini M, van der Meer RW, Rijzewijk LJ, Hooi Ewe S, Siebelink HM, Smit JW, Diamant M, Romijn JA, de Roos A, Leung DY, Lamb HJ, Bax JJ. Myocardial steatosis and biventricular strain and strain rate imaging in patients with type 2 diabetes mellitus. *Circulation*. 2010;122:2538-2544
19. Borisov AB, Ushakov AV, Zagorulko AK, Novikov NY, Selivanova KF, Edwards CA, Russell MW. Intracardiac lipid accumulation, lipoatrophy of muscle cells and expansion of myocardial infarction in type 2 diabetic patients. *Micron*. 2008;39:944-951
20. Bottomley PA. Mr spectroscopy of the human heart: The status and the challenges. *Radiology*. 1994;191:593-612
21. Holloway CJ, Suttie J, Dass S, Neubauer S. Clinical cardiac magnetic resonance spectroscopy. *Prog Cardiovasc Dis*. 2011;54:320-327
22. McMurray JJ, Adamopoulos S, Anker SD, Auricchio A, Bohm M, Dickstein K, Falk V, Filippatos G, Fonseca C, Gomez-Sanchez MA, Jaarsma T, Kober L, Lip GY, Maggioni AP, Parkhomenko A, Pieske BM, Popescu BA, Ronnevik PK, Rutten FH, Schwitter J, Seferovic P, Stepinska J, Trindade PT, Voors AA, Zannad F, Zeiher A. Esc guidelines for the diagnosis and treatment of acute and chronic heart failure 2012: The task force for the diagnosis and treatment of acute and chronic heart failure 2012 of the european society of cardiology. Developed in collaboration with the heart failure association (hfa) of the esc. *Eur Heart J*. 2012;33:1787-1847
23. Vahanian A, Alfieri O, Andreotti F, Antunes MJ, Baron-Esquivias G, Baumgartner H, Borger MA, Carrel TP, De Bonis M, Evangelista A, Falk V, Lung B, Lancellotti P, Pierard L, Price S, Schafers HJ, Schuler G, Stepinska J, Swedberg K, Takkenberg J, Von Oppell UO, Windecker S, Zamorano JL, Zembala M. Guidelines on the management of valvular heart disease (version 2012): The joint task force on the management of valvular heart disease of the european society of cardiology (esc) and the european association for cardio-thoracic surgery (eacts). *Eur J Cardiothorac Surg*. 2012;42:S1-44
24. Sjoli B, Grenne B, Smiseth OA, Edvardsen T, Brunvand H. The advantage of global strain compared to left ventricular ejection fraction to predict outcome after acute myocardial infarction. *Echocardiography*. 2011;28:556-563
25. Ozkan A, Kapadia S, Tuzcu M, Marwick TH. Assessment of left ventricular function in aortic stenosis. *Nat Rev Cardiol*. 2011;8:494-501
26. Lakdawala NK, Thune JJ, Colan SD, Cirino AL, Farrohi F, Rivero J, McDonough B, Sparks E, Orav EJ, Seidman JG, Seidman CE, Ho CY. Subtle abnormalities in contractile function are an early manifestation of sarcomere mutations in dilated cardiomyopathy. *Circ Cardiovasc Genet*. 2012;5:503-510
27. Duan F, Xie M, Wang X, Li Y, He L, Jiang L, Fu Q. Preliminary clinical study of left ventricular myocardial strain in patients with non-ischemic dilated cardiomyopathy by three-dimensional speckle tracking imaging. *Cardiovasc Ultrasound*. 2012;10:8
28. Gotte MJ, Germans T, Russel IK, Zwanenburg JJ, Marcus JT, van Rossum AC, van Veldhuisen DJ. Myocardial strain and torsion quantified by cardiovascular magnetic resonance tissue tagging: Studies in normal and impaired left ventricular function. *J Am Coll Cardiol*. 2006;48:2002-2011
29. Shehata ML, Cheng S, Osman NF, Bluemke DA, Lima JA. Myocardial tissue tagging with cardiovascular magnetic resonance. *J Cardiovasc Magn Reson*. 2009;11:55
30. Edvardsen T, Rosen BD, Pan L, Jerosch-Herold M, Lai S, Hundley WG, Sinha S, Kronmal RA, Bluemke DA, Lima JA. Regional diastolic dysfunction in individuals with left ventricular

hypertrophy measured by tagged magnetic resonance imaging--the multi-ethnic study of atherosclerosis (mesa). *Am Heart J*. 2006;151:109-114

31. Edvardsen T, Gerber BL, Garot J, Bluemke DA, Lima JA, Smiseth OA. Quantitative assessment of intrinsic regional myocardial deformation by doppler strain rate echocardiography in humans: Validation against three-dimensional tagged magnetic resonance imaging. *Circulation*. 2002;106:50-56
32. Teske AJ, De Boeck BW, Melman PG, Sieswerda GT, Doevendans PA, Cramer MJ. Echocardiographic quantification of myocardial function using tissue deformation imaging, a guide to image acquisition and analysis using tissue doppler and speckle tracking. *Cardiovasc Ultrasound*. 2007;5:27
33. Maciver DH. The relative impact of circumferential and longitudinal shortening on left ventricular ejection fraction and stroke volume. *Exp Clin Cardiol*. 2012;17:5-11
34. Bohs LN, Trahey GE. A novel method for angle independent ultrasonic imaging of blood flow and tissue motion. *IEEE Trans Biomed Eng*. 1991;38:280-286
35. Mondillo S, Galderisi M, Mele D, Cameli M, Lomoriello VS, Zaca V, Ballo P, D'Andrea A, Muraru D, Losi M, Agricola E, D'Errico A, Buralli S, Sciomer S, Nistri S, Badano L. Speckle-tracking echocardiography: A new technique for assessing myocardial function. *J Ultrasound Med*. 2011;30:71-83
36. Amundsen BH, Helle-Valle T, Edvardsen T, Torp H, Crosby J, Lyseggen E, Stoylen A, Ihlen H, Lima JA, Smiseth OA, Slordahl SA. Noninvasive myocardial strain measurement by speckle tracking echocardiography: Validation against sonomicrometry and tagged magnetic resonance imaging. *J Am Coll Cardiol*. 2006;47:789-793
37. Seo Y, Ishizu T, Enomoto Y, Sugimori H, Yamamoto M, Machino T, Kawamura R, Aonuma K. Validation of 3-dimensional speckle tracking imaging to quantify regional myocardial deformation. *Circ Cardiovasc Imaging*. 2009;2:451-459
38. Gorcsan J, Tanaka H. [are new myocardial tracking systems of three-dimensional strain a reality in daily clinical practice?]. *Rev Esp Cardiol*. 2011;64:1082-1089
39. Herzka DA, Guttman MA, McVeigh ER. Myocardial tagging with ssfp. *Magn Reson Med*. 2003;49:329-340
40. Stewart BF, Siscovick D, Lind BK, Gardin JM, Gottdiener JS, Smith VE, Kitzman DW, Otto CM. Clinical factors associated with calcific aortic valve disease. *Journal of the American College of Cardiology*. 1997;29:630-634
41. Bonow RO, Carabello BA, Chatterjee K, de Leon AC, Jr., Faxon DP, Freed MD, Gaasch WH, Lytle BW, Nishimura RA, O'Gara PT, O'Rourke RA, Otto CM, Shah PM, Shanewise JS. 2008 focused update incorporated into the acc/aha 2006 guidelines for the management of patients with valvular heart disease: A report of the american college of cardiology/american heart association task force on practice guidelines (writing committee to revise the 1998 guidelines for the management of patients with valvular heart disease). Endorsed by the society of cardiovascular anesthesiologists, society for cardiovascular angiography and interventions, and society of thoracic surgeons. *J Am Coll Cardiol*. 2008;52:e1-142
42. Vahanian A, Alfieri O, Andreotti F, Antunes MJ, Baron-Esquivias G, Baumgartner H, Borger MA, Carrel TP, De Bonis M, Evangelista A, Falk V, Iung B, Lancellotti P, Pierard L, Price S, Schafers HJ, Schuler G, Stepinska J, Swedberg K, Takkenberg J, Von Oppell UO, Windecker S, Zamorano JL, Zembala M. Guidelines on the management of valvular heart disease (version 2012). *Eur Heart J*. 2012;33:2451-2496
43. Schwarz F, Baumann P, Manthey J, Hoffmann M, Schuler G, Mehmel HC, Schmitz W, Kubler W. The effect of aortic valve replacement on survival. *Circulation*. 1982;66:1105-1110
44. Carabello BA. Clinical practice. Aortic stenosis. *N Engl J Med*. 2002;346:677-682
45. Lang RM, Bierig M, Devereux RB, Flachskampf FA, Foster E, Pellikka PA, Picard MH, Roman MJ, Seward J, Shanewise J, Solomon S, Spencer KT, St John Sutton M, Stewart W. Recommendations for chamber quantification. *Eur J Echocardiogr*. 2006;7:79-108

46. Ross J, Jr., Braunwald E. Aortic stenosis. *Circulation*. 1968;38:61-67
47. Monin JL, Monchi M, Gest V, Duval-Moulin AM, Dubois-Rande JL, Gueret P. Aortic stenosis with severe left ventricular dysfunction and low transvalvular pressure gradients: Risk stratification by low-dose dobutamine echocardiography. *J Am Coll Cardiol*. 2001;37:2101-2107
48. Carabello BA. Evaluation and management of patients with aortic stenosis. *Circulation*. 2002;105:1746-1750
49. Yarbrough WM, Mukherjee R, Ikonomidis JS, Zile MR, Spinale FG. Myocardial remodeling with aortic stenosis and after aortic valve replacement: Mechanisms and future prognostic implications. *J Thorac Cardiovasc Surg*. 2012;143:656-664
50. Rosenhek R, Zilberszac R, Schemper M, Czerny M, Mundigler G, Graf S, Bergler-Klein J, Grimm M, Gabriel H, Maurer G. Natural history of very severe aortic stenosis. *Circulation*. 2010;121:151-156
51. Kang DH, Park SJ, Rim JH, Yun SC, Kim DH, Song JM, Choo SJ, Park SW, Song JK, Lee JW, Park PW. Early surgery versus conventional treatment in asymptomatic very severe aortic stenosis. *Circulation*. 2010;121:1502-1509
52. Greve AM, Boman K, Gohlke-Baerwolf C, Kesaniemi YA, Nienaber C, Ray S, Egstrup K, Rossebo AB, Devereux RB, Kober L, Willenheimer R, Wachtell K. Clinical implications of electrocardiographic left ventricular strain and hypertrophy in asymptomatic patients with aortic stenosis: The simvastatin and ezetimibe in aortic stenosis study. *Circulation*. 2012;125:346-353
53. Blais C, Dumesnil JG, Baillot R, Simard S, Doyle D, Pibarot P. Impact of valve prosthesis-patient mismatch on short-term mortality after aortic valve replacement. *Circulation*. 2003;108:983-988
54. Cioffi G, Faggiano P, Vizzardi E, Tarantini L, Cramariuc D, Gerdts E, de Simone G. Prognostic effect of inappropriately high left ventricular mass in asymptomatic severe aortic stenosis. *Heart*. 2011;97:301-307
55. Azevedo CF, Nigri M, Higuchi ML, Pomerantzeff PM, Spina GS, Sampaio RO, Tarasoutchi F, Grinberg M, Rochitte CE. Prognostic significance of myocardial fibrosis quantification by histopathology and magnetic resonance imaging in patients with severe aortic valve disease. *J Am Coll Cardiol*. 2010;56:278-287
56. Zito C, Salvia J, Cusma-Piccione M, Antonini-Canterin F, Lentini S, Oreto G, Di Bella G, Montericcio V, Carerj S. Prognostic significance of valvuloarterial impedance and left ventricular longitudinal function in asymptomatic severe aortic stenosis involving three-cuspid valves. *Am J Cardiol*. 2011;108:1463-1469
57. Stewart S, Jenkins A, Buchan S, McGuire A, Capewell S, McMurray JJ. The current cost of heart failure to the national health service in the uk. *Eur J Heart Fail*. 2002;4:361-371
58. Yancy CW, Jessup M, Bozkurt B, Butler J, Casey DE, Jr., Drazner MH, Fonarow GC, Geraci SA, Horwich T, Januzzi JL, Johnson MR, Kasper EK, Levy WC, Masoudi FA, McBride PE, McMurray JJ, Mitchell JE, Peterson PN, Riegel B, Sam F, Stevenson LW, Tang WH, Tsai EJ, Wilkoff BL. 2013 accf/aha guideline for the management of heart failure: A report of the american college of cardiology foundation/american heart association task force on practice guidelines. *Circulation*. 2013
59. McMurray JJ, Pfeffer MA. Heart failure. *Lancet*. 2005;365:1877-1889
60. Elliott P, Andersson B, Arbustini E, Bilinska Z, Cecchi F, Charron P, Dubourg O, Kuhl U, Maisch B, McKenna WJ, Monserrat L, Pankuweit S, Rapezzi C, Seferovic P, Tavazzi L, Keren A. Classification of the cardiomyopathies: A position statement from the european society of cardiology working group on myocardial and pericardial diseases. *Eur Heart J*. 2008;29:270-276
61. Elliott P. Cardiomyopathy. Diagnosis and management of dilated cardiomyopathy. *Heart*. 2000;84:106-112

62. Neubauer S. The failing heart--an engine out of fuel. *N Engl J Med*. 2007;356:1140-1151
63. Richardson M, Freemantle N, Calvert MJ, Cleland JG, Tavazzi L. Predictors and treatment response with cardiac resynchronization therapy in patients with heart failure characterized by dyssynchrony: A pre-defined analysis from the care-hf trial. *Eur Heart J*. 2007;28:1827-1834
64. Costanzo MR. Selection and treatment of candidates for heart transplantation. *Semin Thorac Cardiovasc Surg*. 1996;8:113-125
65. Paolisso G, De Riu S, Marrazzo G, Verza M, Varricchio M, D'Onofrio F. Insulin resistance and hyperinsulinemia in patients with chronic congestive heart failure. *Metabolism*. 1991;40:972-977
66. Nikolaidis LA, Sturzu A, Stolarski C, Elahi D, Shen YT, Shannon RP. The development of myocardial insulin resistance in conscious dogs with advanced dilated cardiomyopathy. *Cardiovasc Res*. 2004;61:297-306
67. AlZadjali MA, Godfrey V, Khan F, Choy A, Doney AS, Wong AK, Petrie JR, Struthers AD, Lang CC. Insulin resistance is highly prevalent and is associated with reduced exercise tolerance in nondiabetic patients with heart failure. *J Am Coll Cardiol*. 2009;53:747-753
68. Pennell DJ, Sechtem UP, Higgins CB, Manning WJ, Pohost GM, Rademakers FE, van Rossum AC, Shaw LJ, Yucel EK. Clinical indications for cardiovascular magnetic resonance (cmr): Consensus panel report. *J Cardiovasc Magn Reson*. 2004;6:727-765
69. Karamitsos TD, Hudsmith LE, Selvanayagam JB, Neubauer S, Francis JM. Operator induced variability in left ventricular measurements with cardiovascular magnetic resonance is improved after training. *J Cardiovasc Magn Reson*. 2007;9:777-783
70. Hudsmith LE, Petersen SE, Francis JM, Robson MD, Neubauer S. Normal human left and right ventricular and left atrial dimensions using steady state free precession magnetic resonance imaging. *J Cardiovasc Magn Reson*. 2005;7:775-782
71. Stuber M, Spiegel MA, Fischer SE, Scheidegger MB, Danias PG, Pedersen EM, Boesiger P. Single breath-hold slice-following cspamm myocardial tagging. *MAGMA*. 1999;9:85-91
72. Axel L, Dougherty L. Mr imaging of motion with spatial modulation of magnetization. *Radiology*. 1989;171:841-845
73. Donekal S, Ambale-Venkatesh B, Berkowitz S, Wu CO, Choi EY, Fernandes V, Yan R, Harouni AA, Bluemke DA, Lima JA. Inter-study reproducibility of cardiovascular magnetic resonance tagging. *J Cardiovasc Magn Reson*. 2013;15:37
74. Dweck MR, Joshi S, Murigu T, Alpendurada F, Jabbour A, Melina G, Banya W, Gulati A, Roussin I, Raza S, Prasad NA, Wage R, Quarto C, Angeloni E, Refice S, Sheppard M, Cook SA, Kilner PJ, Pennell DJ, Newby DE, Mohiaddin RH, Pepper J, Prasad SK. Midwall fibrosis is an independent predictor of mortality in patients with aortic stenosis. *J Am Coll Cardiol*. 2011;58:1271-1279
75. Assomull RG, Prasad SK, Lyne J, Smith G, Burman ED, Khan M, Sheppard MN, Poole-Wilson PA, Pennell DJ. Cardiovascular magnetic resonance, fibrosis, and prognosis in dilated cardiomyopathy. *J Am Coll Cardiol*. 2006;48:1977-1985
76. Flett AS, Hasleton J, Cook C, Hausenloy D, Quarta G, Ariti C, Muthurangu V, Moon JC. Evaluation of techniques for the quantification of myocardial scar of differing etiology using cardiac magnetic resonance. *JACC Cardiovasc Imaging*. 2011;4:150-156
77. Selvanayagam JB, Jerosch-Herold M, Porto I, Sheridan D, Cheng AS, Petersen SE, Searle N, Channon KM, Banning AP, Neubauer S. Resting myocardial blood flow is impaired in hibernating myocardium: A magnetic resonance study of quantitative perfusion assessment. *Circulation*. 2005;112:3289-3296
78. Cerqueira MD, Weissman NJ, Dilsizian V, Jacobs AK, Kaul S, Laskey WK, Pennell DJ, Rumberger JA, Ryan T, Verani MS. Standardized myocardial segmentation and nomenclature for tomographic imaging of the heart: A statement for healthcare professionals from the

cardiac imaging committee of the council on clinical cardiology of the american heart association. *Circulation*. 2002;105:539-542

79. Simonetti OP, Kim RJ, Fieno DS, Hillenbrand HB, Wu E, Bundy JM, Finn JP, Judd RM. An improved mr imaging technique for the visualization of myocardial infarction. *Radiology*. 2001;218:215-223
80. Karamitsos TD, Leccisotti L, Arnold JR, Recio-Mayoral A, Bhamra-Ariza P, Howells RK, Searle N, Robson MD, Rimoldi OE, Camici PG, Neubauer S, Selvanayagam JB. Relationship between regional myocardial oxygenation and perfusion in patients with coronary artery disease: Insights from cardiovascular magnetic resonance and positron emission tomography. *Circ Cardiovasc Imaging*. 2010;3:32-40
81. Sharma P, Socolow J, Patel S, Pettigrew RI, Oshinski JN. Effect of gd-dtpa-bma on blood and myocardial t1 at 1.5t and 3t in humans. *J Magn Reson Imaging*. 2006;23:323-330
82. Nagel E, Klein C, Paetsch I, Hettwer S, Schnackenburg B, Wegscheider K, Fleck E. Magnetic resonance perfusion measurements for the noninvasive detection of coronary artery disease. *Circulation*. 2003;108:432-437
83. Reingold JS, McGavock JM, Kaka S, Tillery T, Victor RG, Szczepaniak LS. Determination of triglyceride in the human myocardium by magnetic resonance spectroscopy: Reproducibility and sensitivity of the method. *Am J Physiol Endocrinol Metab*. 2005;289:E935-939
84. van der Meer RW, Doornbos J, Kozerke S, Schar M, Bax JJ, Hammer S, Smit JW, Romijn JA, Diamant M, Rijzewijk LJ, de Roos A, Lamb HJ. Metabolic imaging of myocardial triglyceride content: Reproducibility of 1h mr spectroscopy with respiratory navigator gating in volunteers. *Radiology*. 2007;245:251-257
85. Rial B, Robson MD, Neubauer S, Schneider JE. Rapid quantification of myocardial lipid content in humans using single breath-hold 1h mrs at 3 tesla. *Magn Reson Med*. 2011;66:619-624
86. Szczepaniak LS, Nurenberg P, Leonard D, Browning JD, Reingold JS, Grundy S, Hobbs HH, Dobbins RL. Magnetic resonance spectroscopy to measure hepatic triglyceride content: Prevalence of hepatic steatosis in the general population. *Am J Physiol Endocrinol Metab*. 2005;288:E462-468
87. Schaffer JE. Lipotoxicity: When tissues overeat. *Curr Opin Lipidol*. 2003;14:281-287
88. Bilet L, van de Weijer T, Hesselink MK, Glatz JF, Lamb HJ, Wildberger J, Kooi ME, Schrauwen P, Schrauwen-Hinderling VB. Exercise-induced modulation of cardiac lipid content in healthy lean young men. *Basic Res Cardiol*. 2011;106:307-315
89. McGavock JM, Victor RG, Unger RH, Szczepaniak LS. Adiposity of the heart, revisited. *Ann Intern Med*. 2006;144:517-524
90. McGavock JM, Lingvay I, Zib I, Tillery T, Salas N, Unger R, Levine BD, Raskin P, Victor RG, Szczepaniak LS. Cardiac steatosis in diabetes mellitus: A 1h-magnetic resonance spectroscopy study. *Circulation*. 2007;116:1170-1175
91. Biederman RW, Doyle M, Yamrozik J, Williams RB, Rathi VK, Vido D, Caruppannan K, Osman N, Bress V, Rayarao G, Biederman CM, Mankad S, Magovern JA, Reichek N. Physiologic compensation is supranormal in compensated aortic stenosis: Does it return to normal after aortic valve replacement or is it blunted by coexistent coronary artery disease? An intramyocardial magnetic resonance imaging study. *Circulation*. 2005;112:I429-436
92. Baumgartner H, Hung J, Bermejo J, Chambers JB, Evangelista A, Griffin BP, Iung B, Otto CM, Pellikka PA, Quinones M. Echocardiographic assessment of valve stenosis: Eae/ase recommendations for clinical practice. *J Am Soc Echocardiogr*. 2009;22:1-23; quiz 101-102
93. Sharma S, Adrogue JV, Golfman L, Uray I, Lemm J, Youker K, Noon GP, Frazier OH, Taegtmeyer H. Intramyocardial lipid accumulation in the failing human heart resembles the lipotoxic rat heart. *FASEB J*. 2004;18:1692-1700
94. Ge F, Hu C, Hyodo E, Arai K, Zhou S, Lobdell Ht, Walewski JL, Homma S, Berk PD. Cardiomyocyte triglyceride accumulation and reduced ventricular function in mice with

obesity reflect increased long chain fatty acid uptake and de novo fatty acid synthesis. *J Obes*. 2012;2012:205648

95. Katz MH. Performing the analysis. *Multivariable analysis : A pratical guides for clinicians*. Cambridge University Press; 2002:84-116.
96. Zhang Y, Ren J. Role of cardiac steatosis and lipotoxicity in obesity cardiomyopathy. *Hypertension*. 2011;57:148-150
97. Marfella R, Di Filippo C, Portoghese M, Barbieri M, Ferraraccio F, Siniscalchi M, Cacciapuoti F, Rossi F, D'Amico M, Paolisso G. Myocardial lipid accumulation in patients with pressure-overloaded heart and metabolic syndrome[s]. *J Lipid Res*. 2009;50:2314-2323
98. Unger RH. Lipotoxic diseases. *Annu Rev Med*. 2002;53:319-336
99. Goldberg IJ, Trent CM, Schulze PC. Lipid metabolism and toxicity in the heart. *Cell Metab*. 2012;15:805-812
100. Golia G, Milano AD, Dodonov M, Bergamini C, Faggian G, Tomezzoli A, Vassanelli C. Influence of myocardial fibrosis on left ventricular hypertrophy in patients with symptomatic severe aortic stenosis. *Cardiology*. 2011;120:139-145
101. Motoyasu M, Kurita T, Onishi K, Uemura S, Tanigawa T, Okinaka T, Takeda K, Nakano T, Ito M, Sakuma H. Correlation between late gadolinium enhancement and diastolic function in hypertrophic cardiomyopathy assessed by magnetic resonance imaging. *Circ J*. 2008;72:378-383
102. Rijzewijk LJ, van der Meer RW, Smit JW, Diamant M, Bax JJ, Hammer S, Romijn JA, de Roos A, Lamb HJ. Myocardial steatosis is an independent predictor of diastolic dysfunction in type 2 diabetes mellitus. *J Am Coll Cardiol*. 2008;52:1793-1799
103. Iozzo P. Myocardial, perivascular, and epicardial fat. *Diabetes Care*. 2011;34 Suppl 2:S371-379
104. Beyerbacht HP, Lamb HJ, van Der Laarse A, Vliegen HW, Leujes F, Hazekamp MG, de Roos A, van Der Wall EE. Aortic valve replacement in patients with aortic valve stenosis improves myocardial metabolism and diastolic function. *Radiology*. 2001;219:637-643
105. Mannacio V, Di Tommaso L, Stassano P, De Amicis V, Vosa C. Myocardial metabolism and diastolic function after aortic valve replacement for aortic stenosis: Influence of patient-prosthesis mismatch. *Eur J Cardiothorac Surg*. 2012;41:316-321
106. Rajappan K, Rimoldi OE, Camici PG, Bellenger NG, Pennell DJ, Sheridan DJ. Functional changes in coronary microcirculation after valve replacement in patients with aortic stenosis. *Circulation*. 2003;107:3170-3175
107. Delgado V, Tops LF, van Bommel RJ, van der Kley F, Marsan NA, Klautz RJ, Versteegh MI, Holman ER, Schalij MJ, Bax JJ. Strain analysis in patients with severe aortic stenosis and preserved left ventricular ejection fraction undergoing surgical valve replacement. *Eur Heart J*. 2009;30:3037-3047
108. Algahim MF, Sen S, Taegtmeyer H. Bariatric surgery to unload the stressed heart: A metabolic hypothesis. *Am J Physiol Heart Circ Physiol*. 2012;302:H1539-1545
109. Dahl JS, Videbaek L, Poulsen MK, Rudbaek TR, Pellikka PA, Moller JE. Global strain in severe aortic valve stenosis: Relation to clinical outcome after aortic valve replacement. *Circ Cardiovasc Imaging*. 2012;5:613-620
110. Irvine T, Kenny A. Aortic stenosis and angina with normal coronary arteries: The role of coronary flow abnormalities. *Heart*. 1997;78:213-214
111. Rajappan K, Rimoldi OE, Dutka DP, Ariff B, Pennell DJ, Sheridan DJ, Camici PG. Mechanisms of coronary microcirculatory dysfunction in patients with aortic stenosis and angiographically normal coronary arteries. *Circulation*. 2002;105:470-476
112. Steadman CD, Jerosch-Herold M, Grundy B, Rafelt S, Ng LL, Squire IB, Samani NJ, McCann GP. Determinants and functional significance of myocardial perfusion reserve in severe aortic stenosis. *JACC Cardiovasc Imaging*. 2012;5:182-189

113. Clark MA, Arnold SV, Duhay FG, Thompson AK, Keyes MJ, Svensson LG, Bonow RO, Stockwell BT, Cohen DJ. Five-year clinical and economic outcomes among patients with medically managed severe aortic stenosis: Results from a medicare claims analysis. *Circ Cardiovasc Qual Outcomes*. 2012;5:697-704
114. Wong DT, Leung MC, Das R, Liew GY, Williams K, Dundon BK, Molaee P, Teo KS, Meredith IT, Worthley MI, Worthley SG. Diagnostic accuracy of adenosine stress cardiovascular magnetic resonance following acute st-segment elevation myocardial infarction post primary angioplasty. *J Cardiovasc Magn Reson*. 2011;13:62
115. Morton G, Chiribiri A, Ishida M, Hussain ST, Schuster A, Indermuehle A, Perera D, Knuuti J, Baker S, Hedstrom E, Schleyer P, O'Doherty M, Barrington S, Nagel E. Quantification of absolute myocardial perfusion in patients with coronary artery disease: Comparison between cardiovascular magnetic resonance and positron emission tomography. *J Am Coll Cardiol*. 2012;60:1546-1555
116. Jahnke C, Gebker R, Manka R, Schnackenburg B, Fleck E, Paetsch I. Navigator-gated 3d blood oxygen level-dependent cmr at 3.0-t for detection of stress-induced myocardial ischemic reactions. *JACC Cardiovasc Imaging*. 2010;3:375-384
117. Vohringer M, Flewitt JA, Green JD, Dharmakumar R, Wang J, Jr., Tyberg JV, Friedrich MG. Oxygenation-sensitive cmr for assessing vasodilator-induced changes of myocardial oxygenation. *J Cardiovasc Magn Reson*. 2010;12:20
118. Karamitsos TD, Arnold JR, Pegg TJ, Francis JM, Birks J, Jerosch-Herold M, Neubauer S, Selvanayagam JB. Patients with syndrome x have normal transmural myocardial perfusion and oxygenation: A 3-t cardiovascular magnetic resonance imaging study. *Circ Cardiovasc Imaging*. 2012;5:194-200
119. Arnold JR, Karamitsos TD, Bhamra-Ariza P, Francis JM, Searle N, Robson MD, Howells RK, Choudhury RP, Rimoldi OE, Camici PG, Banning AP, Neubauer S, Jerosch-Herold M, Selvanayagam JB. Myocardial oxygenation in coronary artery disease: Insights from blood oxygen level-dependent magnetic resonance imaging at 3 tesla. *J Am Coll Cardiol*. 2012;59:1954-1964
120. Weinsaft JW, Spincemaille P. Bold new directions in myocardial ischemia imaging-myocardial oxygenation assessment by cardiac magnetic resonance. *J Am Coll Cardiol*. 2012;59:1965-1967
121. Fallavollita JA, Malm BJ, Canty JM, Jr. Hibernating myocardium retains metabolic and contractile reserve despite regional reductions in flow, function, and oxygen consumption at rest. *Circ Res*. 2003;92:48-55
122. Ashrafian H, Redwood C, Blair E, Watkins H. Hypertrophic cardiomyopathy:A paradigm for myocardial energy depletion. *Trends Genet*. 2003;19:263-268
123. Crilley JG, Boehm EA, Blair E, Rajagopalan B, Blamire AM, Styles P, McKenna WJ, Ostman-Smith I, Clarke K, Watkins H. Hypertrophic cardiomyopathy due to sarcomeric gene mutations is characterized by impaired energy metabolism irrespective of the degree of hypertrophy. *J Am Coll Cardiol*. 2003;41:1776-1782
124. Briand M, Dumesnil JG, Kadem L, Tongue AG, Rieu R, Garcia D, Pibarot P. Reduced systemic arterial compliance impacts significantly on left ventricular afterload and function in aortic stenosis: Implications for diagnosis and treatment. *J Am Coll Cardiol*. 2005;46:291-298
125. McCann GP, Gan CT, Beek AM, Niessen HW, Vonk Noordegraaf A, van Rossum AC. Extent of mri delayed enhancement of myocardial mass is related to right ventricular dysfunction in pulmonary artery hypertension. *AJR Am J Roentgenol*. 2007;188:349-355
126. Marcus ML, Koyanagi S, Harrison DG, Doty DB, Hiratzka LF, Eastham CL. Abnormalities in the coronary circulation that occur as a consequence of cardiac hypertrophy. *Am J Med*. 1983;75:62-66

127. Marcus ML, Harrison DG, Chilian WM, Koyanagi S, Inou T, Tomanek RJ, Martins JB, Eastham CL, Hiratzka LF. Alterations in the coronary circulation in hypertrophied ventricles. *Circulation*. 1987;75:I19-25
128. Jerosch-Herold M. Quantification of myocardial perfusion by cardiovascular magnetic resonance. *J Cardiovasc Magn Reson*. 2010;12:57
129. Cullen JH, Horsfield MA, Reek CR, Cherryman GR, Barnett DB, Samani NJ. A myocardial perfusion reserve index in humans using first-pass contrast-enhanced magnetic resonance imaging. *J Am Coll Cardiol*. 1999;33:1386-1394
130. Bache RJ, Dai XZ. Myocardial oxygen consumption during exercise in the presence of left ventricular hypertrophy secondary to supravalvular aortic stenosis. *J Am Coll Cardiol*. 1990;15:1157-1164
131. Marcus ML, Doty DB, Hiratzka LF, Wright CB, Eastham CL. Decreased coronary reserve: A mechanism for angina pectoris in patients with aortic stenosis and normal coronary arteries. *N Engl J Med*. 1982;307:1362-1366
132. Laine H, Katoh C, Luotolahti M, Yki-Jarvinen H, Kantola I, Jula A, Takala TO, Ruotsalainen U, Iida H, Haaparanta M, Nuutila P, Knuuti J. Myocardial oxygen consumption is unchanged but efficiency is reduced in patients with essential hypertension and left ventricular hypertrophy. *Circulation*. 1999;100:2425-2430
133. James MA, Saadeh AM, Jones JV. Wall stress and hypertension. *J Cardiovasc Risk*. 2000;7:187-190
134. Karamitsos TD, Dass S, Suttie J, Sever E, Birks J, Holloway CJ, Robson MD, Jerosch-Herold M, Watkins H, Neubauer S. Blunted myocardial oxygenation response during vasodilator stress in patients with hypertrophic cardiomyopathy. *J Am Coll Cardiol*. 2013;61:1169-1176
135. Beache GM, Herzka DA, Boxerman JL, Post WS, Gupta SN, Faranesh AZ, Solaiyappan M, Bottomley PA, Weiss JL, Shapiro EP, Hill MN. Attenuated myocardial vasodilator response in patients with hypertensive hypertrophy revealed by oxygenation-dependent magnetic resonance imaging. *Circulation*. 2001;104:1214-1217
136. Lancellotti P, Donal E, Magne J, Moonen M, O'Connor K, Daubert JC, Pierard LA. Risk stratification in asymptomatic moderate to severe aortic stenosis: The importance of the valvular, arterial and ventricular interplay. *Heart*. 2010;96:1364-1371
137. Trenouth RS, Phelps NC, Neill WA. Determinants of left ventricular hypertrophy and oxygen supply in chronic aortic valve disease. *Circulation*. 1976;53:644-650
138. Kenny A, Wisbey CR, Shapiro LM. Profiles of coronary blood flow velocity in patients with aortic stenosis and the effect of valve replacement: A transthoracic echocardiographic study. *Br Heart J*. 1994;71:57-62
139. Weidemann F, Herrmann S, Stork S, Niemann M, Frantz S, Lange V, Beer M, Gattenlohner S, Voelker W, Ertl G, Strotmann JM. Impact of myocardial fibrosis in patients with symptomatic severe aortic stenosis. *Circulation*. 2009;120:577-584
140. Unger SA, Robinson MA, Horowitz JD. Perhexiline improves symptomatic status in elderly patients with severe aortic stenosis. *Aust N Z J Med*. 1997;27:24-28
141. Davila-Roman VG, Vedala G, Herrero P, de las Fuentes L, Rogers JG, Kelly DP, Gropler RJ. Altered myocardial fatty acid and glucose metabolism in idiopathic dilated cardiomyopathy. *J Am Coll Cardiol*. 2002;40:271-277
142. Funada J, Betts TR, Hodson L, Humphreys SM, Timperley J, Frayn KN, Karpe F. Substrate utilization by the failing human heart by direct quantification using arterio-venous blood sampling. *PLoS One*. 2009;4:e7533
143. Chandler MP, Kerner J, Huang H, Vazquez E, Reszko A, Martini WZ, Hoppel CL, Imai M, Rastogi S, Sabbah HN, Stanley WC. Moderate severity heart failure does not involve a downregulation of myocardial fatty acid oxidation. *Am J Physiol Heart Circ Physiol*. 2004;287:H1538-1543

144. Opie LH, Knuuti J. The adrenergic-fatty acid load in heart failure. *J Am Coll Cardiol*. 2009;54:1637-1646
145. Tuunanen H, Engblom E, Naum A, Scheinin M, Nagren K, Airaksinen J, Nuutila P, Iozzo P, Ukkonen H, Knuuti J. Decreased myocardial free fatty acid uptake in patients with idiopathic dilated cardiomyopathy: Evidence of relationship with insulin resistance and left ventricular dysfunction. *J Card Fail*. 2006;12:644-652
146. Levy S. Secondary prevention after myocardial infarction: In favor of beta-blockers. *J Cardiovasc Pharmacol*. 1990;16 Suppl 6:S50-54
147. Lionetti V, Stanley WC, Recchia FA. Modulating fatty acid oxidation in heart failure. *Cardiovasc Res*. 2011;90:202-209
148. Glenn DJ, Wang F, Nishimoto M, Cruz MC, Uchida Y, Holleran WM, Zhang Y, Yeghiazarians Y, Gardner DG. A murine model of isolated cardiac steatosis leads to cardiomyopathy. *Hypertension*. 2011;57:216-222
149. Tomita T, Wilson L, Chiga M. Idiopathic dilated cardiomyopathy--an evidence of abnormal lipid accumulation accumulation in myocardium. *Am J Cardiovasc Pathol*. 1990;3:81-85
150. Nakae I, Mitsunami K, Yoshino T, Omura T, Tsutamoto T, Matsumoto T, Morikawa S, Inubushi T, Horie M. Clinical features of myocardial triglyceride in different types of cardiomyopathy assessed by proton magnetic resonance spectroscopy: Comparison with myocardial creatine. *J Card Fail*. 2010;16:812-822
151. Suttie JJ, Dass S, Bull S, Holloway C, Banerjee R, Cox P, Pitcher A, Rial B, Francis JM, Schneider J, Robson M, Watkins H, Myerson S, Neubauer S. Cardiac steatosis detected in hypertrophic cardiomyopathy, dilated cardiomyopathy and aortic stenosis. *Circulation*. 2011;124:Abstract17133
152. Schulze PC. Myocardial lipid accumulation and lipotoxicity in heart failure. *J Lipid Res*. 2009;50:2137-2138
153. Cohn JN, Ferrari R, Sharpe N. Cardiac remodeling--concepts and clinical implications: A consensus paper from an international forum on cardiac remodeling. Behalf of an international forum on cardiac remodeling. *J Am Coll Cardiol*. 2000;35:569-582
154. Solomon SD, Anavekar N, Skali H, McMurray JJ, Swedberg K, Yusuf S, Granger CB, Michelson EL, Wang D, Pocock S, Pfeffer MA. Influence of ejection fraction on cardiovascular outcomes in a broad spectrum of heart failure patients. *Circulation*. 2005;112:3738-3744
155. Shah AM, Solomon SD. Myocardial deformation imaging: Current status and future directions. *Circulation*. 2012;125:e244-248
156. Karamitsos TD, Neubauer S. The interplay between cardiac strain and fibrosis in non-ischaemic cardiomyopathies: Insights from cardiovascular magnetic resonance. *Eur J Heart Fail*. 2011;13:927-928
157. Butler CR, Kumar A, Toma M, Thompson R, Chow K, Isaac D, Kim D, Haykowsky M, Friedrich MG, Paterson I. Late gadolinium enhancement in cardiac transplant patients is associated with adverse ventricular functional parameters and clinical outcomes. *Can J Cardiol*. 2013
158. Kelley DE, Goodpaster BH, Storlien L. Muscle triglyceride and insulin resistance. *Annu Rev Nutr*. 2002;22:325-346
159. Kelley DE, Goodpaster BH. Skeletal muscle triglyceride. An aspect of regional adiposity and insulin resistance. *Diabetes Care*. 2001;24:933-941
160. Rijzewijk LJ, Jonker JT, van der Meer RW, Lubberink M, de Jong HW, Romijn JA, Bax JJ, de Roos A, Heine RJ, Twisk JW, Windhorst AD, Lammertsma AA, Smit JW, Diamant M, Lamb HJ. Effects of hepatic triglyceride content on myocardial metabolism in type 2 diabetes. *J Am Coll Cardiol*. 2010;56:225-233
161. McKimmie RL, Daniel KR, Carr JJ, Bowden DW, Freedman BI, Register TC, Hsu FC, Lohman KK, Weinberg RB, Wagenknecht LE. Hepatic steatosis and subclinical cardiovascular disease in a cohort enriched for type 2 diabetes: The diabetes heart study. *Am J Gastroenterol*. 2008;103:3029-3035

162. Kato T, Niizuma S, Inuzuka Y, Kawashima T, Okuda J, Kawamoto A, Tamaki Y, Iwanaga Y, Soga T, Kita T, Kimura T, Shioi T. Analysis of liver metabolism in a rat model of heart failure. *Int J Cardiol*. 2012;161:130-136
163. Graner M, Siren R, Nyman K, Lundbom J, Hakkarainen A, Pentikainen MO, Lauerma K, Lundbom N, Adiels M, Nieminen MS, Taskinen MR. Cardiac steatosis associates with visceral obesity in nondiabetic obese men. *J Clin Endocrinol Metab*. 2013;98:1189-1197
164. Bugianesi E, Gastaldelli A. Hepatic and cardiac steatosis: Are they coupled? *Heart Fail Clin*. 2012;8:663-670
165. van der Meer RW, Hammer S, Lamb HJ, Frolich M, Diamant M, Rijzewijk LJ, de Roos A, Romijn JA, Smit JW. Effects of short-term high-fat, high-energy diet on hepatic and myocardial triglyceride content in healthy men. *J Clin Endocrinol Metab*. 2008;93:2702-2708
166. Zib I, Jacob AN, Lingvay I, Salinas K, McGavock JM, Raskin P, Szczepaniak LS. Effect of pioglitazone therapy on myocardial and hepatic steatosis in insulin-treated patients with type 2 diabetes. *J Investig Med*. 2007;55:230-236
167. Zhou YT, Grayburn P, Karim A, Shimabukuro M, Higa M, Baetens D, Orci L, Unger RH. Lipotoxic heart disease in obese rats: Implications for human obesity. *Proc Natl Acad Sci U S A*. 2000;97:1784-1789
168. van der Meer RW, Rijzewijk LJ, de Jong HW, Lamb HJ, Lubberink M, Romijn JA, Bax JJ, de Roos A, Kamp O, Paulus WJ, Heine RJ, Lammertsma AA, Smit JW, Diamant M. Pioglitazone improves cardiac function and alters myocardial substrate metabolism without affecting cardiac triglyceride accumulation and high-energy phosphate metabolism in patients with well-controlled type 2 diabetes mellitus. *Circulation*. 2009;119:2069-2077
169. Chu Y, Lund DD, Weiss RM, Brooks RM, Doshi H, Hajj GP, Sigmund CD, Heistad DD. Pioglitazone attenuates valvular calcification induced by hypercholesterolemia. *Arterioscler Thromb Vasc Biol*. 2013;33:523-532

APPENDIX 1: EXTENT OF INVOLVEMENT IN THE CURRENT WORK

Aortic stenosis patients

I recruited all the patients and obtained consent myself. Prior to recruitment, I approached all the cardiothoracic surgeons, explaining the nature of the study, getting their permission to recruit severe AS patients referred to them for AVR, and to request for intraoperative myocardial biopsies. Then I attended their outpatient and preadmission clinics to identify suitable candidates. I worked closely with the preadmission cardiothoracic nurses to co-ordinate CMR scan slots and attendance of for pre-operative investigations. Patient information sheet and invitation to take part in the study were sent to eligible patients. This was followed by telephone conversation (after giving them enough time to read and understand the study) to briefly check their eligibility and safety to undergo MRI scan. If they agreed, I would organise CMR scan slot and their transport and if necessary overnight stay if they lived very far away. On the day of arrival, I explained in details about the study, giving them chances to ask questions and also emphasised that tissue biopsies and post AVR scans were optional. At the same time they had to sign MRI safety form as well. After signing informed consent form, physical examination, venepuncture and cannula insertion were performed. After registering the patient on the CMR scanner, I prepared the coil and set up adenosine infusion and gadolinium injector, and connected to the patient while he/she was the scanner. l also made sure that everything worked prior to starting scanning the patient for e.g. BP machine, safety measures, flushing all the lines etc. I performed CMR scan and spectroscopy independently with some technical support from the radiographer. This was necessary as for high risk patients undergoing adenosine stress CMR, the departmental policy is to have a doctor and at least a radiographer during the scan. I have a “licence” from the unit to be able to scan my research patients independently. After scanning the patients, I showed and explained to them their CMR scan images. I also analysed and reported their scan findings, verified by a consultant, and communicated with their surgeons (optional request by the surgeons) their scan findings.

For those patients who consented for tissue biopsy during AVR, I was solely responsible in co-ordinating various people involved to make sure that the biopsy was a success. This involved reminding the surgeon/secretary very early in the morning prior going to theatre, informing the theatre staff (nurses and anesthetist) about the tissue needed for research during AVR, including giving them a copy of the consent form and also informing the pathology team to standby on the day to receive the sample. I collected all the samples by staying in theatre (therefore had the opportunity to observe the procedure), putting it in a pot containing normal saline, then quickly sent the fresh sample to the pathologist for lipid analysis.

For those patients who had agreed to have a repeat CMR scan post AVR, I contacted them again, checking for eligibility and to make sure they did not have any contraindications to MRI for e.g. pacemaker implantation during AVR. If they agreed, study appointment was booked and the same procedure was repeated as before AVR. For asymptomatic patients, some of the patients were obtained from a different project recruiting severe asymptomatic patients (please see under Declaration).

Dilated cardiomyopathy patients

This was part (baseline study) of the multi-centre (a total of 15 centres in the UK and US), randomised, placebo-controlled, double-blinded, Syncria heart failure clinical trial designed and funded by Glaxo Smith Kline (GSK) pharmaceutical company looking at the effect of Albiglutide (glucagon-like peptide, a new anti-diabetic drug) in patients with heart failure due to non-ischaemic dilated cardiomyopathy. I was solely responsible for recruitment and scanning the patients (as per aortic stenosis patients described above), performing randomisation process, and Albiglutide administration (weekly subcutaneous injection for 12 weeks). However, in view of the complexity of the protocol recruitment target was not achieved, and this similarly affected all other sites. Despite this, Oxford was the top recruiting site in the UK and second when compared with the US. Due to the small number of patients, the CMR scan and spectroscopy findings were underpowered to detect the treatment effect. For the purpose of the thesis, the baseline findings of the DCM patients were presented and combined with baseline data from a different project (stated in Declaration and General Methods) to increase the power of the study.

APPENDIX 2: SUPPLEMENTARY TABLES FOR CHAPTER 3

Table 1: Clinical and echocardiographic characteristics (without diabetics)

	Severe Aortic Stenosis		Normal Controls (n = 20)	P value[¶]
	Symptomatic (n = 19)	Asymptomatic (n = 14)		
Age (years)	68±9	63±16	63±4	0.13
Male, n (%)	13 (68)	11 (78)	12 (60)	0.15
Symptoms, n (%)				
Dyspnoea	15 (78)	–	–	
Angina	7 (28)	–	–	
Syncope	1 (4)	–	–	
Past medical history, n (%)			–	
Hypertension	6 (31)	3 (21)	–	
Diabetes	–	–	–	
Dyslipidaemia	3 (15)	2 (14)	–	
Coronary artery disease	–	–	–	
Medications, n (%)				
Beta blockers	4 (16)	–	–	
ACE-I/ARB-II	4 (21)	5 (36)	–	
Statin	6 (31)	3 (21)	–	
Body mass index (kg/m^2)	27±4	27±4	26±4	0.26
Systolic BP (mmHg)	130±16	134±18	130±12	0.70
Diastolic BP (mmHg)	75±10	76±8	76±8	0.93
Heart rate (bpm)	65±10	65±13	62±9	0.67
Echocardiograpy				
Peak AV gradient (mmHg)	82±13	74±14	–	0.12[‡]
E-wave deceleration (ms)	284±116	255±108	210±43	0.10
E/A ratio	0.8±0.4	0.9±0.3	0.9±0.3	0.49
E/E' ratio	14.4±4.7*	12.6±5.4†	9.2±2.7	0.003
Biochemical, mmol/L				
Blood glucose, mmol	5.1±1.0	5.3±0.5	5.1±0.9	0.85
NEFA	0.6±0.2	0.6±0.1	0.5±0.3	0.26
Triglycerides	1.1±0.4	1.2±0.5	1.0±0.3	0.64
Low-density lipoprotein	2.9±1.0	3.1±0.2	3.3±0.9	0.51
High-density lipoprotein	1.4±0.4	1.5±0.3	1.5±0.4	0.78

Values are mean ± SD or percentages.
¶P-values are for one-way analysis of variance (ANOVA) for all groups unless specified.
*P (with post hoc Bonferroni correction) <0.05 vs. normal and >0.05 vs. asymptomatic severe AS.
†P (with post hoc Bonferroni correction) >0.05 vs. normal.
‡P-value is Student *t* test for symptomatic vs. asymptomatic aortic stenosis.
ACE indicates angiotensin-converting enzyme-inhibitors; ARB, angiotensin-receptor antagonist-II; AV, aortic valve; A, atrial contraction; BP, blood pressure; E, early diastolic filling phase; E', mitral annular velocity; NEFA, non-esterified fatty acids.

Table 2: Cardiovascular MRI and spectroscopy (without diabetics)

	Severe Aortic Stenosis		Normal Control (n = 20)	P value¶
	Symptomatic (n = 19)	Asymptomatic (n = 14)		
Lipid/water ratio (%)	0.90±0.46*	0.75±0.36†	0.45±0.17	<0.001
Circumferential strain (%)	-16.6± 2.6*	-18.1±2.9†	-20.7±2.0	<0.001
Longitudinal strain (%)	-12.6±2.2*	-13.2±2.9†	-16.6±1.6	<0.001
Circumferential diastolic SR (s^{-1})	53±13*	59±12†	76±12	<0.001
Longitudinal diastolic SR (s^{-1})	42±12*	40±14†	54±12	0.006
LV ejection fraction (%)	74±6*	73±8†	69±4	0.003
LV end-diastolic volume (ml)	145±49	143±27	143±28	0.96
LV end-systolic volume (ml)	38±20	39±16	45±11	0.46
LV mass index (g/m^2)	97±36*	94±29†	54±13	<0.001
LV wall thickness (mm)	16±2*	15±3†	9±1	<0.001
LGE present, n (%)	15 (79)‡	9 (64)	2 (10)	<0.001
Aortic valve area (cm^2)	0.84±0.10	0.86±0.14	–	0.61χ

Values are mean ± SD or percentages.
¶P values are for one-way analysis of variance (ANOVA) for all groups unless specified.
*P (with post hoc Bonferroni correction) <0.05 vs. normal and >0.05 vs. asymptomatic severe AS,
†P (with post hoc Bonferroni correction) <0.05 vs. normal.
‡P (with post hoc Bonferroni correction) <0.05 vs. asymptomatic severe AS and normal.
χ P-value is Student t test for symptomatic vs. asymptomatic aortic stenosis.
LV indicates left ventricular; LGE, late gadolinium enhancement; SR, strain rate.

Table 3. Cardiac MRI and spectroscopy before and after AVR in symptomatic AS after excluding diabetics (6 diabetics before and 4 after AVR).

Cardiac MRI and Spectroscopy	All symptomatic AS patients[§] (n = 19)	Follow-up patients (n = 9)		Controls
		Pre AVR	Post AVR	
Cardiac lipid/water	0.90±0.46	0.97±0.49	0.40±0.21*	0.45±0.17
Circumferential strain	-16.6±2.6	-17.4±1.9	-20.7±1.8*	-20.7±2.0
Circumferential diastolic strain rate	53±13	56±11	76±13*	76±12
Longitudinal strain	-12.6±2.2	-13.2±2.1	-14.0±2.4[†]	-16.6±1.6
Longitudinal diastolic strain rate	42±12	43±5	56±14*	53±12
Left ventricular mass index	97±36	101±41	73±21[‡]	54±13
Left ventricular ejection fraction	74±6	75±6	74±5[†]	69±4

[§]All 6 diabetics were in the symptomatic group, therefore cardiac MRI and spectroscopy parameters for asymptomatic AS remain the same as in Table 1 of the manuscript.

*$p<0.05$ versus pre AVR and >0.05 versus controls; [†]$p>0.05$ versus pre AVR and <0.05 versus controls; [‡]$p<0.05$ versus pre AVR and controls.
Note: For strain, n=8 were used for follow-up analysis as one patient was excluded due to presence of left bundle branch block post AVR.

APPENDIX 3: PROPOSED CLINICAL TRIAL ARISING FROM CHAPTER 3

Background: In AS, myocardial TG is increased and correlates with the degree of LV strain impairment. Myocardial steatosis and strain impairment improve significantly after AVR, suggesting that myocardial lipotoxicity may contribute to the pathophysiology of AS. Steatosis regression, achieved by metabolic modulator drugs may become a potential new therapeutic option to delay onset of symptoms or LV dysfunction.

Proposed metabolic modulator: Aleglitazar is one of the glitazar family of drugs which and combines the PPAR gamma effects (targeting peripheral insulin sensitivity) with the PPAR alpha effects (targeting dyslipidaemia), and is currently used for treating patients with diabetes mellitus (DM)**.**

Proposed clinical trial design: A pilot study (placebo-controlled, double-blind) to evaluate the safety of PPAR agonist (Aleglitazar) and its effects on myocardial TG content and LV function (strain) in patients with moderate-severe AS.

Relevant previous studies using PPAR: Troglitazone lowered myocardial TG and ceramide, prevented cardiac dysfunction in obese diabetic rats.[167] Pioglitazone reduced myocardial and hepatic steatosis in insulin-treated human type 2 DM,[166] but only reduced hepatic steatosis in well-controlled human type 2 DM.[168] Pioglitazone has also been shown to attenuate calcification and reduce lipid content of the aortic valve.[169] There have been inconsistent reports from animal studies on the effect of PPAR agonist on LVH which is either protective or pro-hypertrophic. Hypoglycaemia in non-diabetic subjects has been shown to be comparable with placebo. Recently, Aleglitazar doses of <300 mcg, cardiovascular safety profile have been shown to be better than Pioglitazone.

Hypothesis: In patients with moderate-severe AS and elevated myocardial TG, treatment with Aleglitazar will reduce myocardial TG and improve myocardial function (strain).

Study design: 30 patients with moderate-severe AS will undergo screening ^{1}H-MRS to identify patients with elevated myocardial TG (lipid/water ratio >0.5). Eligible patients will be given 6 months of either Aleglitazar or placebo. Primary endpoints include myocardial TG content using ^{1}H-MRS and LV strain using MR tagging. Secondary endpoints include LVH regression, valve gradient and area, pericardial, visceral and abdominal subcutaneous fat assessed by MRI and exercise capacity. Safety measures include heart failure from symptoms or physical examination, weight gain and hypoglycaemia.

Eligibility: Inclusion criteria - isolated moderate-severe AS (not planned for AVR) aged >18, no other significant valvular pathology, no contraindications to MRI, myocardial TG >0.5. Exclusion criteria - underlying cardiomyopathy, poor LV function, significant CAD, uncontrolled hypertension, diabetes, CHF by history, clinical examiantion or current use of CHF medications, liver impairment, pregnancy, lactating, BMI >35, concurrent use of fibrates or PPAR agonists, fasting serum TG >4.5mmol/L, GFR <30.

Expected value of results: If positive effect on primary and/or secondary outcome is demonstrated, to plan a multicentre outcome study powered for outcome**.** If positive, Aleglitazar treatment for chronic aortic stenosis may ultimately become routine clinical practice.

APPENDIX 4: PAPERS AND ABSTRACTS ARISING DURING COURSE OF DPHIL

PAPERS

Mahmod M, Bull S, Suttie JJ, Pal N, Holloway C, Dass S, Myerson SG, Schneider JE, De Silva R, Petrou M, Sayeed R, Taggart D, Westaby S, Clelland C, Francis JM, Ashrafian H, Karamitsos TD, Neubauer S. *Myocardial Steatosis and Left Ventricular Contractile Dysfunction in Patients with Severe Aortic Stenosis.* Circ Cardiovasc Imaging published online July 5, 2013. DOI: 10.1161/CIRCIMAGING.113.000559.

Mahmod M, Karamitsos TD, Suttie JJ, Myerson SG, Neubauer S, Francis JM. *Prevalence of cardiomyopathy in asymptomatic patients with left bundle branch block referred for cardiovascular magnetic resonance imaging*. Int J Cardiovasc Imaging. 2012 Jun;28(5):1133-40.

Mahmod M, Pal N, Lewis A, Dass S, De Silva R, Petrou M, Sayeed R, Taggart D, Westaby S, Francis JM, Ashrafian H, Neubauer S, Karamitsos TD. *Impaired Myocardial Oxygenation Response during Vasodilator Stress in Patients with Severe Aortic Stenosis: insights from Oxygenation-sensitive Cardiovascular Magnetic Resonance.* The paper is under review by Circulation.

Mahmod M, Suttie J, Karamitsos T, Ashrafian H, Neubauer S. *Myocardial Steatosis and Left Ventricular Contractile Dysfunction in Dilated Cardiomyopathy*. The paper is in preparation.

Holloway C, Ntusi N, Suttie J, **Mahmod M**, Wainwright E, Clutton G, Hancock G, Beak P, Tajar A, Piechnik SK, Schneider JE, Angus B, Clarke K, Dorrell L, Neubauer S. *Comprehensive cardiac magnetic resonance imaging and spectroscopy reveals a high burden of myocardial disease in HIV patients*. Circulation. 2013 Jul 1. [Epub ahead of print] doi: 10.1161/ CIRCULATIONAHA.113.001719.

Dass S, Suttie JJ, Piechnik SK, Ferreira VM, Holloway CJ, Banerjee R, **Mahmod M**, Cochlin L, Karamitsos TD, Robson MD, Watkins H, Neubauer S. *Myocardial tissue characterization using magnetic resonance noncontrast t1 mapping in hypertrophic and dilated cardiomyopathy*. Circ Cardiovasc Imaging. 2012 Nov;5(6):726-33.

ABSTRACTS

Mahmod M, Bull S, Suttie JJ, Nikhil Pal, Holloway C, Banerjee R, Dass S, Ashrafian H, Schneider JE, Myerson SG, Francis JM, Karamitsos TD and Neubauer S. *Myocardial steatosis and impaired energetics are independent predictors of regional contractile function in patients with severe aortic stenosis.* Journal of Cardiovascular Magnetic Resonance 2013, 15(Suppl 1):O27. Oral presentation at SCMR, San Francisco 2013.

Mahmod M, Karamitsos TD, Suttie JJ, Myerson SG, Neubauer S, Francis JM. Prevalence of *cardiomyopathy in asymptomatic patients with left bundle branch block referred for cardiovascular magnetic resonance imaging.* Poster presentation at BSCMR, Leicester 2011 and BCS, Manchester 2011.

Dass S, Holloway C, Suttie J, **Mahmod M**, Sever E, Watkins H, Neubauer S, Karamitsos TD. *Patients with Dilated Cardiomyopathy (DCM) have appropriate myocardial oxygenation response to vasodilator stress*. Journal of Cardiovascular Magnetic Resonance 2013, 15(Suppl 1):O68. Oral presentation at SCMR, San Francisco 2013.

Holloway C, Ntusi N, Suttie J, **Mahmod M**, Wainwright E, Clutton G, Hancock G, Beak P, Tajar A, Piechnik SK, Schneider JE, Angus B, Clarke K, Dorrell L, Neubauer S. *Comprehensive cardiac magnetic resonance imaging and spectroscopy reveals a high burden of myocardial disease in HIV patients*. Journal of Cardiovascular Magnetic Resonance 2013, 15(Suppl 1):O25. Oral presentation at SCMR, San Francisco 2013.